SMART ELECTROSTATIC CROP SPRAYING USING REMOTE SENSING TECHNOLOGY

A thesis submitted in partial fulfilment of the requirements for the degree of Doctor of Philosophy (Ph.D.)

In

Centre for Electronic Systems Research

Electronic and Computer Engineering

College of Engineering, Design and Physical Sciences

Brunel University London

By

Murtadha Jaleel Ibraheem Al-Mamury

Supervised by

Prof Wamadeva Balachandran

June 2015

Declaration

This is to certify that:

i. The thesis comprises only my original work towards the Ph.D. except where indicated.

ii. Due acknowledgement has been made in the text to all other material used.

Murtadha Jaleel Al-Mamury

ABSTRACT

For this thesis, smart spraying robot was designed, constructed and tested to validate the concept of smart pest control. Electrostatic charging of sprayed pesticide was realized in a spray nozzle design that improved plant coverage and reduced wasted pesticide as well as soil pollution. A thorough investigation into electrostatic spraying was conducted, which was accompanied by extensive simulations and experimentation. The results obtained from the simulation experimentation on industry standard electrostatic spray system (ESS) nozzles along with laboratory testing of these nozzles, detecting spray coverage using water sensitive paper and additional optical spray visualization methods gave the necessary insight and experience required to develop a new spray nozzle. Additional COMSOL simulation and experimentation were carried out on a Fan Hydraulic Spray Nozzle (FHSN), the results of which allowed for the effective addition of electrostatic induction capabilities, thereby transforming the (FHSN) into Electrostatic Induction Spray Nozzle (EISN) which is one of the prime parts of the smart spraying system. SOLIDWORKS software was used in the designing parts of this nozzle which were then manufactured using a 3D printer. An AL05D robotic manipulator and a TTRK tracked platform from Lynxmotion ™ were the mini mobile robot components selected for the feasibility study of the smart electrostatic crop spraying system. This mobile robot was equipped with a CCD digital camera, a range detector, and path mark detector to provide the necessary sensors required by the smart electrostatic spray system. A Windows™ based mobile computer in addition to an ARDUINO™ based orksmicrocontroller system were chosen to provide the computational power required by the system. These were arranged in a master – slave configuration, with the main processing for images and motion being conducted inside the master computer using programs created by Matlab smart ™ software. The execution of motion commands and the operation of the range and path mark detection along with operating the spray nozzle were performed on the slave computer using C as the programming language. The manufactured smart electrostatic spray system moves along cotton crop rows with a camera that scans the selected plant for pest infestation on the upper and lower surfaces of plant leaves. When a pest is detected, the spray nozzle is targeted on it at the appropriate distance, and a burst of pesticide destroys it. The results of experiments have shown that using the electrostatic induction system improves coverage 3 to 4 fold and reduces soil contamination by 2 to 4 fold. The system has plenty of room for performance improvement, and future development will make it adaptable for application to other crops and applications.

Dedication

All the devotion to Allah the Almighty for his infinite kindness and mercy throughout my life, who gave me the ability and confidence to complete my studies.

Additional dedications to my wife for her patience and support, the members of my family, Basma, Huthiafa, Hayder, Ali, Muhtadha, Fadak and to all my brothers and sisters.

ACKNOWLEDGEMENTS

TABLE OF CONTENTS

LIST OF TABLES

LIST OF FIGURES

LIST OF ABBREVIATIONS

Abbreviations	Definition
A	Ampere
ADC	Analogue to Digital Converter
ALU	Arithmetic Logic Unit
CCD camera	Charge Coupled Camera Device
CKD	Complete Knock Down
CMOS	Complementary Metal Oxide Semiconductor
CPU	Central Processing Unit
CMR	Charge to Mass Ratio
CV	Coefficient of Variation
cm^2	Square centimetre
D	Distance
2D	Two Dimensions
3D	Three Dimensions
DC	Direct Current
DV	Droplet Volume
FEM	Finite Element Model
EEPROM	Electrically Eraseable Programmable Read Only Memory
EHDA	Electro Hydrodynamics Atomization
ESS	Electrostatic Spraying System
FHSN	Fan Hydraulic Spray Nozzle
ha	Hectare (area unit of agricultural land)
h	Hour
EISN	Electrostatic Induction Spray Nozzle
I/O	Input / Output

kPa	Kilopascal
L	Litre
LED	Light Emitting Diode
m^2	Square metre
MIPS	Mega Instruction Per Second.
MOS FET	Metal Oxide Semiconductor Field Effect Transistor
m	metre
MMD	Mass Median Diameter
MPa	Mega Pascal
mm	Millimetre
ms	Millisecond
ml	Millilitre
ng	Nano game
OSP	Oil Sensitive Paper
PSI	Pounds per Square Inch
PC	Personal Computer
PVC	Polymer of Vinyl Chloride
PAC	Post Atomization Charging
PMI	Product and Manufacturing Information
QFN/MLF	Quad Flat No-Lead or Micro Lead Flat Pack, a king of IVC Pac
RISC	Reduced Instruction Set Computer
rpm	Revolutions per minute
SE	Spot Elimination
SRAM	Static Random Access Memory
SPW	Sweet potato whitefly

SPI	Serial Peripheral Interface, a kind of serial bus
TQFP	Thin Quad Flat Pack, a kind of modern IC packaging
USB	Universal Serial Bus
USART	Universal Sichnonous Asynchronous Receiver Transmitter
µg	Micro grame
V	Volt
VMD	Volume Median Diameter
VRM	Voltage Regulator Module
WSP	Water Sensitive Paper

LIST OF SYMBOLS

Symbol	
σ	Liquid conductivity
τ	Time
ε_0	Permittivity
C	Coulomb
V	Volt
E	Electric field
N	Newton (Kg/s^2)
Fe	Electrostatic force
Fg	Gravitational force
Ed	Drag force
A	Ampere
I E	Induction electrode
q/m	Charge to mass ratio
kV	Kilovolt
s	Second
min	Minute
Q/M	Charge to mass ratio
μh	Micro Ampere
μm	Micron
Qp	Electrical charge
Ωm	Resistivity
$\mu S/m$	Micro Siemens per metre
ρ	Space charge density (C/m^3)
Q	entrapment air flow rate (m^3/s)
I	Induction current (A)
M	Liquid mass flow rate (kg/s)
D	Water Density (kg/m^3)
V	Water flow rate (m^3/s)
q	Charge to mass ratio (C/Kg) (alternative to q/m)
F	Spread factor correction of droplet size on the water sensitive paper

CHAPTER ONE: INTRODUCTION

1.1. Description of Iraqi location and climatic conditions

Iraq is a country in Western Asia, which borders Turkey to the north, Iran to the east, Kuwait to the southeast, Saudi Arabia to the south, Jordan to the southwest, and Syria to the west. The southern part of Iraq is within the Arabian Peninsula. The country lies between latitudes' 5 29 ° and 22 ° 37 N, and longitudes 45 ° 38 and '45 ° 48 east, occupying an estimated area of 438,317 km^2. This location means it has intensely hot and dry summers lasting from May to October, with peak temperatures often reaching 49°C (120°f) in the shade. In the summer months, there are two types of wind. The south-east, dry, dusty wind, with speeds of up to 80 kilometers per hour (50 mph), which occurs from April to early June, and again from late September until November, can last for one day at the beginning or end of the season, but for several days at other times. From mid-June to mid-September, the prevailing wind comes from the north and northwest, which is constant, only occasionally being absent during this period. Winters, lasting from December to March, are damp and comparatively cold, with temperatures averaging about 10°c (50°f), whilst spring and autumn are brief transition periods. Normally, no rain falls from the end of May to the end of September and with an average annual rainfall of less than 38 cm (15 in), agriculture is dependent on irrigation. Iraq has two major rivers, the Tigris and the Euphrates, which run in a southeasterly through the Centre of the country, flowing into the Shatt al-Arab that runs into the Arabian Gulf. Owing to these rivers, significant amounts of fertile land can be created, especially in the region that is located between them, often referred to as Mesopotamia, which is the world's oldest civilisation. Mesopotamia refers to the ancient name of Iraq, and it is here that nearly all the agricultural production of the country is found.

1.2. Variety of crops grown in Iraq

The factors described above have resulted in great agricultural diversity across the whole of the country. Cotton is grown in different areas including, the northern, central and southern parts owing to the appropriate climatic conditions during the summer season [1]. In fact, Iraq is one of the top countries in the world producing cotton [2]. Cotton is the fourth most important strategic crop in Iraq, after wheat, barley and corn in securing foreign exchange. The plant provides the raw material for the textile industry and oil for certain products, hence playing a big role in the country's economy. State factories and other companies that have

been created by the government depend on its production, producing cotton clothing and other items for domestic consumption and also for exporting. In sum, the socioeconomic importance of cotton is clear as many thousands of people working in agriculture, industry and trade rely upon the crop.

In the last fifteen years, a significant drop was recorded in the production of cotton plants and there are several reasons behind this. For instance, it has been indirectly attributed to changes in the weather, such as lack of rain water, greenhouse gases influence and land salinization. In addition, there has been a marked increase in insect infections during all the stages of the plant life cycle. Despite pesticides being used to control insects in crops, cotton is still suffering from several that appear with the growth of the plant.

1.3. Types of pests infesting cotton plants

Pests can be identified as organisms that infect plants, causing losses, directly or indirectly, in all stages of growth, even after storage of the harvest, thereby damaging agricultural production in terms of quantity and quality. Different types of pests begin their life cycle by laying their eggs on the plants and those found in Iraq are described below.

1.3.1. Thirps tabaci: It is yellow in colour, also having yellow wings and the female lays 10 to 30 white eggs on the leaves, resulting in 6-8 generations each year. The insect larvae and adult absorb the juices of the plant, thereby damaging its chlorophyll. This leads to the leaves curling upwards and silver infection spots appearing on their under surfaces, resulting in poor and late plant growth.

Figure 1.1: Photograph of Thirps tabaci.

1.3.2. Empoasca Iybica: An insect that is light green in colour with wings that are also green transparent. The female lays 50 to 60 eggs in the plant tissues, which leads to several generations per year. The adult insect absorbs juice from the leaves, which causes flowers and fruit to drop and in cases of severe infestation kills the plant.

Figure 1.2: Photograph of Empoasca Iybica.

1.3.3. Aphis-gosspii: Has a dark green colour and its eggs hatch inside the female, appearing as a multiple births of 9 to 12-day nymphs, resulting in several generations per year. It sucks the sap of plants causing the leaves to wrinkle and eventually to turn over, thus leading to the plant dying.

Figure 01.3: Photograph of Aphis- gosspii.

1.3.4. Bemisia tabaci: Orange and yellow in colour but is often covered in a waxy material, which gives it a white appearance. The female lays eggs on the undersurface of the leaves and the adults suck plant sap such that yellow spots appear and eventually black mushroom-like growth is seen, which kills the plant.

Figure 1.4: Photograph of Bemisia tabaci.

1.3.5. Agrotis yplilon: This moth is covered with dark brown spots, and the grubs are clay coloured with three dark stripes on their backs. The female lays her eggs in the soil individually in sets of 300 or even more, leading to 3 to 4 generations per year. The grubs bite the stems of seedlings of the cotton plants causing them to droop and then die because their tops are touching the soil.

Figure 1.5: Photograph of Agrotis yplilon.

1.3.6. Crentiades pallidos: Small-sized insect pale green in colour. The insect nymphs move rapidly across the leaves and feed on the juices of the floral buds and leaf veins, which results in both dropping off.

Figure 1.6: Photograph of Crentiades pallidos.

1.3.7. Tetraychus telarius: This very small insect is oval shaped, light red or dark orange and has two black spots on its back. It makes a yellow mosaic on the upper leaf surface, after sucking plant juices from the veins, weakens the plant and hence stunts growth.

Figure 1.7: Photograph of Tetraychus telarius.

1.3.8. Spodoptera littoralis: Is a polyphagous adult moth up to 2 cm long with a wingspan of approximately 4 cm. The fully developed larvae are 35 to 45 mm long, with their colour varying from grey to reddish or yellowish. Their eggs are laid in batches and are covered with orange-brown hairs.

Figure 1.8: Photograph of Spodoptera littoralis.

This is the most destructive of all of the insects described above [3]. In fact, this insect and two other reasons have led to a reduction the percentage of cultivated land in Iraq. These other reasons being high atmospheric pollution in recent years, and the high cost of the raw materials for chemical pesticides used to control pests. The cotton plant needs a long growing season of at least six months and sometimes as much ten before it can be harvested, whilst *Spodoptera littoralis* can deposit as many as 1,200 eggs on one leaf in one week. Furthermore, the incubation period ranges from three to seven weeks depending on the weather conditions. Controlling of insects is an urgent issue if cotton plant production is to be protected. In order to keep production robust, large amounts of pesticides have had to be used at great cost, which has resulted in Iraq and some other Arab countries being the highest users

of chemicals in their agriculture, being also used for fertilizers [4]. The challenge is how to reduce the use of pesticides, whilst at the same time reducing the numbers of harmful insects. It is contended here, that the solution lies in selecting a suitable spraying system, one that provides the optimum dose for controlling pests, whilst also avoiding drift and the electrostatic spraying method has delivered the best results to this end [5].

1.4. Crop spraying techniques used at present in Iraq

Chemical treatment methods adopted by the Iraqi government vary according to the size of the cultivated land. For example, in vast open spaces owned by the government agricultural lands, aerial crop spraying of agricultural pests has been commonly employed. While, in smaller areas owned by the farmers, crops are sprayed using attachments to farm vehicles and spraying by hand is applied to small holdings as well as inside greenhouses. In all the cases, the spraying is inefficient for the following reasons.

1. The aforementioned high temperatures in Iraq during the summer (growing season of cotton) months of up to 50 degrees Celsius or 120 degrees Fahrenheit, which results in rapid evaporation of the fine droplets of pesticides, thereby reducing their efficacy.

2. These methods lead to much pesticide ending up underneath the plants directly on the ground rather than on them, thus requiring the quantities to be higher.

3. Aerial spraying is particularly poor at hitting the intended targets.

4. Failure to achieve full coverage for all infected areas.

5. The methods often fail to penetrate to the under surfaces of the leaves of plants and so the cause of the infection remains untouched.

1.5. Motivations

Several factors have prompted the decision to carry out the current research aimed at addressing these problems.

1. The need to reduce the huge amounts of money spent on pesticides and chemicals.

2. Enormous amounts of chemical materials are consumed to protect cotton plants from infection of insects, including pesticides, insecticides and herbicides.

3. Great amount of drift in the air and on the soil due to the use of overdose amount causing environmental pollution and increased soil contaminations. Furthermore, the side effect of the drift on the neighbor's crops and on the health of farm workers.

4. The reluctance of farmers for cultivation of cotton crop during the recent years due to reducing the annual production caused by infection of the insects.

5. Reducing patch of cotton farmland due to cultivating alternative crops that have a short period of growth and give good economic benefit.

6. Decline of cotton production due to insect infection and subsequent decline of cotton textile industry and other cottage industry products from cotton.

7. Cotton plant cultivation contributes with the other crops in completing agriculture cycle. It means some of the crops should be planted one after the other. These crops are corn wheat, alfalfa, barley and cotton the reason for this cycle is to provide some of elements nutrition from the residual material after the harvest to the next plant which is planted after and to maintain the soil fertility. Stopping cultivation of the cotton plant in these lands influenced on the productions of these crops and on the soil fertility level.

1.6. Aim and objectives

The aim of this study is development a smart electrostatic crop spraying system to protect cotton plants from pest's infestation in Iraq.

The Objectives:

1- To carry out literature review to identify the state-of-the-art electrostatic crop spraying techniques that can be adopted for use in Iraq.

2- To develop a smart electrostatic crop spraying system suitable for cotton fields in Iraq.

3- Perform numerical modelling and simulation to obtain optimal design parameters of a smart electrostatic nozzle.

4- Based on the results of the simulation, design and manufacture a novel induction charging nozzle using SOLIDWORKS and 3D printer.

5- Assembly of mini robot with CCD camera, sensors for range finding and path mark detectors in addition to other sensors to achieve a smart spraying system.

6- Experimental investigation of the smart electrostatic crop spraying system using idealized cotton plants and artificial insects.

1.7. Methodology

Figure 1.9 illustrates the steps of the methodology followed in conducting this research which can be summarised as follows:

To understand the theory and design of the induction spray nozzle, two types of experiments were carried out using hardware and software processes. The hardware testing involved using industry standard spraying nozzles, namely an electrostatic spraying system nozzle (ESS) and a fan hydraulic spray nozzle (FHSN). Two types of artificial cotton plants were placed in a Faraday pail to eliminate the influence of external fields on conducted tests. The faraday pail was manufactured from steel sheet mesh and an aluminum frame wired to form a continuous conducting frame. A graphics design software package like SOLIDWORKS or AutoCAD would be employed to design the shape of cotton leaves, which would then be constructed from aluminum metal and paperboard for the purpose being to mimic the real leaves of the cotton plant. The aim of the experiments that used the electrostatic spraying system nozzle was to gain comprehensive knowledge about its working principles. The next consideration was how to use the knowledge obtained from these experiments to build a more efficient spraying system. The new experimental set-up was to employ a mobile robot and a novel induction nozzle, with the former being selected on the basis of the planting of cotton and so as to be compatible with plant size during fumigation season and to be capable of holding and maneuvering the induction nozzle type and size chosen for the intelligent spraying process. The mobile robot would consist of an electric vehicle with a manipulator arm to which the nozzle was attached. The results of the fan hydraulic spray nozzle experiments and simulations guided the design of the novel induction nozzle designed for this project, which was built using some software can be designed and built the shape of the nozzle will be used in this study. For the second part of the methodology, two types of software were employed: PC based and microcontroller based. These were used to control the movement of the vehicle and the manipulator's arm. The other functions of these software programs were to analyse the images captured by the camera attached to the manipulator arm beside the nozzle for cotton pest signature using image processing methods and to control the timing and duration of induction hydraulic nozzle spraying operation to apply direct pesticide spray application

on   the   pest   without   the   need   to   cover   the   entire   plat   with   pesticide.
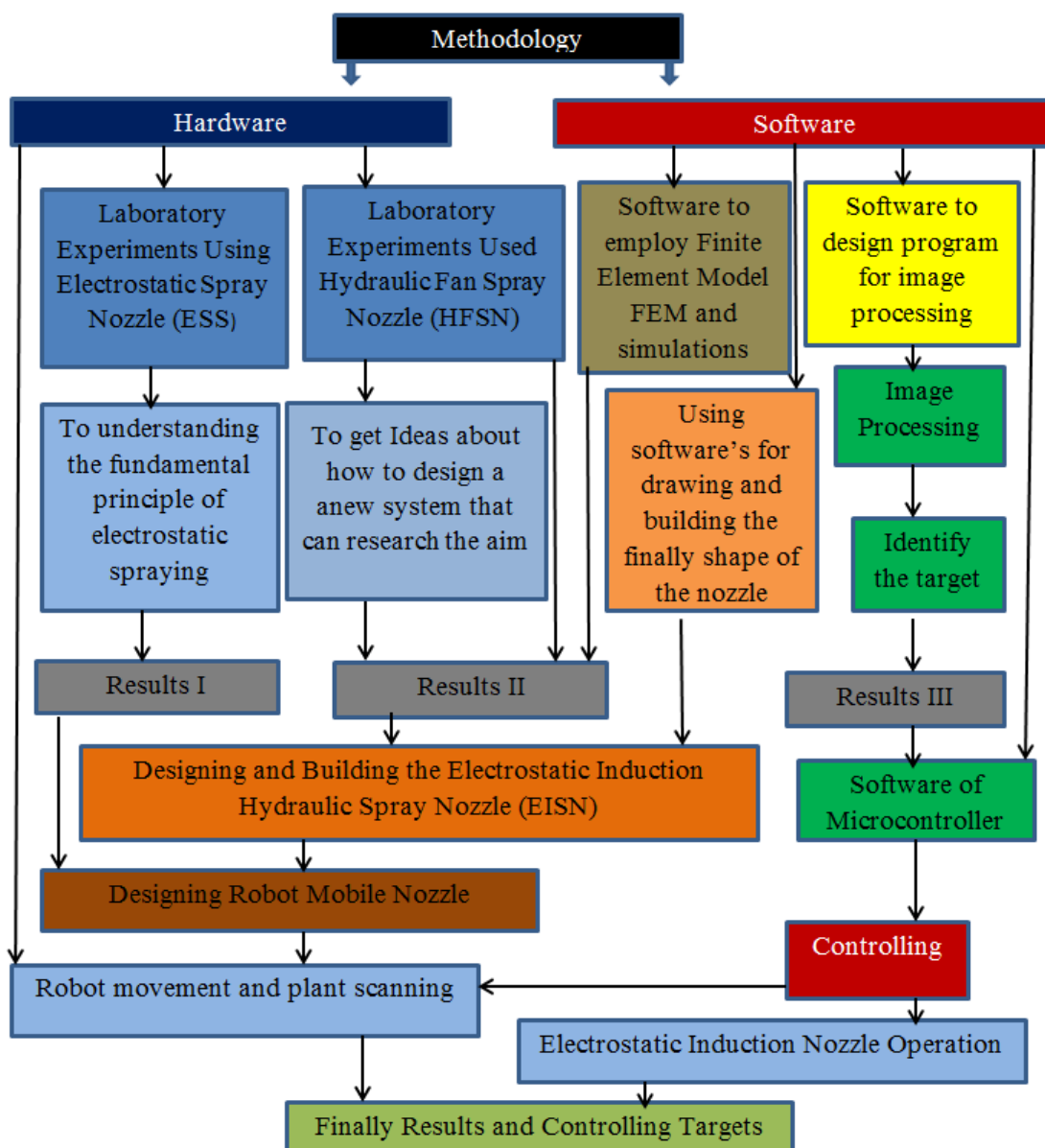
Figure 1.9: Describe the processing of methodology.

1.8. Contributions to Knowledge

It has become clear that electrostatic spraying yields more coverage area and deep penetration in the spatial canopy of plants compared to conventional systems. Despite researchers having used this technology in order to improve nozzle efficiency, performance and uniform distribution deposition on the targets, there are still large amounts of money and huge quantities of pesticides wasted, because the leaves that do not need remediation are still being treated by farmers and workers. This condition can be controlled by targeting the infested

area only, thus giving large reductions in wasted chemical materials, which would result in decreased environmental pollution and better utilisation of financial resources. This research has addressed the gap in knowledge regarding the development of a more efficient spraying system than those presently available. Specifically, smart pesticide spraying system was developed with a nozzle attached to the gripper of a mobile robot along with a CCD camera for locating insect positions on plant leaves. After positioning the nozzle so as to target pests within its spraying range, the machine delivers short bursts of pesticide spray to exterminate them without subjecting non-infested parts of the plants to the chemical. A novel induction charging electrostatic spray nozzle capable of generating pulsed charged sprays was designed using COMSOL. Computer simulation of electric fields helped to identify the optimal induction electrode geometry needed. The fan spray nozzle housing was designed and fabricated using 3D printing. This nozzle is capable of producing short duration pulsed spray of a desired amount to cover the pests location without unwanted over spraying and soil contamination.

A mobile robot system was constructed from kits supplied by Lynxmotion™ and the computing system was arranged with a master-slave approach. The slave computer receives robot motion, nozzle positioning and spraying action commands from the master computer. The master computer sends a series of motion commands that move the attached camera in a search path that assists in locating a given type of pest. Once the targets to be exterminated have been selected by processing the received images from the CCD camera attached next to the spraying nozzle, the nozzle is put into the correct position and a burst of pesticide is applied. The master computer is a Windows-based notebook computer while the slave computer is an Arduino mega 2560 microcontroller board along with additional circuitries and hardware that assist in operating the smart nozzle system.

1.9. Organization of the thesis.

This thesis comprises seven chapters, and the content of each is described briefly below.

Chapter 2 contains a literature review of electrostatic crop spraying in agricultural applications. The review covers the history of the electrostatic phenomenon and its earlier applications in the field of industry. A comprehensive description of induction charging methods and their application between 1978 and 2013 is provided. The factors that cause spray drift and soil contamination are also discussed. In addition, the factors affecting nozzle efficiency and performance are covered. Finally in this chapter, there is an investigation into

the use of water sensitive paper in experiments relating to electrostatic spraying in agriculture.

Chapter 3 describes the theoretical background to agricultural electrostatic crop spraying. In addition, the types of charging methods used in electrostatic applications are explained, which include corona charging, conduction charging and induction charging. Next, experiments using induction charging with electrostatic spraying systems are carried out, and the results are reported so as to understand principles underpinning this form of spraying. Specifically, these experiments study the effect of using different levels of induction nozzle and air pressure as well as nozzle to target distances on the values of the electrostatic parameters. These parameters are the spray current, charge to mass ratio, value of deposition on the targets, coverage area on both surfaces (top and underside of leaves) of the target and the soil contamination level.

Chapter 4 focuses on the design of a suitable induction charging nozzle that can be used in the harsh weather of Iraq. That is, owing to the aforementioned high temperatures in the country of up 50 degrees Centigrade the selected nozzle has to produce an appropriate droplet size. Eventually, a small hydraulic fan spray nozzle was selected and converted into an induction charging hydraulic spray nozzle. The process of designing the new nozzle was dependent on the properties of the fan spray nozzle and on the simulation results of the COMSOL software used. Subsequently, SOLIDWORKS software and a 3D printer were used to build the novel smart induction nozzle. All of these processes and equipment are discussed in this chapter.

Chapter 5 presents the designing of the smart electrostatic system. All of the details regarding the assembling of the mini mobile robot are provided as well as those of the sensors attached to the robot for enabling the system to work. These sensors are responsible for controlling the robot's movement and setting the target nozzle distances. In addition, the training exercises for testing the ability of the electrostatic system to control an individual target and group of targets at different positions are explained, and the results obtained provided.

Chapter 6 describes the laboratory experiments conducted using the newly developed smart electrostatic system. These include the outcomes of experiments aimed at increasing of the depositing of pesticide on the target locations and reducing the amount of soil contaminants. The operating parameters, such as spray charge to mass ratio, spray burst duration, cone

angle of spray, and robot trajectory are investigated. It emerges that all of these desired objectives were achieved with the new smart electrostatic spraying system.

Chapter 7 presents a summary of all the main results of the study and suggestions for the future works are made.

1.10. List of Publications.

Conference papers:

1. Al-Mamury, Murtadha, Balachandran, Wamadeva, Al-Raweshidy, Hamed and Manivannan, Nadarajah" Designing Induction Nozzle for Controlling Cotton Insect in Iraq". The COMSOL Conference 2015 Grenoble. France.

2. **M Al-Mamury, N Manivannan**, H Al-Raweshidy and W Balachandran" Mobile robot based electrostatic spray system for controlling pests on cotton plants in Iraq". IOP Electrostatic 2015 International Conference, 12-16-April, Solent Southampton University, UK.

3. **Murtadha Al-Mamury**, Nadarajah Manivannan, Hamed Al-Raweshidy and Wamadeva Balachandran "Intelligent Electrostatic Induction Hydraulic Spray Nozzle for controlling Cotton Plant Insects ".12-16-April Solent Southampton University. IOP Electrostatic 2015.

4. **Al-Mamury, Murtadha**, Balachandran, Wamadeva, Al-Raweshidy, Hamed and Manivannan, Nadarajah. Computation Model of Electrostatic Spraying in Agriculture Industry" Excerpt from the Proceedings of the 2014 COMSOL Conference in Cambridge. UK.

5. **Murtadha Al-Mamury**, Wamadeva Balachandran, Hamed Al-Raweshidy and Nadarajah Manivannan. "Intelligent Electrostatic Crop spraying" ILASS – Europe 2014, 26th Annual Conference on Liquid Atomization and Spray Systems, Sep. 2014, Bremen, Germany.

6-**Murtadha Al-Mamury**, Wamadeva Balachandran and Hamed Al-Raweshidy "intelligent electrostatic crop spraying for controlling cotton worm *spodopetra littorals*.", ResCon , 2014, Brunel University, UK

7-**Murtadha Al-Mamury**, Wamadeva Balachandran and Hamed Al-Raweshidy" experimental study of electrostatic induction charging of spray nozzle", ResCon, 2013, Brunel University, UK.

CHAPTER TWO: REVIEW OF THE RELEVANT LITERATURE

2.1. Introduction

In this chapter, brief definitions of the electrostatic phenomenon and electrostatic spraying in agriculture applications are provided. Types of charging methods and classification of the articles published in induction charging in agriculture for the last thirty-five years are discussed. Furthermore, the factors affecting on nozzle efficiency and performance are considered. Finally, use of water sensitive paper to estimate the results of electrostatic spray in laboratory and field applications is discussed.

2.2. Background

In the 1600s, when the phenomenon of electrostatic force was discovered, the simple explanation assigned to it was the attraction forces between two objects having different values of electric potential. At that time, there was no notion how to apply it in practical applications, so nobody understood its usefulness. In fact, the first attempts at industrial applications did not happen for another three hundred years, and these were to do with the paint spraying of grounded objects in the 1950s.

The term electrospray, when the phenomenon of electrostatic force was discovered, the simple explanation assigned to it was the holds for doing so. The first is when the liquid becomes atomized by some mechanical or aerodynamic means, and then the droplets are charged, a process called Post Atomization Charging (PAC). It is widely used in industrial and commercial applications of which crop spraying is one example. The second method is when the charged droplets are produced by Electro Hydrodynamics Atomization (EHDA). This is caused by (EHD) related instabilities being produced at the surface of the liquid by an electric field. EHDA depends on liquid conductivity, which has resulted in the division of liquids into three categories: conductive, semi-conductive and insulating according to the charge relaxation time τ [6] Atomisation will occur based on conductivity σ and permittivity ε of the liquid as illustrated in the table [7]:

Table 2.1: Classification of liquids, Huneiti [7].

$\sigma < 18^{-8}\,Sm^{-1}$	$10^{-8} < \sigma < 10^{-4}\,Sm^{-1}$	$\sigma > 10^{-4}\,Sm^{-1}$
Insulating Liquids	Semiconducting Liquids	Conducting Liquids
• Long relaxation time, so charge carriers take a long time to reach the surface when an electric field is applied. • Cannot be sprayed by induction, due to lack of charge carriers. Charge injection necessary to atomize these liquids by EHDA. Example: Corn oil. $$\sigma = 5x10^{-11}Sm^{-1}$$ $$\tau = 4.8\ s$$ $$\varepsilon = 2.7$$	• Moderate relaxation time. • Relaxation time and droplet formation times are comparable. • Ideal for EHDA. • Stable jet obtained as a result of tangential stress and surface charge induced by the (radial) electrostatic field. Example: Ethylene glycol $$\sigma = 1x10^{-6}\,Sm^{-1}$$ $$\tau = 0.4\ ms$$ $$\varepsilon = 41$$	• Short relaxation time. • Charge relaxation time must be shorter than the droplet formation time. • Surface becomes an equipotential when subjected to an electric field. • Harder to attain EHDA. • Ideal for charging by induction. • Example: Tap water $$\sigma = 5x10^{-2}\,Sm^{-1}$$ $$\tau = 21ns$$ $$\varepsilon = 80$$

Electrospray is defined as the process of simultaneous droplet generation and charging, which happens when the electric force is stronger than the surface tension force. It consists of charged droplet generation, conveyance of particles to the target object and target deposition [8]. Liquid coming out from the nozzle at high pressure is subjected to an electric field, with this pressure causing elongation of the meniscus so as to form a jet spindle. This process allows for the generation of fine droplets of charge of magnitude close to one-half of the Rayleigh limit, which is the magnitude of charge on droplets that overcomes the surface tension force, thereby resulting in their fission [9]. The interactions that happen between charges on the surface of the liquid and the applied electric field give out two results: the first being the acceleration of the liquid and subsequent disruption into droplets, whilst the second is the build-up of the charges on the droplets [6].

Agricultural applications began after the success in the industrial field, with the first pertaining to the development of pesticide materials in powder form. Subsequently, electrostatic techniques were applied to liquid agricultural pesticides and herbicides, because

there are a number of benefits in using the electrostatic principle in spraying technology, which include: good distribution of droplets/particles, more uniform deposits on the surfaces of the intended targets as well as low or even no drift. Furthermore, pollination and biomaterial in agriculture have delivered satisfactory results through electrostatic application. However, the direct application of electrostatic paint spraying equipment in orchards is not feasible for three reasons, as explained [10].

1- The object in electrostatic painting to be coated is located relatively close to the paint gun (usually < 50 cm), which results in a significant increase in deposition efficiency on the object surface due to the high voltage applied to the gun. However, in orchard spraying the object to be coated is often much further away from the sprayer and hence, the technique is not effective.

2- In electrostatic painting, the process takes place in controlled environment with the conditions characterised as having minimum outside influences. But in the case of agricultural spraying, this takes place under a range of environmental conditions, such as temperature, relative humidity, wind velocity, and vibration, which can hinder spraying.

3- There are different skills requirements between operators working in the two different fields. Regarding electrostatic painting, the equipment is usually maintained by a full-time technician and the spraying is carried out by a skilled operator. While in the context of agriculture, pesticide spraying is only one of a number of operations that a farmer must carry out and thus, the equipment must be simple to operate, extremely robust, and reliable.

In general, electrostatic applications have been applied in several domains regardless of the percentage of the efficiency of this technique.

2.3. Classification of the literature review into three-time periods

In order to understand the developments that happened in the last quarter of the twentieth century regarding electrostatic spray application, this is classified into three stages, because each of those identified focuses on distinct aspects of how to advance this technology.

2.3.1. Papers published in period between 1978 and 1988

The first study during this period, conducted by Law, focused on designing an induction nozzle for producing fine droplets using a lower voltage when compared to corona charging. The latter method was used at that time in agricultural applications and needed voltages of

more than 20 kV. The induction nozzle design has good properties and can achieve high values in the applications. It provides a compact, cheaply fabricated droplet charging method and dependability has been greatly increased by the complete embedding of its electrode in order to prevent mechanical damage and personal hazard. The results of this early experiment were good as they fitted well with the design constraints imposed. The close spacing of the electrode to the droplet formation zone within the charging nozzle now permitted greatly reduced design requirements regarding size, output voltage and current drain of the power supplies necessary for operating an electrostatic – déposition system. It produced sprays of the desired size (such, as 30 to 50, µm volume median diameter) and created a 1.6×10^6 V/m charge-inducing field at the droplet formation zone with a corresponding -14 µC/m^2 surface charge density on the grounded liquid jet (i.e. a free electron surface density of approximately 108/mm^2). In addition, it could be used with low levels of high voltage supplies ranging from 0.85 to 1.0 kV [11].

Field experiments were conducted by Law on four types of plant: cabbage, broccoli, cotton and corn. Spherical shaped metal targets were fixed inside the rows of plants in order to determine the amount of the deposition on them. Two types of nozzles were used: an induction nozzle operated with and without electrostatic charging, and a conventional nozzle. The purpose of this study was to determine the increases in the amount of spray deposition attributable to electrostatics application and compare these Figures with those for the conventional one. The results obtained indicated that the charged versus uncharged deposition increase ranged from 1.8-fold to 7-fold. However, deposition-limiting conditions were encountered with certain plants at charge/mass levels as low as -1.6 mC/kg and charged versus conventional deposition benefits for these diverse plants ranged from 1.9 fold to 4.4 fold [12].

The applied levels of voltage and air pressure are factors influencing pesticide spraying efficiency, which were studied by Frost and Law, who wanted to determine their influence on nozzle performance. Four voltages were used, 0.5, 1.0, 2.0, and 3.0 kV, and six air pressure values ranging between 69 and 414 kN/m^2. The results showed that the charge to mass ratio increased with both increasing electrode voltage and increasing atomizing air pressure. By contrast, the charge to mass ratio decreased with both increasing the liquid flow rate and nozzle orifice diameter [13]. The relationship between the charge to mass ratio and liquid flow rate with nozzle orifice diameter was found to be inversely proportional in a study conducted by Inculetet *et al*. In this research, electrostatic and mechanical sprayers were

used in an apple orchard, 8 hectares in area, containing 2,000 trees. 1000 were allocated for experimenting using electrostatic assisted spraying, whilst the rest were assigned for testing with mechanical spraying, and the purpose was to compare the efficiency of the two in depositing pesticides. The results obtained illustrated that the deposition was markedly improved on the upper canopy of apple trees and more uniform distribution within the whole plant when compared with conventional (mechanical) application. In general, the results were classified into different tree parts. Regarding the upper canopies of the trees, this region received 85% more deposition of pesticide and approximately the same deposition was found on the lower canopies. Moreover, electrostatic assisted spraying yielded better uniform distribution of the pesticides within the whole tree. In fact, the total variation in deposition over the whole tree was within 3% for electrostatic spraying as compared with 49% for mechanical [14].

A comparative study between electrostatic induction and conventional spraying was conducted by Law and Lane. The first nozzle produced fine droplets of 25µm size VMD, and those for the second ranged in size from 150 to 200 µm. The experimental works was carried out in a laboratory, with the purpose being to investigate the effects of point presence on the target and the intensity that spray-droplet charging has upon the mass transfer of spray liquid by droplet deposition onto the target and the charge transfer to the target system as partitioned into point discharge and droplet deposition current. The results obtained illustrate that **1)** The number of charged droplets onto smooth metal increased seven-fold for spherical, and planar targets compared with uncharged spray; 2) Electrostatic spraying deposition onto a vertical planar target increased 24 fold compared with a conventional hydraulic-atomizing nozzle; and 3) Spray deposition onto the sides of a vertically oriented planar target was typically at least 80 percent more than onto the planar target in its horizontal orientation. Figure 2.1 shows the trend in the surface charge to mass ratio magnitude versus spray cloud current for spherical targets [15].
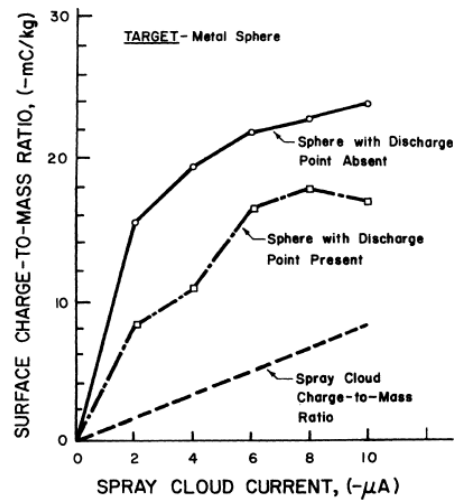
Figure 2.1: The relationship between the charge to mass ratio values versus spray cloud current for spherical targets, Law and Lane [15].

To overcome the major problems with induction charging of spray from a hydraulic nozzle and so be able to design a workable system, a study was conducted by Merchant and Green. A small flat fan nozzle tip was used and connected to a high voltage supply with a range of 0-10KV. The purpose of this experiment was to investigate how to overcome the major obstacles in induction charging spraying using a hydraulic nozzle and consequently, understanding how a workable system could be designed. The results obtained can be summarised as follows: The maximum charge to mass ratio achieved was 2 mC/kg at a nozzle voltage of 9 kV. Charging increased the uniformity of deposit on cylindrical artificial targets by providing underside deposits and increasing those on the sides of the targets. In addition, charging increased the total deposit on the artificial targets by a factor of 1.6 to 2.8 at a nozzle speed of 2 m/s and an operating voltage of 6 kV. Also, the droplet sizes exhibited differences between the charged and uncharged systems. Regarding which, it can be seen that the volume contained in drops above 250 μm diameter is less in the charged case (an average of 1.5 % of the total) than in the uncharged case (an average of 7.2 % of the total). Figure 2.2 shows the distribution of spray volume by drop diameter [16].
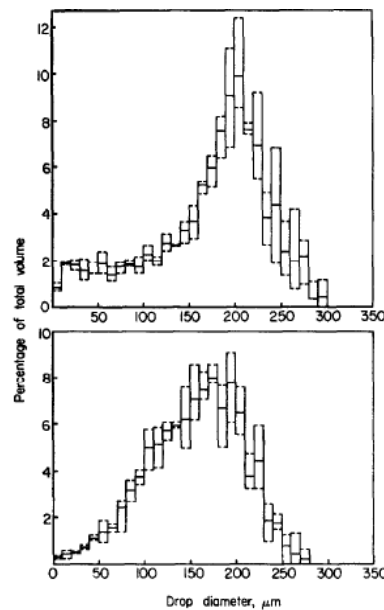
Figure 2.2: Distribution of spray volume by drop diameter: uncharged spray (top); and charged spray (bottom). Solid lines represent mean values, whilst broken lines show the maximum and minimum values measured Merchant and Green [16].

Image and space charge forces play a very important role in enhancing the deposition of liquid on the target. The former is limited to when the droplet is a negligible distance from the target while the latter relates to driving the charged droplets over greater distances within the plant canopy. These two forces become evident when the electrostatic forces predominate over mechanical forces like drag and gravity. Several experiments were conducted in the field and laboratories in order to measure both of these values. One of these is a study carried out on orchard trees conducted by Castle and Inculet using an electrostatic spray system developed at the University of Western Ontario. It uses a number of air shear nozzles which, when exposed to air velocities in the order of 300 km/h, atomize the liquid pesticides into a very dense fine spray (MMD of 80 μm). The electrode is embedded flush with the surface and is energised from an 18 kV high-voltage power supply connected to a tractor's battery. The main purpose of this study was to present a way of applying electric space charge theory to liquid droplets and to show some experimental results that demonstrated improved deposition. The results obtained are summarised [10]:

1) Image forces have a negligible effect on pesticide deposition;

2) Since the drag force predominates in high-velocity regions, the space charge forces will have a negligible effect and hence, the mechanical depositions will predominate;

3) When the space charge forces are larger than both the gravitational and drag forces, enhanced deposition should be expected due to electrostatic forces;

4) There is no significant effect between the electrostatic and mechanical forces on the deposition on the lower parts of the tree. Electrostatic forces provide more than 85% of pesticides deposition on the upper part of the plant compared to the condition when no electrostatic forces are applied;

5) Space charge improves the uniformity of deposition on the tree. For example, the ratio of residue in the upper and lower part of the plant is 0.95 with charging while the same ratio without charging is 0.51;

6). Space charge law effectiveness was observed in several field testing's and, in general, there is agreement between the analytical results and experimental deposition. Table 2.2 shown [10] provides the results of the above experiments.

Table 2.2: Force ratios for particle diameters 50 several field testing's and, in general, there is agreement between the analytical, Castle and Inculet [10].

Electrostatic Forces	Droplet Diameter	Position A		Position B	
		Fe / Fg	Fe/ Fd	Fe / Fg	Fe / Fd
Image force	50μm	0.15	0.0001	0.15	0.01
	100 μm	0.3	0.001	0.3	0.1
Space charge force	50 μm	6	0.006	60	5.5
	100 μm	3	0.01	30	11
Space charge induction force	50 μm	12	0.012	120	11
	100 μm	6	0.01	60	22

The meanings of Fe , Fg and Ed are Electrostatic force, Gravitational force and Drag force, respectively.

The nozzle designed by Law in 1978 was used and tested again by Law in two places. The first was in a field cultivated with crops and vegetation, including, crop rows, planar turf grass type crops and orchard trees. The other one was executed in a laboratory on different metallic shaped targets, including spherical and planar forms, with vertical and horizontal orientations. The aim was to provide an overview of research and development efforts directed towards the incorporation of electrostatic forces for increasing mass transfer efficiency of the basic droplet-deposition process inherent in the application of agricultural pesticides to living plant systems. The results obtained from this study indicated that the deposition efficiency of an induction nozzle increased from two to seven-fold for the various

models and biological targets, as compared to similar uncharged sprays and conventionally applied ones. Table 2.3 indicates the superiority of induction charged spraying over the conventional one in terms of deposition efficiency [8].

Table 2.3: Relative increases in spray deposition onto various agronomic plants and model targets as a result of electrostatic spray application, Law [8].

Type Target	Application Comparison	
	Charged Versus Uncharged	Charged Versus Conventional
Cabbage heads	7.0**	2.9
Broccoli plant	1.8**	1.9**
Cotton plants	2.5**	N/A
Corn plants	2.0**	4.4**
Smooth metal sphere	7.0**	7.8**
Metal sphere with point	3.5**	3.5**
Horizontal metal plate	2.5**	1.6**
Vertical metal plate	3.0**	24.0**

*Significant difference ($p < 0.01$)

On a grass strip in a field, the induction charging nozzle type ConJet Boom and a conventional one were used in experiments conducted in a study by Inculet *et al*. This had two aims: 1- finding a sufficiently large charge to mass ratio to develop the necessary electrical attraction forces; 2 - atomization of the liquid into small enough particles for the electrostatic force to be effective, yet large enough for the droplets not to evaporate or be easily entrained by winds. The results demonstrated that the induction charging nozzle improved coverage of the vegetation (up to 40% increase over conventional mechanical spraying using the same mechanical sprayer without charging the droplets). The development and experimental work carried out in this project showed that with relatively simple modifications to a standard unrefined crop sprayer a substantial increase in the efficiency of deposition can be achieved and hence, reduce environmental drift [17].

In an experimental work on the barley plant, three types of nozzles that formed different droplet sizes were used by Lake and Marchant. The variables investigated were nozzle size, nozzle height, charge and wind speed. In addition to these, vertical and horizontal targets

were distributed within the plant rows. The purpose of this study was to measure the effect of charged spray from a hydraulic nozzle on deposition on targets between the rows of the plant. The results obtained indicated that the charging increased the deposition on the vertical targets and tended to decrease it on horizontal ones. In the wind, the upper surface of the horizontal target showed no effect of electrostatic charging on spray deposits. The wind tended to increase the deposits from uncharged spray on the vertical target, whilst decreasing those from charged spray. Additionally, the model developed was used to explain some of the unexplained effects, for example, those related to nozzle orifice size and wind. Figure 2.3 shows the relationship between the deposition on the target and nozzle size, nozzle target and nozzle type [18].
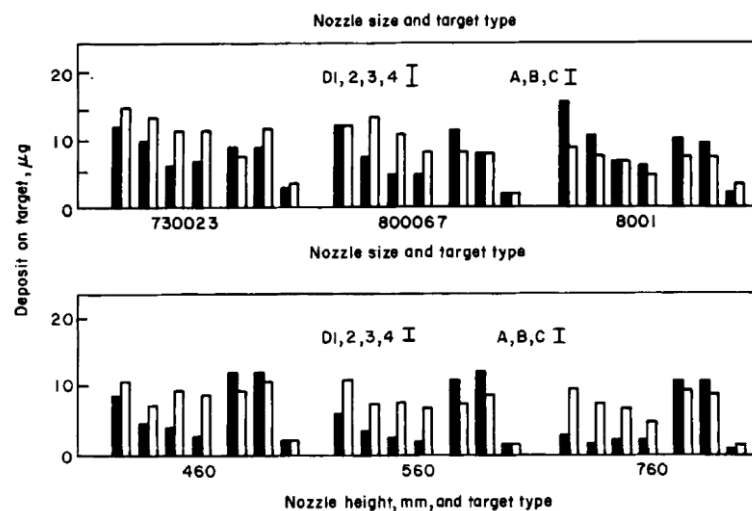
Figure 2.3: The relationship between the deposition on the target and nozzle size, nozzle target and nozzle type. The letters A, B, and C represent horizontal targets, whilst D1,2,3 and 4 represent the vertical targets and black column bar, white colum bar represent charged and uncharged sprays, respectively, Lake and Marchant [18].

In the theoretical field, development of a model for enhancing space charge deposition of airborne particulates within an electrostatically shielded target system has been studied by Law and Bowen. The purpose of this study was to present a theoretical basis of the new concept of electroporation of airborne particulates and the four principles for the charged particles involved are listed below:

1) The electric mobility of an airborne particle charged by the ionised field process is a linear function of the particle radius;

2) The resultant space-charge field that exists within a target region is due to the superposition of the fields generated by all species of charged airborne particles within that region;

3) The charge to mass ratio varies inversely with the radius for particles charged by the ionised field process;

4) The fraction of saturation charge which a particle attains in the ionised field charging process is independent of particle radius. In general, dual particle-specie offers further benefit to the management of the total space–charge external to the target as a means of lessening the present limitation on the overall electrostatic deposition process caused by the induced corona at the earth points and edges on the target boundary [19].

In order to evaluate experimentally the contribution of electrostatic forces in improving the depositional characteristic of fine droplets carried in high-velocity air streams and to document the beneficial effects, a comparative study was conducted by Law and Cooper. Two types of nozzles were used, one with small droplets with a size of 30 μm (VMD) and the other big droplets, sized 370 μm (VMD). The results obtained revealed that the former did not reach the magnitude of that observed during conventional spraying by the latter. Moreover, when managing finely divided droplets in the 20 to 40μm range, the electrostatic force increased deposition by 1.5 to 2.9 fold when compared to conventional spraying. Additionally, electrostatic wrap around benefits were observed at radial distances as close as 2.5 m, where the air carrier velocity averaged above 15 m/s as far away as 8 m [20].

A comparative study between two mathematical models of the transport of charged spray that were put forward by Lake and Marchant and Dix and Marchant was conducted by Hadfield. Specifically, this paper compared the results from these two models by measuring charged spray deposits in well-defined conditions and their relationship with droplet size. The findings showed that Dix and Marchant's model gave closer agreement to the measured results than that of Lake and Marchant and consequently, the variation in charge and droplet size has an important impact on constructing a correction model of deposition distribution. Figure 2.4 illustrates the effect of droplet size on the charge to mass ratio [21].
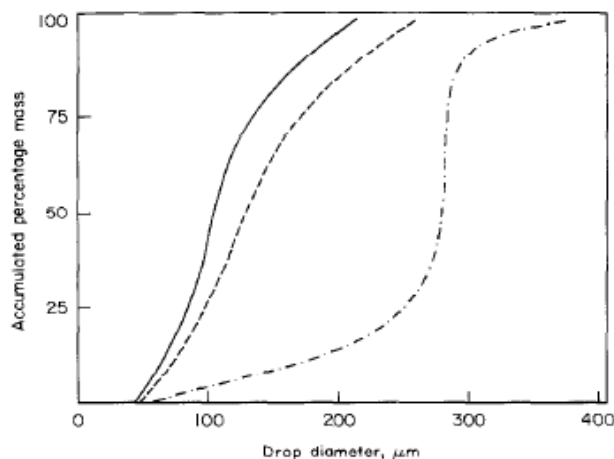
Figure 2.4: The relationship between the droplet sizes and accumulated percentage mass measured. Drop size spectra: ____, 4000 rev/min; - - -, 3000 rev/min; - . - , 2000 rev/min, Hadfield [21].

An embedded electrode electrostatic spray nozzle was used on a field planted with barley by Law *et al* , being operated at 172 kPa (25 psi) to atomize the pesticide liquid to 40 μm (VMD). The purpose of the experiments was to determine the spatial distribution of the droplet mass and charge transfer characterising these various modes of electrostatic cereal-crop spraying. The results obtained from this study can be summarised as follows: The values of droplet charging ranged between 1.5 and 4.5 mC/kg, which resulted in increased spray deposition onto all plant surfaces within the cereal crop tested. Additionally, these increases were from 5.5fold for the top halves of the barley leaves, to 2.5 fold for their base halves and to 1.5 fold on the lower growing broadleaf weeds. Finally, approximately 10 fold and 34 fold greater charges were collected by the barley plant as compared with a weed and the underlying soil, respectively, as shown in Figure 2.5 [22].
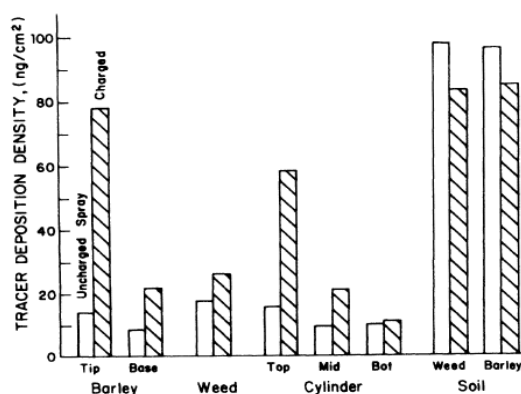
Figure 2.5: Average charged versus uncharged spray deposition achieved at stated locations throughout a barley-weed-soil target system, Law *et al* [22].

In another study, experiments using the flat fan hydraulic spray type Teejet 800 were conducted by Marchant and Wilson. The nozzle was operated with two levels of air pressure values, 200 and 600 kPa, to atomize the water flow rate into fine droplets and the power supply that was connected to the nozzle provided a high voltage in the range of 1 to 6 kV. The purpose of this study was to predict the properties of a liquid sheet emerging from a flat fan hydraulic spray nozzle and to produce a formula for the charge to mass ratio of the spray. The results indicated that both the original and the modified equations predicted that charge to mass ratio increases with greater charging voltage and nozzle angle but reduces with an increase in the nozzle orifice area and the electrode spacing. So whilst the original equation predicted that the effect of increasing pressure reduces the charge to mass ratio, the modified equation predicted that the effect depends on the nominal spray angle. Furthermore, the charge to mass ratio was predicted to increase with increasing pressure for brass nozzles having angles of less than 66^{0} and to decrease for larger angles. In addition to these outcomes, the equation predicted that the charge to mass ratio was considered reasonably acceptable up to an operating voltage of 2 kV [23].

In laboratory experiments, an induction nozzle and metal–spherical target with and without a point were used in a study by Law and Cooper. The nozzle was connected to a 700V electric power source to charge the spray and operated at 138 kPa to give 30 µm droplets a study by considered reasonably was to document space charge field losses caused by induced target coronas and to establish any polarity–dependent advantage that could be exploited for improving electrostatic crop spraying. The results indicated that the masses of the charged deposition for an ionised target were 1.5 and 1.8 fold for the positive and negative sprays, respectively and four-fold for a non-ionized target regardless of spray polarity. In general, target deposition values with negative spray treatments were 410 ng/cm^2 and 180 ng/cm^2 for target-points-absent and target-points-present, respectively, while the positive spray treatments values were 393ng/cm^2 and 150 ng/cm^2. The table 2.4 has been given general for the significant value [24].

Table 2.4: shows peak interior electric fields during transient spray trials onto a parallel-plate target, Law and Cooper [24].

Point Condition	Spray-Cloud Current (-µA)		
	1	2	3
Absent	54.6	62.1	53.4
Interior	53.4	61.6	58.6
Exterior	53.4	52.5[a]	46.8[a]

*Significant difference for point-absent treatment mean of the same spray cloud current ($p < 0.05$).

Three types of nozzles made of brass "Teejet type 800067" (Spraying Systems Co., Wheaton, Illinois) with artificial targets consisting of vertical columns of horizontal discs were used by Lake in his work. These nozzles were operated at air pressure of 300 kPa to produce 212 µm (VMD) droplets and were connected to high power supply of 5 kV. The purpose of the study was to measure the deposits from electrostatically charged hydraulic nozzles on the vertical columns of horizontal discs. A summary of the results is that: 1- disc spacing had only a small effect on the target deposits. 2- With no wind, total target deposits with charged spray increased with greater target spacing, but there was no such effect with uncharged spray. 3- The effect of wind was generally a decrease in target deposits with the charged spray. 4- Deposits on the underside of discs were low with both charged and uncharged spray under all conditions (see Figure 2.6) [25].
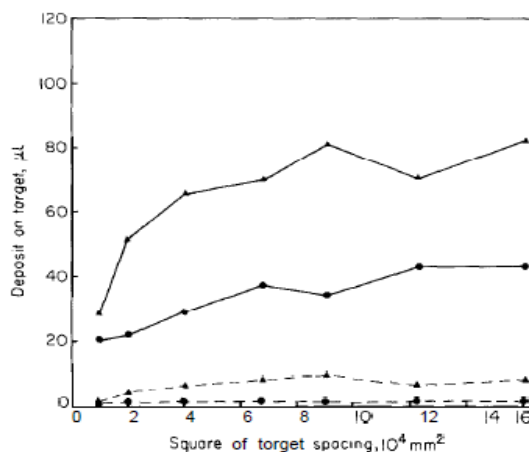
Figure 2.6: The effect of target spacing in wind: ▲——▲ Charged spray, upper disc surfaces; ●——●
uncharged spray, upper disc surfaces; ▲――▲ charged spray, lower disc surfaces; ●――● ;
uncharged spray, lower disc surfaces, Lake [25].

2.3.1.1. Conclusion to the first period

This time period can be characterised in terms of two important objectives. The first was increasing the amount and value of deposition on the surfaces of the intended targets, which included both the front and back surfaces. The second objective was comparing the efficiency of the pesticide application methods of novel systems using electrostatic spraying with the conventional or classic system. The reason for this comparative work was to encourage workers in the agricultural field to use electrostatic spraying because it was more efficient. Some mathematical formulae and predictive equations were tested during these projects, such as in studies by Inculet [17] and Hadfield [21]. The aim regarding these was to reduce the amount of pesticide waste by controlling the droplet size distribution and decreasing the level of drift.

2.3.2. Papers published in the period between 1989 and 2000

An electrostatic sprayer equipped with a pneumatic atomizing mechanism and induction charging of liquid film was developed by Bologa and Makalsky. The aim of this study was to investigate the influence of the interaction of high-speed air flow with liquid film and to find out how the electric field distribution in the nozzle affects the efficiency of the electrostatic sprayer. The results showed that intensification of the turbulent interaction of the airflow with the liquid film in the initial zone of its formation in the electric field made it possible to change the size of droplets and to increase the spray cloud current. Moreover, the values of

the charge to mass ratio exceeded 6 to 8 times the corresponding values for existing electrostatic sprayers and Figure 2.7 illustrates this interaction [26].
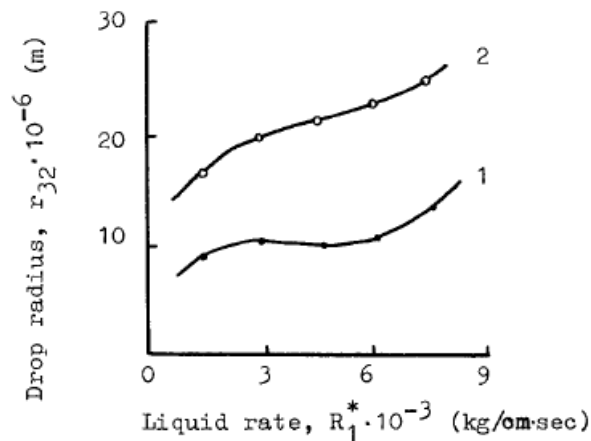
Figure 2.7: The dependence of the aerosol drop radius on liquid rate from a unit of the nozzle edge length of the sprayer in the presence (1) and in the absence (2) of a turbulent spraying of liquid, Bologa and Makalsky [26].

In aerial work, two nozzles were used by Inculet and Fischer when they developed a novel system that consisted of generating two coplanar clouds of insecticides. One formed the port side wing and the other the starboard side. The first type was the spraying system nozzle SS-11004 negatively charged with liquid insecticide while under the strong positive electric field of an induction electrode I E (+). The second type was an SS-110015 charged positively by an induction electrode I E (-), which was connected to a 36 kV supply. The results obtained indicated that the electrically charged spray influences the spray deposition and the effects become more pronounced especially with fine droplets, but it could also enhance deposition (recovery) under arid conditions. Additionally, it emerged that charging coarse spray electrostatically does not influence spray deposition significantly [27].

In order to determine theoretically the feasibility and experimentally to confirm the practicality of focused or target–selective deposition of agricultural sprays, an induction nozzle with a copper sphere (row target) of 75 cm diameter was used in laboratory tests conducted by Giles. Polyethylene film with a thickness of 0.1mm and a dielectric constant of 2.3 was use underneath earthed targets. The results of the study indicate that passive manipulation by increasing the air–gap spacing between the dielectric film and the underlying earthed planar boundaries that ranged from 0 to 4cm significantly increases lower hemisphere spray deposition, whilst decreasing film deposition. While the active manipulation of the film

4 cm above the earthed plane by recharging it to a surface charge density of 15 $\mu C/m^2$ resulted in greatly increased target and decreased film deposition. Additionally, electrical charging of aerodynamically–delivered spray droplets, in combination with the lifting and recharging of the dielectric film, resulted in an 84% to 16% ratio of target sphere to non-target film deposition compared to a corresponding 44% to 56% ratio for uncharged spray deposition along a 31cm section of one sphere and the adjacent film of the test row [28].

An electrostatic induction handgun sprayer with two embedded-electrodes charging and a conventional spray with high volume application were used by Law *et al*. This was tested in laboratory experiments as well as on rows of strawberry plants in a greenhouse. The aim was to evaluate several recent air-assisted electrostatic crop-sprayer machines incorporating this specific type of pesticide spray-charging capability. A second aim was to compare the laboratory and field-test outcomes to establish whether the deposition efficiency and insect control efficacy could be attributed to this reduced–volume aerodynamic-electrostatic application technology. The findings obtained from this study suggested that the air-assisted charged sprayer deposited significantly more insecticide onto plant foliage than the high volume conventional spray method. These values were 1.29 $\mu g/cm^2$ and 0.35 $\mu g/cm^2$, giving a 3.7 fold electrode position benefit. Finally, the results of the air–assisted charged sprayer showed that it was appropriate for penetrating charge conductive pesticide to inner plant regions and electrostatically depositing droplets onto leaf undersides through its space charge field [29].

An electrostatic induction twin nozzle especially constructed for generating fine droplets of pesticides with a metal plant model was used by Machowski and Balachandran in a greenhouse**.** The nozzle was operated at air pressure ranges of 0.3 - 0.8 MPa to atomize 0.5 L min^{-1} of solution into fine droplets and the high voltage connected to the nozzle was 2.5 kV. The aim of this research was to design and construct an induction charging electrode arrangement in an electrostatic spraying nozzle for greenhouse application. Laplace's equation, with the finite element software ALGOR, was used to solve the modelling calculation of the field distribution in the vicinity of the nozzle. The results obtained indicated that the reverse field modelling technique can be used successfully to optimise an induction electrode arrangement for twin fluid nozzles with respect to the charging efficiency of spray droplets. Moreover, the level of measured charge to mass ratio increases proportionally to the applied voltage. As a result, significant improvement of deposition

efficiency on the underside of leaves was seen when high potential was applied to the charging electrode (see Figure 2.8) [30].
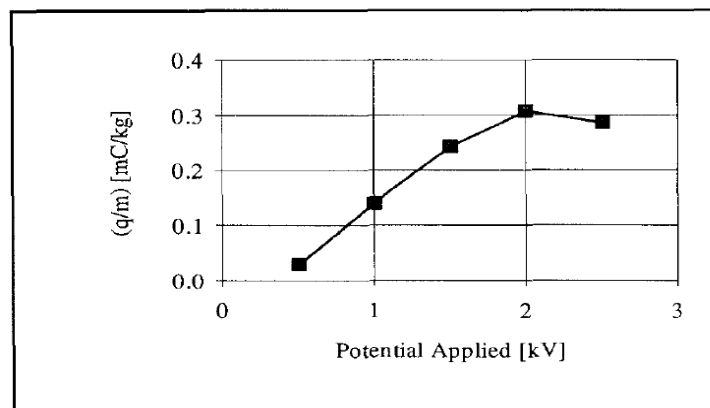
Figure 2.8: Charge to Mass ratio (q/m) of the spray generated by a "TL" fog generator, Machowski and Balachandran [30].

In the experimental field, a study that included several operating conditions was conducted by Law *et al*. The nozzle operated at an air pressure of 207 kPa (30 psi) to atomize the water flow rate of 73mL/min into fine charged droplets of 20-50 μm connected to as connected to a high power supply ranging from 1-3 kV and a Faraday cage was used to collect the charged spray from different distances between 0 and 50 cm so that the current of droplets could be measured. The purpose of this study was to present as a function of the degree of bounding of the charge spray–cloud, the experimentally observed effect being hypothesised as space charge suppression of induction spray charging. The results regarding the charge conditions demonstrated that the capability to charge electrically conductive spray by an electrostatic induction nozzle linearly diminishes by 41% from a -7.3 mC/kg value of charge to mass one of -4.3 mC/kg. In addition to this, the countering space-charge effect of the dispensed negative spray cloud is attributed to being the cause of this reduced effectiveness in the induction charge-transfer process at the earthed droplet-formation liquid jet within the dielectric nozzle body [31].

Jahannama *et al* used an air-assisted induction charging nozzle type, namely a MaxCharge, based on the original design of Law from 1978. However, the material of this nozzle is different to that of Law ranging from 1-3 kV and a Faraday cage was used to collect the charge influence of the charging electrode on the primary atomization zone. The theoretical program employed in the study was the VOF model, which was used to simulate two phases, air and water. In addition, the FLUENT CFD package was used to give an account of the mixing and atomizing process inside the nozzle. The aim was to compare the performance of

this nozzle with the Law's original. The results obtained indicate that the droplet size distributions of horizontal sprays showed a significant difference between the charged and uncharged cases, whereas there was no remarkable difference between the vertical ones. Moreover, the computational results confirmed that the creation of a vortex and negative pressure field in the middle part of the nozzle plays a significant role during the mixing of the fluids and the liquid atomization processes. Figures 2.9 shows droplet size distributions for charged and uncharged sprays in the horizontal situation [32].
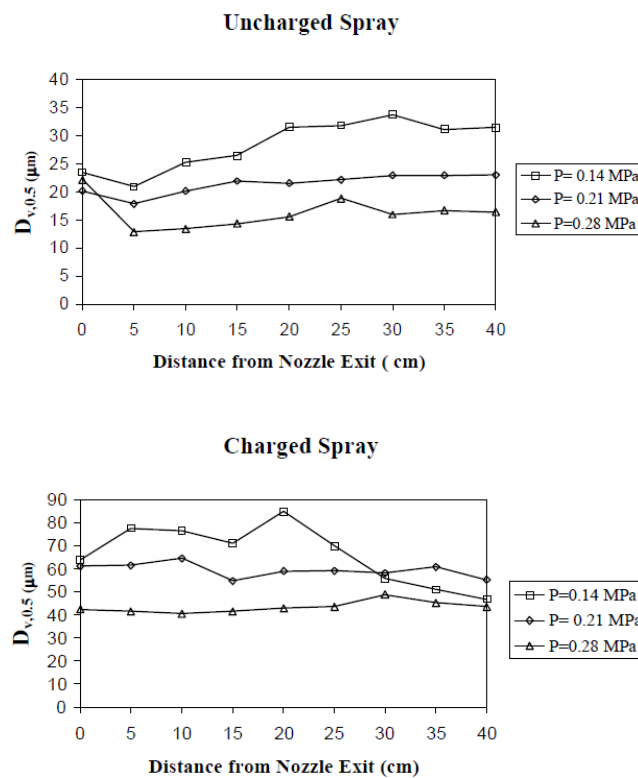
Figures 2.9: Droplet size distributions for charged and uncharged sprays in a horizontal situation, Jahannama *et al* [32].

2.3.2.1 Conclusion of the second period

In this period, the studies concentrated on new aspects of the electrostatic spray phenomenon. In particular, the focus was no nozzle technique, which led to new nozzle designs that improved deposition and nozzle efficiency. The first concern was regarding how to develop a suitable nozzle for crop spraying, that is, one the increased the amount of deposition on the intended targets and to this end, researchers conducted experiments using different geometry of nozzles. The second concern was to explain the nature of the interaction inside the nozzle between the air pressure and the liquid as well as to study the interaction involved in

changing the sizes of charged droplets and the amount of the deposition. Finally, all of these nozzle experiments aimed to increase the amount of deposition on both surfaces of the targets.

2.3.3. Papers published in the period between 2001 and 2013

The first study in this period involved experimental and theoretical work conducted by Cook and Law. The induction nozzle designed by Law in 1978 was used in the experimentation, with the purpose being to investigate and explain why the performance of a dielectric embedded-electrode induction spray charging nozzle is affected by the charged cloud of droplets it generates. Poisson's equation was solved using a COMSOL finite element axisymmetric model consisting of 3,704 triangular elements and 1,946 nodes for various placements of nearby earthed surfaces. The results obtained from this study showed that [33]:

1) The potential due to the presence of the negatively charged cloud issuing from an electrostatic induction spray charging nozzle can become substantially larger in magnitude than the positive electrode potential within the dielectric charging nozzle;

2) A grounded Faraday cage placed axially downstream in the cloud effectively suppresses the potential produced by the charged cloud by limiting its size and hence, negatively affects the nozzle performance as well as the location of the grounded boundary.

Figure 2.10 shows the distribution of potential and voltage obtained with and without space charge.
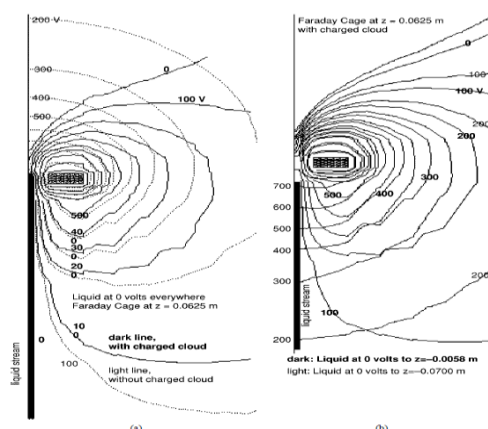
Figure 2.10: (a) Potential, volts, without and with a space charge with the liquid grounded everywhere. (b) Potential, volts, with a space charge and with the liquid grounded at various locations (0–1000 V shown), Robert and Law [33].

An electrostatic pressure swirl nozzle with a brass ring electrode was used by Laryea and Young No on orchard trees and the experiments were conducted under charged and uncharged conditions. The aim of this study was to develop a suitable electrostatic nozzle for an orchard sprayer. The results showed that the droplet size exhibits an increase in the VMD as the applied voltages are increased and decreases when the operating pressure is increased (Figures 2.11 and 2.12 illustrate such effects). Moreover, the spray width increases as the axial distance is increased, but the applied voltages have no effect on this width and this could affect the spray trajectory. In addition, under all conditions, the charged spray shows an increase in spray deposit and drift reduction as compared to the uncharged spray [34].
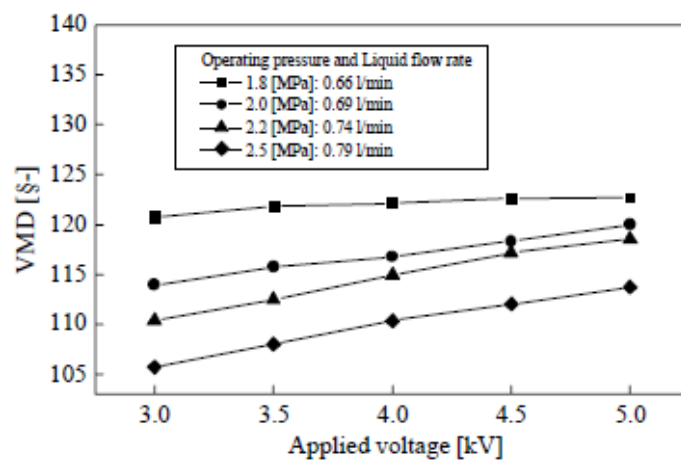
Figure 2.11: The effect of applied voltage on volume median diameter, Laryea and No [34].
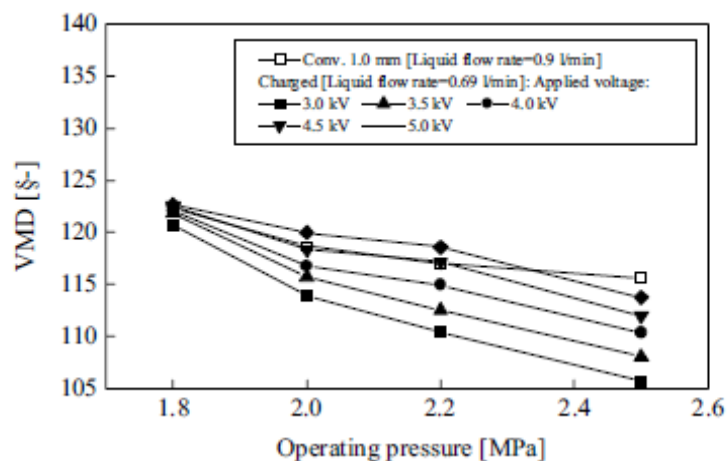
Figure2.12: The effect of operating parameters on volume median diameter, Laryea and No [34].

A comparison study between conduction and induction charging in liquid spraying was carried out by Zhao *et al* [35]. The aim was to clarify that the differences that pertain to the charging mechanism, electric field distribution, energy conversion and the effect of space

charge theoretically and experimentally for three-electrode conduction and induction charging management. The results obtained explained that the three-electrode spraying system, conduction and induction charging differ both in the source of charge and electric field distribution. Furthermore, the target current in induction charging depends only upon the space charge field, which causes a larger electrode current and surface discharge at a lower voltage. For the three-electrode geometry, conduction charging produces larger current and smaller electrode leakage current when compared to induction charging. In addition, as the nozzle-to-target distance increases, the space charge effect increases and the target current decreases (see Figure 2.13)[35].
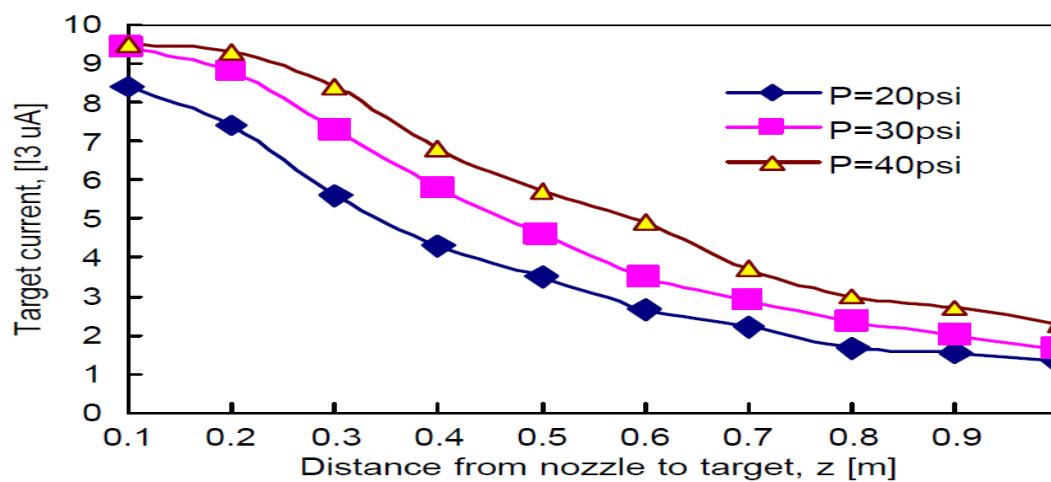
Figure 2.13: Relationship between target current and distance to target when U ism, electric field distribution, Zhao *et al* [35].

In a theoretical study, Zhao used FLUENT software to model the charged droplet trajectories towards a spherical target for different droplet sizes, charge to mass ratios and nozzle-to-target distances. The purpose of this simulation was to determine the conditions for maximum deposition, while reducing the drift of charged droplets to nearby ground in the electrostatic pesticide spraying process for uniform sized droplet sprays. The results obtained indicate that an increase in the charge to mass ratio increases the deposition significantly, while the radial drift may also increase. Moreover, the droplet size, charge to mass ratio and nozzle-to-target distance need to be carefully selected in order to achieve the best results [36].

Two types of spray nozzles, electrostatic and conventional, were implemented to control the sweet potato whitefly (SWF) pests of cotton in the UK in experimentation work undertaken by Latheef *et a* [37].The first spray system assembled was the electrostatic spray boom, which included a large number (82) of spray charging nozzles that were necessary to

accomplish a spray rate of 4.68 l/ha. These were operated at an air pressure of 482.7 kPa so as to atomize a flow rate 225 ml/min of pesticide into fine droplets and they were connected to a high-voltage supply with an output that ranged from 1 to 13 kV. The second type of nozzle in a boom set-up was the conventional spray applicator, which was attached to provide an application rate of 46.8 Lha^{-1} at 193.1 kPa. Four treatment applications were carried out, three with electrostatic spray, two charged and the third without, whilst the last involved conventional spraying. There were two main aims, with the first being to determine whether electrostatic charged sprays could be effectively used to achieve season-long control of whiteflies using pest control materials of diverse chemistries. The second aim was to ascertain whether the low spray rate (4.68 L/ha) required by the current prototype electrostatic spray charging nozzles would favor the development of resistance in whiteflies to mixtures of insecticides compared with conventional spray applications at 46.8 /ha. The results obtained can be summarised as follows: 1) the potential exists for obtaining increased efficacy against whiteflies using an electrostatic spray charging system. 2) Electrostatic treatments are as good as conventional ones and the amount of water used is 10 times less. 3) counts of whitefly adults in electrostatic charged spray treatments are comparable with those regarding conventional sprays. However, counts of dead adults in electrostatic treatments are greater than those under conventional means after spraying with insecticides [37].

Maynaghet *et al* conducted a series of laboratory experiments using an electrostatic sprayer with an ultrasonic nozzle. The operational condition for these experiments included the following factors: two nozzle charging electrodes of radii 10 and 15 millimeters, which were connected to four levels of high voltage supply: 1.5, 3.0, 5.0 and 7 kV, in sequence. Furthermore, six levels of air flow speeds of 14, 14.9, 17, 20.2, 21.6 and 22.0 m/s were used to atomize three levels of water flow rates, which were 5, 12 and 25 ms^{-1}. Finally, four levels of horizontal distances between the electrode and nozzle tip of 1.5, 6, 10 and 15 millimeters, respectively, were deployed. The aim of this study was to evaluate and quantify the charging of the droplets created by an electrostatic sprayer with an ultrasonic nozzle. The results obtained show that while increasing the liquid flow rate, the charged spray current increased at first then started dropping (Figure 2.14) and the reason for this relates to ionisation. In addition, increasing the electrode distances caused increases in the amount of the spray current (see Figure 2.15). Finally, the optimum combination of independent parameters was found to be as follows [38]:

Flow rate = 5 ml/min, high voltage = 3 kV,   12100 (rpm) 20.2 (ms^{-1}) radius of electrode = 15 mm and horizontal distance = 10 mm
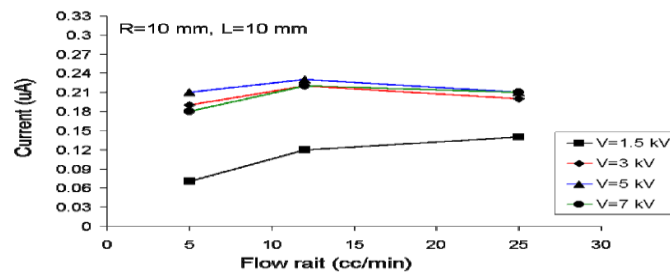
Figure 2.14: The effect of liquid flow rate on the target current, Maynagh *et al* [38].
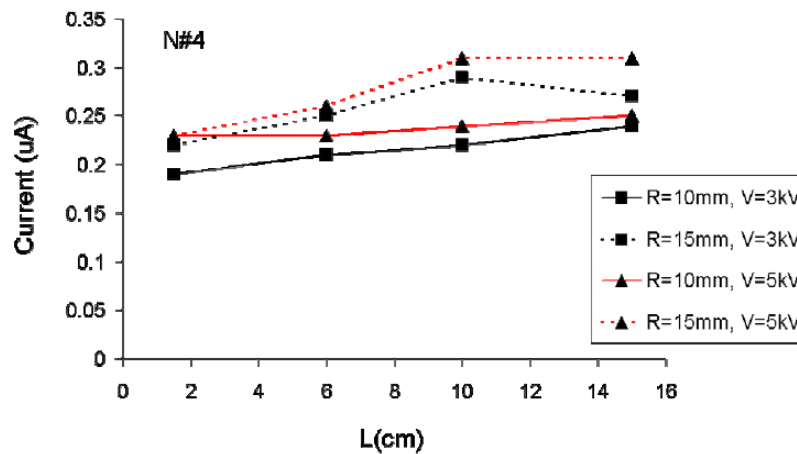
Figure 2.15: The effect of electrode distance on the current value Maynagh *et al* [38].

Nader *et al* investigated the dynamics of induction charging for spherical particles assuming finite volume and surface conductivities by using mathematical and simulation models. The purpose of this study was to illustrate a simulation model for investigating the induction charging of spherical particles with finite surface conductivity. In addition, the aim was to investigate the effect of volume conductivity on the surface layer, surface layer thickness and particle permittivity. The results showed that an increase in the contact area between the particle and the electrode significantly shortens the charging time. Charge accumulation on the particle's surface was fastest for a hemisphere having the largest contact area and slowest for a particle with a point contact. It was demonstrated that even for a short relaxation time constant, the actual charging time constant can be significantly larger, if the contact area is large, due to high contact resistance. Assuming a small finite contact area with the grounded electrode, fixed permittivity and bulk conductivity, the conductivity for the surface area was

varied. The results of these simulations show that when conductivity of the surface layer increases, charge accumulation on the particle's surface is faster. For fixed values of the conductivities, increasing the particle's permittivity results in slightly faster charging. However, the effect of increasing the permittivity is negligible when compared to the effect conductivity [39].

In lab experiments, an air-assisted electrostatic induction charging spray- (AEISC) system was investigated by Maski and Durairaj. It operated with higher and lower flow rates depending on nozzle condition. When the jet diameter was 0.35mm, it provided 30, 45, and 60 ml/min, which represented the lower water flow rate. The high water flow rates used were 250, 450 and 600 ml/min when the nozzle jet diameter was 1.0 mm. The nozzle electrode was connected to a high-voltage supply with an output that ranged from 3kV to 4 kV for charging the spray liquid. A Faraday pail was used to collect the droplets generated and to measure the chargeability in order to calculate the charge to mass ratio. The objective of this study was to investigate the spray chargeability of an air-assisted electrostatic induction charging spray with due consideration to the effects of electrode voltage, spray liquid flow rate and liquid properties. The results indicated that increasing the electrode voltage between 3 and 4 kV and decreasing liquid flow rates to 30 ml/min maximizes spray chargeability to about 18.5 mC/kg for ground water and 7.5 mC/kg for tank water sprays. The rate of increasing spray chargeability with decreasing liquid flow rate was higher in the lower flow rates than at the higher ones of 250, 450, and 600 ml/ min. The reason for this was attributed to the larger surface area of finely atomized spray-droplets exposed to the applied electric field strength. In general, this means that the charge to mass ratio increases as spray flow rate decreases and its response is non-linear with flow rates in the two distinct ranges mentioned above. Figure 2.16 shows the relationship between the charge to mass ratio and liquid flow rate [40].
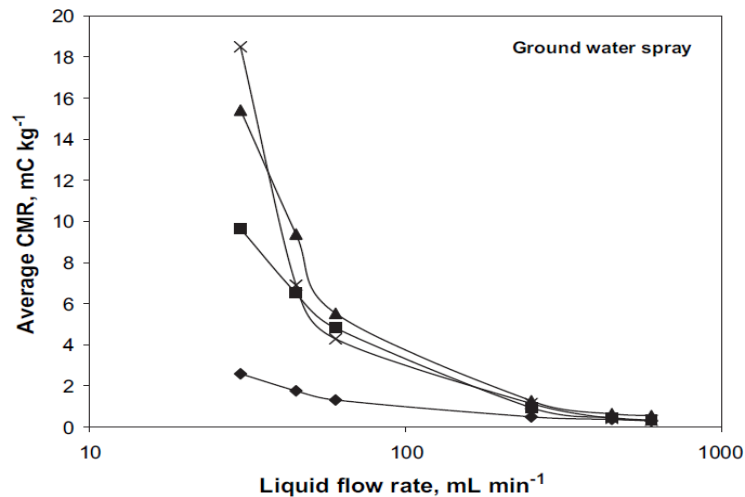
Figure 2.16: The relationship between the charge mass ratio and liquid flow rate, Maski and Durairaj [40].

In the same year, Maski and Durairaj studied the values of depositions on the upper leaves (adaxial) and bottom leaves (abaxial) of an artificial cotton plant with other parameters, which were: spray charging, application speed, height and the orientation of the target. The artificial plant leaf orientations were 0^0, 30^0, 45^0 and 60^0 to the horizontal (below a sheet of aluminum). The high voltage power supply connected to the spraying system was 7.5 kV, while the application speed moves were 0.278, 0.417, and 0.555 m/s. The fluorescent tracer technique was used to determine the spray deposition. The objective of this study was to investigate the effect of these parameters on the values of deposition on abaxial (underside) and adaxial (upper) leaf surfaces. The results can be summarised as: 1) the uncharged case (0 kV) was nearly zero value on the abaxial surface (under) and increased for all target heights, whereas the deposition value of the adaxial surface (upper) yielded the maximum 2) the abaxial deposition of charged spray gradually increased with the target orientation from 30^0 above to 30^0 below the leaves, whereas the adaxial deposition was maximum at 0^0 (horizontal) orientation. 3) The lower height always received a higher adaxial deposition (2.0 mg/cm^2) than the higher (0.95 m) and 4) an increase in abaxial deposition (1.5 mg /cm^2) with the spray charge being distinct at all target heights [41].

Toljic *et al* [42] employed COMSOL, finite element analysis software package, in order to investigate the relationship between the value of charge on a conductive particle and the particle radius in the process of induction charging. The aim was to determine the value of the radius exponent in the charge to radius dependency for the conductive particles atomized in an electric field. The results obtained explained that the single most predominant parameter

affecting the particle charge to radius dependency is the ligament length. Moreover, the exponent in the particle charge to radius dependency is equal to two when the particle is in direct contact with the bulk material. In addition, the maximum charge to mass ratio in liquid spraying will be achieved by maximising the ligament length [42].

Turning to applications in the field, two types of nozzles were compared on wheat plants by Esehaghbeygi *et al*. The first, air-assisted electrostatic induction charging required a high-velocity air flow (30 m/s) within the spraying head assembly to keep the charge in the electrode 8 kV. The second, a spinning charging. The aim was to determine the value of this with a disc speed of 2000 rpm. The aim of this study was to investigate the effectiveness of different herbicide application methods of electrostatic charge and spinning discs under natural weed flora in an irrigated wheat field. The obtained results indicated that electrostatic forces on small droplets are more prominent than gravitational ones and spray droplets can provide an improved deposition with reduced drift. Despite the spinning disc nozzle having more droplet uniformity, it does not significantly improve herbicide efficacy in dense canopy compared with the electrostatic charging sprayer. Furthermore, the spinning disc sprayer decreased water use and so was cheaper to operate, but did not improve herbicide efficacy [43].

Bayat and Sarıhan conducted experiments on maize plants used six spraying methods. The types of nozzles used were (1) conventional boom manufactured with domestic cone (DCN; Toyman Company Đzmir, Turkey), (2) boom with tail boom plus domestic cone (TBDCN), (3) air induction (AI; Spraying System Co. USA), (4) twin jet (TJ; Spraying System Co. USA), (5) air assisted spraying with domestic cone (AADCN) and (6) air assisted TX cone (AATX; Spraying System Co. USA. These nozzles were used at two stages of the plants' growth, the first when the height ranged between 50 and 60 cm and the second when it was > 210 cm. Two application rates of pesticide were used during the growth of the plants, 150 and 300 l/ha. Water sensitive paper was used to determine the coverage rate achieved. The purpose of this study was to determine the efficiency of different types of new nozzles and air-assisted spraying in second-crop maize by measuring spray deposits, coverage, and deposits as losses on the ground. The results revealed that the air-assisted domestic cone nozzles with an application volume of 300 Lha^{-}1 achieved the highest deposits for both plant stages, with the coverage rates being 21.3% and 27.6%, respectively. This increase over conventional spraying was remarkable especially in the second application period on the

middle and bottom parts of the plants. In addition, the ground deposits as losses in both application volumes in the second period were lower than those in the first period [44].

In order to protect tobacco plants, a hollow cone nozzle was used in a study conducted by Chao *et al*. The nozzle was operated at different spray heights, (0.2 m, 0.3 m, 0.4 m) and different spray angles (90°, 45°, and 0°). To atomize the flow rate into fine droplets, the air pressure ranged from 0.4 to 0.6 MPa and water sensitive paper was used to evaluate spray coverage, whereas the spray deposition was measured by a quantitative method (Allura-Red). The aim was to investigate the potential effects of spray height and spray angle on the spraying of the upper side of the leaves, the penetration of the spray liquid and the uniformity of the liquid distribution on the dense crop. The results obtained indicated that the spray coverage on tobacco plants decreased from the upper to lower layers. The deposition value of the upper layer increased as the height grew and the maximum value was located at 0.4 m. Moreover, the utilisation of liquid rate was lower than 45% at a spray angle of 0° and above 50% when it was 90°. Furthermore, the coverage of liquid was 52.9 - 86.0%, 29.5 - 52.7% and 18.7 - 39.6% for the upper, middle and lower layers, respectively [43].

Five different spray delivery systems were used by Roten *et al* on a land plot planted with potato plants. The nozzles were the conventional boom, a canopy submerged drop sprayer combination, a pneumatic electrostatic spraying system, an air-assisted rotary atomizer and a high-volume air-assisted boom. The purpose of this study was to assess deposition from conventional and novel spray delivery systems in a potato canopy and investigate a digitised method for the analysis of this deposition. The results indicated that the deposition on the upper side of a leaf increased by 82% to 97% for all treatments when compared to conventional treatments. Secondly, all those that consisted of one or more novel technology consistently gave higher coverage to the underside of the potato leaves than the conventional boom. Thirdly, the drop-sprayer and both electrostatic spraying system (charged and uncharged) treatments were similar in both the lower and middle canopy of the plant. Fourthly, the air–assisted rotary and air-assisted sustained gave the best coverage in the middle strata with 4.8% and 7.7% margin of increase in the coverage area, respectively, compared with conventional spraying. Fifthly, the hardest to reach area, i.e. the underside of the leaf at the lower canopy level, was covered best by the air-assisted rotary nozzle using the conventional method by 6%, electrostatic spraying charging (ESS) by 5.64%, and the air–assisted treatment by 3.71%. Sixth and last, the conventional boom consistently achieved the

least amount of deposition to the underside of the leaf only ranging from 0.1 to 0.41% at best [45].

An electrostatic spraying nozzle, type MBP 4.0, with a 15 L capacity that uses the pneumatic principle for the formation and fractionation of droplets was experimented on in work carried out by Sasaki *et al*. A Faraday pail was used to collect the charged spray from five different distances, 0, 1, 2, 3, 4 and 5m in order to determine the intensity of charge on the droplets. Artificial targets made of wood were constructed and fixed with two metal plates to evaluate deposition, one in transverse and the other in longitudinal alignment to the spraying jet. The aim of this study was to evaluate the factors that affect electrostatic spraying, especially the effect of the distance between the spray tip and the target, the charge to mass ratio (q/m) and the liquid deposition under different positions relative to the target. The results obtained demonstrated that the q/m ratio is inversely proportional to the distance between the sprayer and the target. Additionally, the system was more efficient regarding to droplet deposition when the target was longitudinal to the spray jet. Furthermore, the minimum q/m ratio on which the liquid deposition was increased by the electrostatic system was 0.6 mC kg^{-1}[46].

Mamidi *et al* designed a hand-held electrostatic induction pressure swirl nozzle and used it in laboratory experiments with different artificial targets, including a glass beaker, plastic ball and aluminum. This nozzle had two swirl holes of diameter 1.0 mm and the orifice disc a hole of diameter 0.8mm. The position of the nozzle electrode ranged from 1.0 mm to 7.0 mm and was connected to a high voltage supply ranging between 0 and 10 kV. All the experiments were conducted in ambient conditions. The nozzle operated at air pressure ranging from 0 - 35 psi in order to atomize a water flow rate of 350 ml/min into fine droplets. The purpose of this study was to establish the optimisation of certain parameters, including the electrode position, applied pressure, electrical conductivity of the spray liquid, and applied voltage so as to enhance the efficiency of a system, thus making it attractive to small and medium scale farmers. A remarkable phenomenon, the "wraparound effect", was utilised, which provided underside deposition efficiently with increased uniformity. In fact, the deposition of liquid quantity was enhanced 2-3 fold when this effect was included. Moreover, the charge to mass ratio increased with the applied voltage and the maximum achieved was 0.419 mC/kg at 3.25 kV (see Figure 2.17). In addition, the charge to mass ratio increased with increases in both the air pressure and the electrode distance (see Figure 2.18). In fact, even a 1.0mm difference in the electrode position could change the system from being fully efficient to completely inefficient [47] .
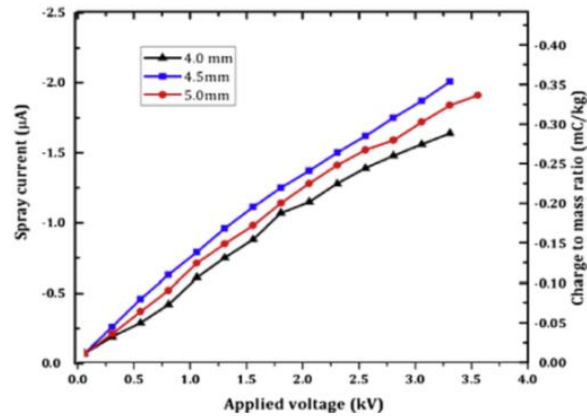
Figure 2.17: The effects of applied voltage on spray current and CMR at various electrode positions, Mamidi *et al* [47].
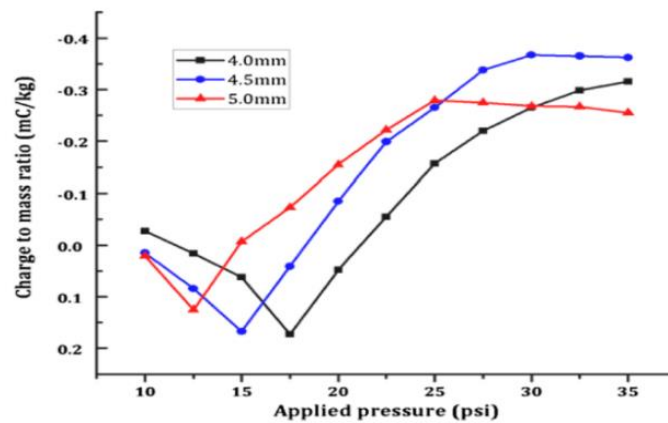
Figure 2.18: The relationship between the charge mass ratio and applied pressure Mamidi *et al* [47].

To explain the relationship between nozzle orifices and droplet size under different air speeds, Martin and Carlton used an electrostatic induction charging nozzle (Spectrum Electrostatic Sprayers, Houston, Tex.) in laboratory experiments. The nozzle orifice diameters were 1.19 and 1.70 mm. The operational wind and air speeds ranged between 24 to 346 km/h and 177 to 306 km/h, respectively. In all the spray testing, the air pressure used to atomize the liquid was 517 kPa and the nozzle electrode ring was connected to a positive voltage of 6 kV to induce a negative charge on the spray. The study had two objectives: first, to quantify the effects of typical fixed-wing airspeeds and nozzle orifice sizes on the atomization of charged spray. The second objective was to quantify the electrostatic performance characteristics (q/m, charge to mass ratio) of the nozzle for each of the test orifices and at every airspeed tested. The results obtained showed that an increase in nozzle orifice size increased the coarseness of the spray droplet spectra at all airspeeds tested. In

addition to this, increases in airspeed produced smaller spray droplets for all the nozzle orifices tested. Figure 2.19 illustrates the findings [48].
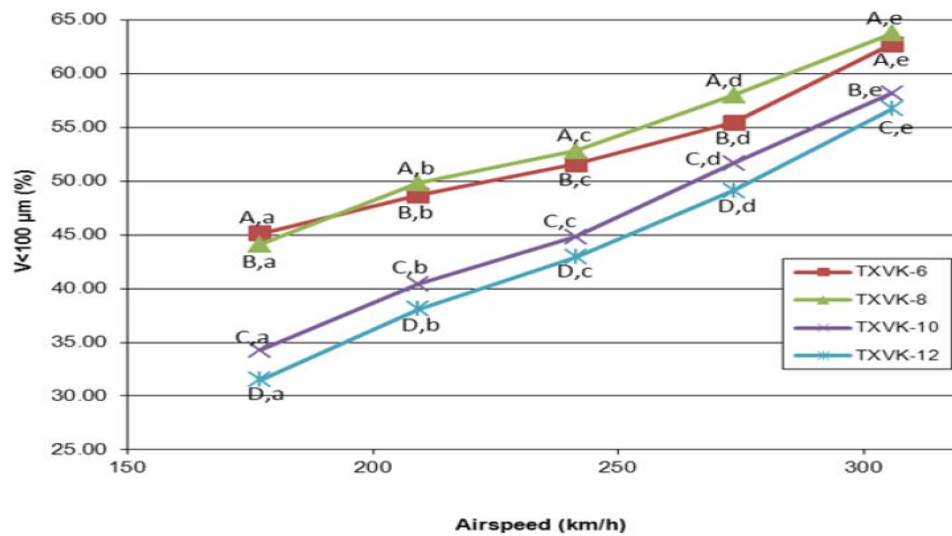
Figure 2.19: Effects of airspeed and nozzle orifice size on the percent of the spray volume that is contained in spray droplets of 100 μm or less from the Brazilian aerial electrostatic nozzle, Martin and Carlton [48].

An air-assisted induction charged nozzle spray was used by Patel *et al* in air atmosphere at ambient conditions (Temperature 20 degrees ^{0}C, Relative humidity = 46% plus minus 3%)**.** The diameter of the nozzle orifices was 1.60 mm and the air pressure entered the nozzle through five holes into the atomization zone. A nozzle embedded electrode was placed inside the nozzle at 4.0 mm from the nozzle tip and the air pressure used was 145 psi to atomize the water at a flow rate of 90 ml/min into fine droplets. In addition, the values of voltage used ranged from 0-3 kV. The purpose of this study was to perform materialistic investigations regarding electrode material in accordance with the theory behind the use of specific materials in electrostatic spraying for high voltage applications. The materials tested were: nickel, copper, stainless steel, brass, and aluminum. The findings showed that the experimental results had good agreement with the relevant theoretical explanations. Specifically, nickel proved to be a good alternative as an electrode material for high voltage application in electrostatic spray nozzles since the performance of its electrode was better than the others in terms of charge to mass ratio and the mechanical parameters mentioned in subsequent sections (see Figure 2.20) [49]:
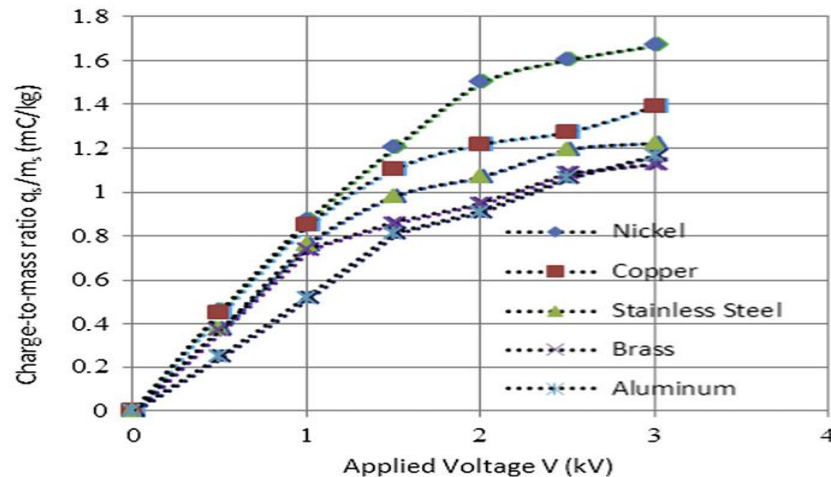
Figure 2.20: Variation of charge to mass qs/ms (mC/kg) with applied electrode voltage kV, Patel *et al* [49].

Another study conducted by Laryea and Young No used the same electrostatic pressure–swirl

nozzles with two types of orchard apple trees, namely M9 and M26. Their aim was to evaluate the contribution of electrostatic forces on spray deposition by using a traditional orchard sprayer and the effect of the sprayer fan speed on spray deposition. The three levels of fan speed were 1000, 1500, and 2000 rpm. The results showed that a significant difference could be observed at the top level for one pass and at the middle level for two passes, at 2000 rpm. In addition, it emerged that the charged spray proved superior to the uncharged one, at a fan speed of 2000 rpm with both passes for both types of trees [50]

2.3.2.1. Conclusions to the third period between 2001 and 2013

This period represents a big advance compared to the two previous ones. It is characterised by the use of advanced technology with excellent software, such as, MATLAB, FLUENT and COMSOL, which have been providing much greater understanding regarding the factors affecting nozzle behavior and deposition value than before. In addition how to improve the nozzle efficiency by selecting the types of nozzle materials and identifying other important factors has been at the forefront during this period. For instance, understanding has been acquired regarding the interactions between the inside and outside of the nozzle in relation to how these affect the efficiency of the application. Finally, during this period, some formulae aimed at predictions the drift value and atomization behaviors have been constructed. The computer simulation models developed have facilitated better understanding of induction charging nozzles for agricultural spraying.

2.4. Factors that have an effect on electrostatic spraying efficiency

Figure 2.23 illustrates four factors that can impact on the efficiency of the induction nozzle and on the electrostatic spraying agricultural application, these being: nozzle geometry, nozzle air pressure, nozzle induction voltage and the properties of the sprayed liquid used. The nozzle geometry factor is determined by three things: the nozzle electrode material, the nozzle electrode radius and the distance between the nozzle electrode and the nozzle liquid film. That is, the value of surface charge on the spread liquid and the chargeability value on the droplet surface depend on these three aspects. For example, if the nozzle distance is the right distance from the nozzle liquid film, the value of the surface charge on the latter will be satisfactory. Furthermore, when the radius of the nozzle and the electrode are the correct size along with the conductivity of the material being high, this will give a value of surface charge to the droplets in the range of the Rayleigh limit, i.e. they will have sufficient chargeability. The second factor is the nozzle air pressure, which controls the volume of the spray and the type of droplet size distribution. For instance, increasing the level of nozzle air pressure means there will be a greater volume of nozzle spray.

On the other hand, the droplet size distribution depends on the pressure levels and can be split into three categories, two of which are beyond the scope of the electrostatic forces zone. The first pertains to small droplets that evaporate through the atmosphere due to their tiny mass and drag forces, while the second refers to big droplets that drop onto the soil due to gravitational force. These two types constitute the total liquid spray drift. Finally, the third category coming within the limits of the electrostatic zone provides the values of the target deposition and coverage area. The liquid spread properties, such as viscosity and surface tension, have effects on the droplet size distribution. They play an inverse role to the electrostatic forces and try to avoid the atomization process or weaken it. Specifically, high values of surface tension and viscosity will make the process insufficient by producing big sized droplets as well as increasing the amount of drift due to gravitational force. Hence, to produce droplet size within the electrostatic forces zone, suitable air pressure is needed in order to destroy the forces of surface tension and viscosity. The fourth factor in nozzle performance and efficiency, as shown in Figure 2.21, is the induction voltage level, which is important for determining the value of the surface charge on the liquid film and then on the surface of the droplets. If the value of the chargeability on the surface of the droplet is within the Rayleigh limit and the droplet size falls within the electrostatic forces zone, the numbers of charged droplets on the intended target is going to increase. Furthermore, the numbers of

the charged droplets reaching the back surfaces of the target due to the role of electric field lines also increases. That is, the probability of increasing the deposition and coverage area on the front and back surfaces of the target will rise, whereas the drift and soil contamination values will drop owing to the dominant electrostatic forces controlling the distribution of the droplets onto the targets. As a result, the amount of chemicals used and the money spent for spraying are reduced.

Nozzle electrode radius

Electrode distance

Nozzle geometry

Electrode material

Nozzle performance and efficiency

Effect of level of voltage value

Levels of air pressure

On chargeability of liquid surface

Properties of liquid spread

Amount of flow rate

On the chargeability of droplets

Droplet size and distribution

On the number of charged droplet on the target

Sizes of average droplets located in electrostatic zone

Sizes of small droplets that are subjected to evaporation and to drag forces

Sizes of big droplets that are subjected to gravitational forces

On deposition value

On coverage area

On drift volume

On amount of chemical materials

On amount of soil contamination

On money spent

Figure 2.21: Explained the factors that affect the nozzle performance and efficiency.

2.5. Factors affecting atomization properties

The spraying operation involves changing a liquid sheet into smaller droplets by using different devices called atomizers and just as with different nozzles being used different

liquids types can be applied. For example, water, oil, emulsion, alcohol and other liquids can be mixed to make new solutions. Many studies have focused on liquid atomization inside and outside the atomizer in order to identify the behavior of interaction that occurs. Specifically, the purpose of these studies was to understand the atomization mechanisms completely in order to use them well in the applications and they have led to the discovery of several factors. These can be divided into two groups, which should be well known by researchers and anyone who intends to work in this field. The first group consists of external forces which are relevant to devices (equipment) and weather conditions, while the second pertains to the internal forces which relate to the liquid properties [51].

Deposition quantity and distribution on the target, risk of spray drift and mode of action and uptake of the chemical particles at the target surface are three functions influenced by external forces. While the droplet size velocity and volume distribution, distribution pattern, entrained air characteristic, spray structure and the structure of individual droplets are influenced by internal factors [52][53]. Results reported in [54] indicate that a change in liquid properties due to the use of adjuvant materials causes significant change in the spray quality for a flat fan nozzle. Three features of the spraying process have been changed according to nozzle type: atomization trajectory, droplet size and droplet distribution. Results obtained from three types of hydraulic nozzle demonstrated that the reduction in the surface tension of liquid tends to reduce droplet size [55], while this increases with nozzle size increase and decreases with nozzle angle as well as with rising pressure [56][23].

2.5.1. Charge to Mass Ratio

This refers to the amount of spray current (measured in Coulombs) divided by the mass flow rate (measured by units of mass) also known as chargeability, which is the total amount of electrostatic charge that is carried by the spray droplets and is a measure of the performance of the nozzle system [49]. This is very important for the optimisation of the system operational parameters and effectiveness of charged spray application [40]. For, from this value the optimum peak of the nozzle design under experimental conditions can be shown in addition to evaluating and estimating the change of the value of deposition and drift [50]. Several electrostatic processes depend on this value which governs the behavior of particle trajectories in a charged cloud of particles [57][58][54] [55]. Factors impacted by it are electrode voltage, liquid flow rate, the type of liquid, nozzle angle, nozzle orifice area, pressure and the velocity of droplet distribution [59][60][61][62][38][25][21]Inverse

proportionality has been found between the charge to mass ratio and nozzle target distance [63]. The reasons for this are a long path, which leads to loss of electrical charge and the droplets being subject to air pressure resistance during their trajectory. On the other hand, the value of the charge mass ratio becomes non-linear with voltage increases above 2 kV, which can be attributed to ionisation of the air in the charging region [56]. The final parameters that need to be identified are: the high voltage magnitude, nozzle to target distance and droplet size, which are chosen so as to yield the best possible results [36].

2.5.2. Droplet size and distribution

Droplet size distribution is one of the three important features that determine the efficiency of electrostatic spraying technique (see the Figure 2.23), with the other two being the ability of the nozzle to generate the desired droplet size efficiently and the construction design having the capacity to generate high voltage [62]. Factors that must be considered when selecting the droplet size are: environmental conditions (temperature, humidity, relative humidity and wind velocity), charge to mass ratio, the velocity of the charged droplets and the type of target [34]. The characteristics of the droplets govern the trajectory of liquid sheet and hence, can increase in efficiency of the pesticide application [64]. That is, the trajectory of the liquid sheet is a function of some of its characteristics, such as: surface density, liquid density and sheet thickness. In addition, droplet diameter and the droplet size distributed can be affected by changing the voltage [61] and/or the water flow feed rate [65][66].

2.5.3. Back ionisation

This phenomenon occurs during electrostatic processing and has profound consequences. It is due to droplet deposition between the earthed target and the nearby charged spray cloud as a result of electric field intensification [67]. Given the importance of deposition, it is crucial to understand which factors influence or reduce its efficiency. Two reasons account for the electrical migration back towards the electrified cloud where droplet coalescence is likely to occur. The first is the ionic discharge from target points that can neutralise part of the oppositely charged spray cloud, which can cancel beneficial Columbic forces leading to the probable collapse of the droplet-driving space-charge field. Secondly, all momentum fluxes and charges associated with gas discharge can be shown to repel droplets from the target [68].

2.5.4. The drift

This has a negative impact on pesticide application in terms of the amount of fluid lost through the spraying process. Some of this is lost as a vapor or small droplets in the atmosphere due to their very light mass, known as exo-drift [69].While conversely, some is lost on the ground due to gravitational forces owing to the droplets having a large mass, termed endo-drift [10] (see flowchart in Figure 2.3). The third way through which droplets are lost is when they are off target owing to drag forces. This can be attributed to several reasons, including: characteristics of the pesticide solution, weather conditions, droplet size, travel speed, nozzle type, boom height, spray pressure, nozzle spacing as well as the level of attention and skill of the operator [5]. The size of the spray angle plays an important role in determining the drift amount, regarding which it has been found that a fan angle of 110°

increases airborne drift by 29 percent more than one of 80° [70]. In addition to this, wind speed, the absorption coefficient and surface roughness lead to increases in the drift amount [71][72].

The results of drift include damage to neighboring crops that are not resistant to the pesticide, spoiled ecosystems, contaminated waterways and threats to human health. The last is particularly of concern in areas known to have intensive agriculture and relatively small fields that are scattered and close to living spaces and hence, the need for a good understanding of drift from field sprayers is of high priority [73][74]. Drift not only has a negative environmental impact, for it also results in wasted pesticide and consequently, unnecessary expenditure. In agriculture, most of the pesticides types used are aqueous based liquids and more than 90 percent of them are applied by the spraying method, which means that the amounts of exo- and endo- drift are seriously on the increase.

2.6. Existing challenges

Despite researchers through their great efforts having achieved satisfactory results in agricultural application of electrostatic sprayers, too many chemicals are still being used, substantial amounts of money continue to be wasted owing to inefficiency and the problems of drift and soil contamination remain unresolved. In the first ten years covered by this literature review, researchers focused on two things: increasing the amount of charge mass ratio on the living target by comparing the values obtained from the methods that used induction voltage with those that did not. The second focus during this period pertained to

comparing the efficiency of the induction nozzle with the conventional one. Two factors remained unaddressed at this time: the amount of overdosing of the chemical material and huge quantities of wasted money. While during the second stage, the interest lay in the geometry of nozzle and which of the different types could produce the highest deposition values on the target. At this time, there was little concern about drift loss and the amount of pesticides being used and instead, drift was considered only a secondary result caused by several primary factors. During the third period of the literature review, it became apparent that the work was concentrated on using advanced software simulation nozzle models. These studies sought to comprehend the role of internal and external conditions in nozzle efficiency so as to be able to increase the amounts of the deposition on the targets. A little research has been carried out investigating drift behavior through mathematical formulae so as to reduce the losses from the agricultural application. From the projects and studies that have been reviewed, it is clear that the drift amount and overdosing with chemicals still lack sound remedies. Issues that still remain unresolved are:

1- Conventional inefficient nozzles are still used in many applications;

2- The whole plant is still being treated even when there are parts that do not need it and hence, local infection detection needs to be pursued;

3- No advanced technology has been developed to control the duration of the operation of nozzles.

In order to address the above, the aim of this project was to design a system of electrostatic spraying through the use of new technology. This system includes a novel induction charging nozzle, mobile robot, CCD camera, software and hardware to control the nozzle operating and the robot's movement. Regarding the software, the induction nozzle design involved drawing on the results from COMSOL simulations of models. This provides the ability to scan the whole plant and identify the target area of infection from the results of image processing. In addition, the system being mobile gives it the versatility to seek out a range of insects across the crop from a variety of positions. To this end, the mobile robot comprises two main parts: an arm manipulator and an electronic vehicle. The novel induction nozzle is attached to the arm manipulator of the system next to a CCD camera. Finally, MATLAB and Arduino software control all the induction nozzle operations, movement of the robot, image processing and the amount of the pesticides applied.

2.7. Conclusions and contributions

It has become clear that electrostatic spraying yields more coverage area and deeper penetration into the spatial canopy of plants when compared to conventional systems. Even though researchers have used this technology for some time now to improve nozzle efficiency, performance and to provide uniform distribution of deposition on the target, as explained above, large quantities of money and huge amount of pesticides are wasted because leaves that do not need remediation are being treated farmers and workers. This situation can be addressed by targeting only the infested area, which will not only greatly reduce the amounts of wasted chemical materials and hence, save money, for it would also result in less environmental pollution. This Ph.D. research has been carried out so as to address these issues. Smart pesticide spraying system has been developed involving a nozzle attached to the gripper of a mobile robot along with a CCD camera, which is used to locate insect positions on plant leaves. Subsequently, the nozzle is positioned so as to put the target within its spraying field and then, short bursts of pesticide spray are made to exterminate insects without subjecting non-infested parts of the plants to unnecessary treatment.

The mobile robot system was constructed from kits supplied by Lynxmotion™ robot system was constructed from kits supplied by coverage area and deeper penetration into the spatial canopy of plants when compared to conventional systems. Even though researchers have used this technology for some time now to improve nozzle move the attached camera next to the spray nozzle on a search path aimed at locating a given type of pest. The targets are selected for extermination after processing received images and subsequently the nozzle is put in the correct position, with a burst of pesticide on the targeted insect then being applied. The master computer is a Windows-based notebook computer, while the slave is an Arduino mega 2560 microcontroller board along with additional circuitries and hardware that assist in operating the smart nozzle system.

2.8. Water Sensitive Paper

2.8.1. Introduction

There is a considerable interest in improving the efficiency of coverage from spraying activities for agricultural applications. To visualise the coverage obtained, water sensitive paper (WSP) is used [75], which is a common method for evaluating spraying techniques [76]. In particular, it has been widely employed for determining of the distribution of the droplets and their size. Furthermore, this method under ambient conditions can provide

important information regarding spray deposition efficiency [74] and quick evaluation of spray coverage [77]. It is common practice in the laboratory to use artificial targets to study spray deposition characteristics [77][78]. WSP is yellow in colour and changes to dark blue after being subjected to aqueous droplets being deposited on it [79][80][81]. This colour change is due to the reaction of the water with the bromophenol blue indicator contained in the coating, which changes blue with a pH between 2.8-4.6   [82][83]. It's role is to calibrate and check the sprayer pattern which helps in correcting boom height, spotting irregularities in the spray system area, measuring droplet size, keeping the environment clean by eliminating drift and counting the number of droplets as well as their distribution on the target.

When a water droplet contacts WSP, it creates a stain that is larger than the original droplet as a result of the water being adsorbed into the paper surrounding the site of impact [84]. Droplet sizing is possible when an appropriate spread factor or calibration equation is developed to convert the size of the WSP stains into an estimation of the droplet size [75]. That is, it is possible to determine the approximate diameter and volume of the original droplet that formed the stain on the WSP, by dividing the measured spot diameter by a spread factor. This operation is feasible when it is assumed that all the droplets have same physical properties under the same atmospheric conditions [85]. The analysis of WSP involves manual processing [86] or automatic image analysis using a software package [87] and microscopic measurement [85]. Reviews regarding the use and effectiveness of some of these software packages have been published and their limiting factors investigated [88][89], which means they have the capacity to evaluate information about droplets. WSP can also be used to determine accurately the lethal dose on the target and increase the probability of contact between the pest and the pesticide, the impact density and the uniformity of deposition of spray onto the selected surfaces [90]. The use of WSP in testing comes with some disadvantages; in particular, the process of manual analysis is slow with or without the aid of a magnifying glass [83]. Some other limitations that must be considered when using WSP are:

1. The colour of the unstained areas on the water WSP can be changed when the distance between the stains is decreasing [83];

2. If droplet diameter is less than 50μm, this will be insufficient to create visible results on the WSP [78][82];

3. WSP is not used under high humidity conditions (i.e. >80%) because this will make it unreadable [91].

The lack of standard images that can be obtained affects the accurate measurement of the stain properties, which is the most common difficulty faced when evaluating the performance of the software application [81]. In spite of the advances in digital imaging technology that have increased the resolution capabilities for analysing spray particle sizing and distribution from different passive sampler, there remain difficulties in the evaluation of the homogeneity on the card and for samples with droplets that overlap [87]. The best approach to solving these problems is by conducting comparisons with reference cards with known coverage and droplet size [22]. In the work conducted in this study, WSP has been used to compare the area coverage and the number of droplets on both surfaces of an artificial cotton leaf using an agricultural induction charging nozzle.

2.8.2. Water sensitive paper applications

WSP has been used in different sciences and applications both in the field and laboratory. To demonstrate its significance, summaries of some of researchers conducted using WSP are presented here. Previous research has shown that there is just 1% difference between two methods being used to estimate the volume and number median diameter, these being visual microscopic classification and a computer program [88]. However, it was noted that the microscopic method was slower than that using a computer program. In other work, three imaging systems (USDA-ARS, Swath Kit camera-based system and the Droplet Scan scanner-based system) were described and the results compared with those of two sets of WSP. There was a high correlation for the three image systems used for droplet spectral parameters of DV0.1, DV0.5, and DV0.9, but less consistent results relative to the span measurements. These outcomes gave the researchers confidence in using WSP to compare their results using the software package [85].

The relative performance of eight image processing software programs, both commercial and experimental, used in analysing results obtained using WSP (Gotas, Stain Master, mage Tool,

Stain Analysis, Agro Scan, Droplet Scan and Spray_imageI and II) was compared. The results showed that Spray-imageII with its overlapped feature provided the highest accuracy for coverage and droplet size spectrum measurement, when compared to the other software tested [82]. A strong relation between the values of the measured diameter and volume of droplets emerged from using four different software programs (CIR, e- Sprinkle, DepositScan and Conta-Gotas) and manual analysis. However, there were great differences between the numerical values measured for the same test paper [83]. Experiments to determine the droplet characteristics of seven agriculture spray nozzles were carried out, with the purpose of the study being to develop a practical alternative to the conventional approach of Spot Elimination (SE) from WSP surfaces. The results gave a linear relationship between the minimum SR (Spot Roundness) value and volume median diameter of the droplets. Moreover, it was determined that the spot roundness values can be employed for an elimination procedure of overlapped spots as well as for non-circular spots on a WSP surface [76].

A method to determine the amount of sprayed liquid for several commercial orchard sprays with different types of air discharge systems (conventional, cross flow and directional spouts) was presented, with both WSP and blotting paper being used. The experimental results indicated that the former was suitable for the proposed technique, because it could generate the spray distribution, spot density, spot size and a histogram of spot size as well as the distance between spots, although it has to be acknowledged that in practice it is very hard to adjust a sprayer used on trees that are characterised by their randomness [86]. A fully automatic methodology based on image processing was used to evaluate the quality of spray application sampled by several WSPs. The experimental data obtained indicated that one with appropriate scanning resolutions can provide good results, not only in terms of stains, size and spectra factors, but also, in relation to the homogeneity of coverage [87].

The software package Image J for image processing results obtained using WSP was used to estimate the spray characteristics of different types. The results indicated that there is a close relationship between the simulated superficial coverage and the computed form, thus showing that this relationship is independent of the type of spraying system used. This means it is easy to estimate the overlap between the droplets and certain spraying characteristics, such as: the volume median diameter (VMD), the coefficient of variation (CV), impact density, the degree of uniform deposition as well as the coverage surface area as WSP can now be analysed electronically [78]. WSP was used to determine pesticide performance on the cotton plant. Specifically, for a fixed area of spray coverage, every part of the used WSP was

labelled, digitised at a special resolution of about 5000 pixels/cm^2 and subsequently subjected to image analysis using two scatter plot tools in ENVI 4.3 for Windows (ITT Industries, Boulder, CO). The results of an experimental and theoretical modelling approach demonstrate how a combination avoiding pesticide waste and increasing spray coverage can markedly reduce pesticide usage, whilst at the same time increasing performance.

To determine the number and size effect of spot and image area on accuracy of measurement, and to evaluate the utility of the image analysis for assessments of spray deposition and distribution, three sets of images, namely single speck, mixed speck and uniform speck size were prepared. The results obtained were:

1) The accuracy of image analysis for sizing single specks increased as spot size increased;

2) The size of the image and the size and number of the specks (within the image) had a significant effect on speck sizing and percentage area coverage measurement;

3) The size and number of specks were not accurately measured for small and dense images made up of small ones [80].

A comparison study was carried out both in the field and laboratory to calculate the ratio of WSP to oil sensitive paper (OSP) spot size for different concentrations of oil in water mixtures. Field experiment results did not agree with predicted values, which could have been due to larger water spots touching, or oil spots separating into several globules as the water portion of the spray droplet evaporated. However, water spot to oil spot diameter ratios measured for the laboratory sprayed WSP and OSP were similar to those predicted [75].

CHAPTER THREE: BACKGROUND TO AGRICULTURAL ELECTROSTATIC CROP SPRAYING

3.1. Introduction

In this chapter, some experiments are conducted using the electrostatic spraying system (ESS) with artificial plants in the laboratory. The purpose of these experiments is to achieve full understanding of the principles underpinning the application of the electrostatic spraying system. This knowledge will be applied when designing the new induction nozzle. The parameters of electrostatics that are tested are the flow rate, spray current, charge to mass ratio, and space charge density. In addition, examination of the liquid atomization and measuring the droplet size for charged and uncharged droplets are included in this chapter along with the other experiments.

3.2. Background to the atomization study

The atomization of liquids is a technology used in many industrial operations and the importance of droplet size information has increased considerably over time. Nowadays, this has a broad range of applications, including: spray drying, evaporative cooling, combustion, and agriculture. What is of key importance with sprays is the droplet size distribution. The concern is to achieve a high coverage area and good uniform distribution on the intended targets. In agriculture, pesticides are used to protect crops against pests and diseases, with more than 90% of these being applied as aqueous-based sprays [35]. During this process, a large portion of the spray volume is lost as airborne drift through and beneath plants, especially when conventional methods are employed. Moreover, the amount of deposition on the intended target is inadequate due to the influence of gravitational and drag forces on the mass of the droplets generated. As a result, less than 25% of pesticides fall on their targets. Electrostatic spraying systems have provided the best results for farmers and agricultural workers when applying pesticides. They have many advantages over traditional systems, if used in correct way, as they can improve the plant canopy penetration [92]. Finally, the researchers have used different methods to charge the spray to identify the best method depending on the type of application required.

3.3. Electrostatic forces physical conditions and the basic principles

The electrostatic spray theory evolved based on two fundamental premises:

(1) Electrostatic spraying can be treated as an equilibrium end - state problem;

(2) The spray process is complex as it involves several interacting variable that need to be accounted for, if the desired application is to be successful [65].

These two statements form the conceptual framework from which all investigation proceeds.

Two physical conditions must be met in order to incorporate an electric force into a pesticide spray application, which are:

1-Each spray droplet must be given a significant net electrical charge Q_p equivalent to 0.5-1.5x10^6 for a 50 μm droplet.

2-The charged droplet must be acted upon by an electric field E, which may be self-generated or may be imposed by other nearby charge assemblies including charged bodies (e.g. metallic electrodes and other charged droplets) [66].

A brief description for these kinds of charging is provided next.

3.4. The types of the charging methods

There are three main methods of charging applied to pesticides: corona, conduction and induction.

3.4.1. Ionized/Corona Charging: It is routinely used in a variety of commercial and industrial processes ranging from xerography to electrostatic precipitation. Great care must be taken when using this process for agricultural spray the intended target is in maintaining long term charging reliability. For ionized – field charging, a D.C. voltage is applied with a magnitude sufficient to cause dielectric breakdown of the air surrounding a sharp curved active electrode in the zone, such as a metal needle or wire. A high voltage electrode releases a large number of positive or negative ions around which ions with dissimilar charge gather. The saturation charge depends upon the particle's dielectric constant, surface area and the electrical characteristics of the corona charge. A liquid droplet is charged with the same polarity as the electrode after intensive bombardment by the free ions and the basic theory behind this phenomenon is clearly explained by Law [22]. This charging method can be applied to both pressure and rotary atomizers.

3.4.2. Contact charge: This is when high potential is directly connected and maintained to the nozzle or to the liquid flow system, with the charge transfer being by conduction. The charge transfer capability by conduction from a metal nozzle through the issuing liquid jet depends upon the electrical properties of the liquid comprising the continuous jet. This system works well with conductive liquid [23].

3.4.3. Induction charging: This involves using an electric field to induce charges onto the droplets. In this method, the atomization is achieved conventionally by forcing pressurized liquid through a nozzle and charging the resultant spray by induction, thus avoiding direct contact of the spray liquid with the potentially hazardous high voltage and it provides a spray that disperses charged droplets effectively as a result of Columbic repulsion, which are subsequently attracted to grounded targets [24][25]. The charge on the droplet is opposite to that of the electrode [26] and theoretically the spray liquid should be conductive. The induction charging method will work within a resistivity limit of 10^{-1} to 10^{6} Ωm [27]. This method is widely used in agriculture and is a good alternative to the ionized and contact field methods due to it employing low voltage and hence, is safer than the other forms of charging. The level of droplet charge imparted by this method depends upon the relative time of the charge transfer to the droplet formation zone when compared with that required for droplet formation.

The best method among these three is induction charging, because in addition to being safer it has the following advantages:

1. The high voltage does not directly contact the liquid;

2. The electric field strength is below the breakdown strength of the air, so its working voltage can be lower and electrode insulation becomes easier;

3. In principle, there is a very small current drawn from the power supply, therefore its capacity can be very small [28];

4. Since the electrostatic force counteracts the surface tension force, it will produce smaller, more uniform sized droplets;

5. Since like charges repel, the atomized droplets are dispersed more uniformly in the entrained air;

6. As the charged particles produce space charge forces and image attraction, they result in enhanced attractive and adhesion forces to the leaves.

In general, electrostatically charged sprays increase the mass transfer of pesticides onto plant targets, which can generally not be achieved when using the conventional methods of applying agricultural chemicals.

3.5. Experimental set-up of the electrostatic spraying system

The experiment was conducted in the Laboratory of Centre for Electronic Systems Research of the Department of Electronics & Computer Engineering in the College of Engineering, Design and Physical Sciences at Brunel University. A photograph of the experimental set-up is shown in Figure 3.1.
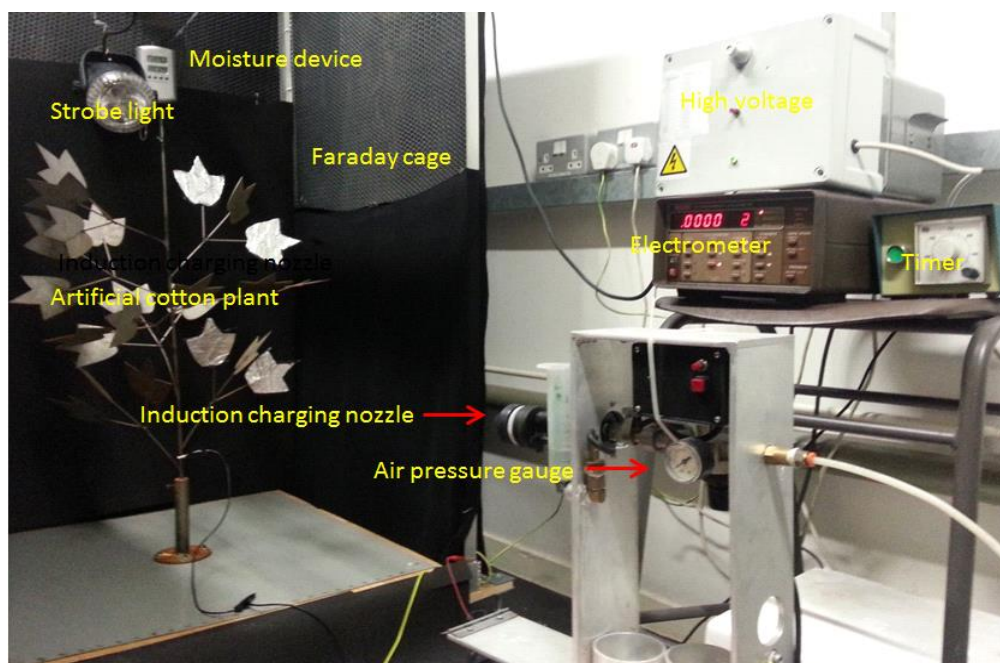
Figure 3.1: The experimental setup.

In the laboratory experiment, a twin fluid nozzle (Electrostatic Spraying Systems Co) (ESS) was used to generate sprays of tap water to mimic pesticide ones and the value of its electric conductivity was 620 μS/m. And air pressure to generate the droplets after mixing with the water, which was maintained by an air compressor Condor MDR2/11 bar, type Clark rebel air no.50 model, connected through a solenoid valve and monitored by a simple pressure gauge via a length of insulated plastic tubing (see Figure 3.2).

Figure 3.2: Type of compressor used in the experimental set-up.

Different levels of pressure were used with this induction nozzle ranging from 5 to 60 psi depending on the experimental situation. A timer device was connected to the nozzle to monitor the duration of its operation, which was set to different lengths of time. A high voltage supply (Emco model 7200) was directly connected to the electrode of the induction nozzle in order to provide the nozzle voltage potential. A grounded Faraday pail (140 cm x 90cm x 90cm) was manufactured and used in order to isolate the experiments from the rest of the laboratory electrically. This was made of an aluminum frame and sheet mesh. A polyethylene sheet was placed around the chamber to avoid having the water droplets passing through the wall to the outside and it was completely isolated from the ground by being stood on a wooden table top with four small plastic legs. The purpose of the using Faraday pail was to minimise external electrical interference. A small hole drilled into the bottom of the pail and through the wooden table served to drain the sprayed water into a plastic container underneath. A strobe light and four ordinary small lights were attached inside and on the ceiling of the Faraday pail, respectively. The purpose of these lights was to create clear opportunities to capture pictures of the nozzle spray via a high-speed camera, namely, a Casio EXILIM EX-FH25 with 30-1000 fps and a description of the camera is provided in [93]. Placed inside the Faraday pail was a device to monitor the relative humidity and temperature. An artificial cotton plant made of metal with different leaf orientations was constructed standing inside a metal holder. The reason for the plant being made of metal was to achieve good conduction so as to mimic a real cotton plant. SOLIDWORKS software was used to design leaf shape such that it replicated the actual area and dimensions of that of cotton (100x100mm)[94]. The shape of the cotton leaf drawn by this software is presented in Figure 3.3.
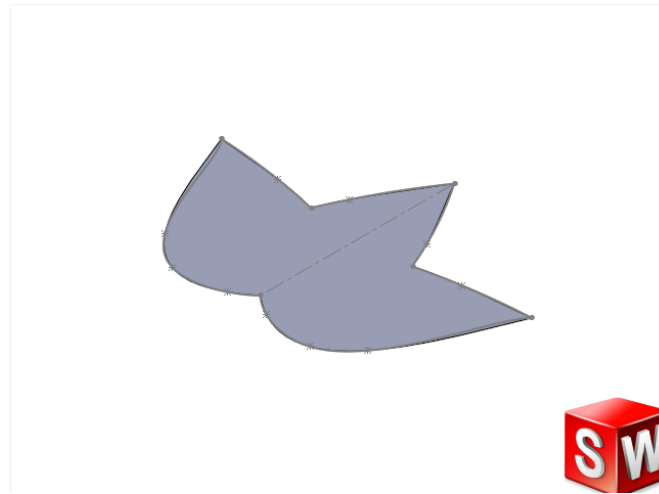
Figure 3.3: Leaf of a cotton plant manufactured by SOLIDWORKS.

A model 617 electrometer was connected to the artificial plant to measure the spray current (charge deposition) on the leaves used. The spraying was performed with and without charging in order to investigate the effect of electrostatic forces on the deposition value on the plant leaves. In addition, water sensitive paper was attached to the two faces of the plant leaves in order to capture the droplet size distribution and the coverage area. Different nozzle-artificial plant distances were used, these being: 25 cm, 50 cm, 75 cm, 100 cm, and 125 cm. The reason for applying different distances was to determine that which could achieve high deposition on the target with low drift. The factors that needed to be tested were the water flow rate, air flow rate, spray current, charge to mass ratio, space charge density, coverage area and droplet size distribution.

To monitor the nozzle air pressure, an air pressure gauge was connected to the nozzle. For checking the induction voltage of the nozzle, a high voltage probe was connected between the nozzle electrode and a multimeter, as shown in Figure 3.4. To obtain the correct value of induction charging voltage, the reading on the multimeter had to be multiplied by 1,000 and this number represented the constant value of the high voltage probe.
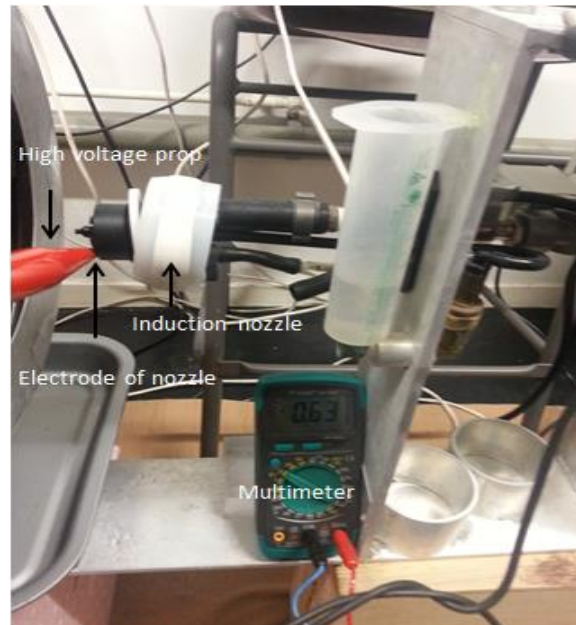
Figure 3.4: The process for checking the level of induction voltage.

The high-speed camera was used to capture the spray at different pressures. This was in order to be able to measure the droplet size distribution and coverage area which was done in two ways. First, an image processing program run by Matlab was used to analysis the samples of the microscopic pictures of the water sensitive papers used and then, Image J software was employed for the same purpose. Subsequently, the results obtained were compared. The procedures for determining the optimal values for the different properties are summarized below.

3.5.1. Measurement of the water flowrate

The flow rate was measured for different air pressures, starting with 5 psi and ending at 60 psi, as mentioned above. It was found that the flow rate increased when the nozzle air pressure increased. Figure 3.5 presents this relationship.
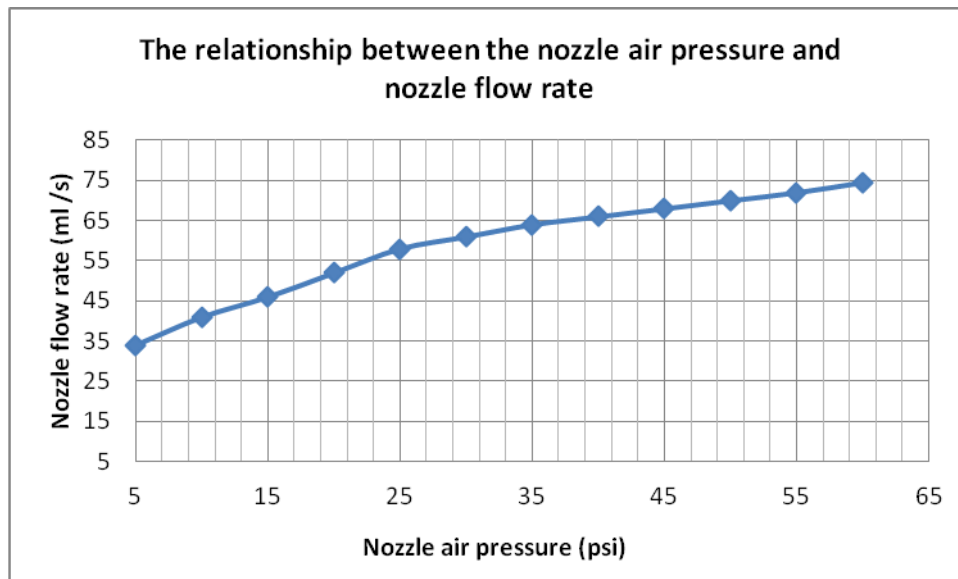
Figure 3.5: The values of the flow rate at different levels of air pressure.

3.5.2 Measuring the air flow rate

To measure the volume of air flow, a rotameter device was needed, which was attached between the air compressor and the induction nozzle. Figure 3.6 illustrates how the rotameter (Ki instrument) was connected in the experimental set-up.
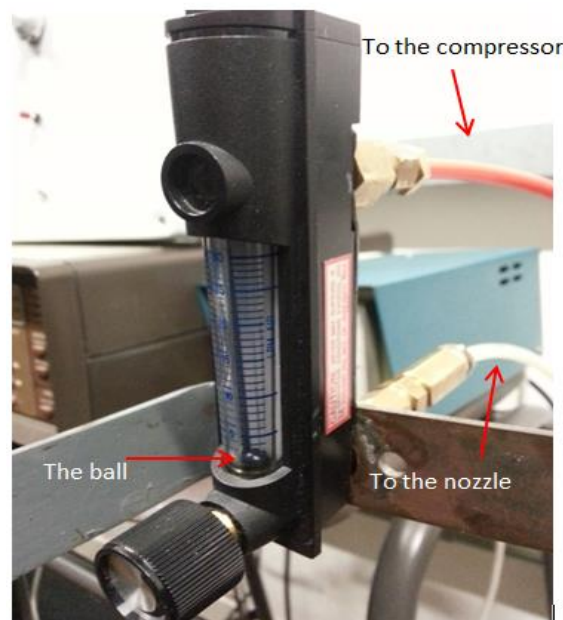
Figure 3.6: The attachment of the rotometer device in the experimental setup.

The plotted results obtained from the experiments are provided in Figure 3.7, in which it can be seen that a direct relationship is found between the air flow rate and air pressure levels of the nozzle.
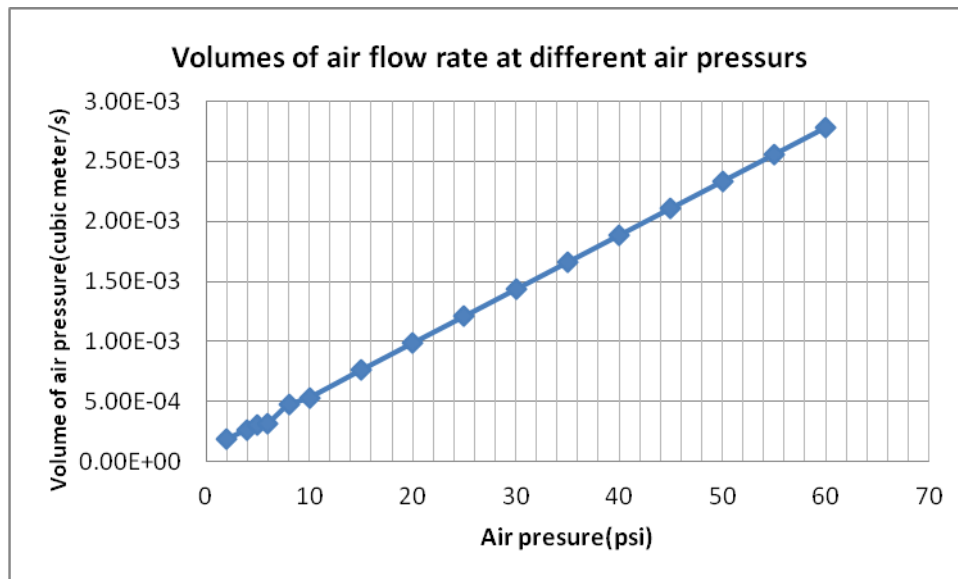
Figure 3.7: The values of the nozzle air flow at different pressures.

3.5.3. Measuring of the spray current

An electrometer was connected to the artificial plant leaves to measure the spray current reaching them. In order to check the spray current on one face of the leaf, insulating tape was used to cover the other, as shown in Figure 3.8.
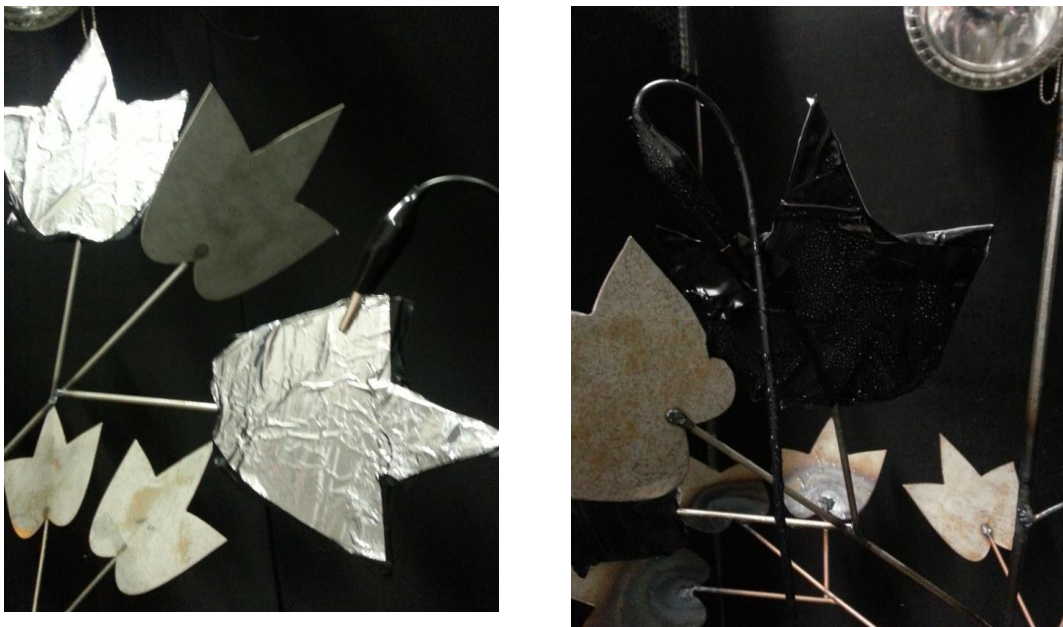
Figure 3.8: How the plant leaves were connected to the electrometer (left) insulating tape being used to cover the surface of the leaf (right).

The results for the spray current are presented in Figure 3.9, showing that it increases when the air pressure is increased and when the nozzle target distances reduced. The spray current ranged in 1 to five µA to 125 cm and 25 cm distances, respectively. Although high values are obtained at 25 cm, and 50 cm, the suitable distances that can be used for the electrostatic nozzle are between 50 cm and 75 cm. The reason for this is because distances below 50 cm are too close to the plant, whilst those over 100 cm are too far away. That is, the rejected distances do not achieve sufficient spray current for the nozzle to penetrate the internal parts of the plant. The results obtained from this study are in good agreement with those reported by Maynagh *et al*. and Sasaki *et al* [38][46] as well as being located within the range mentioned by Law [11].
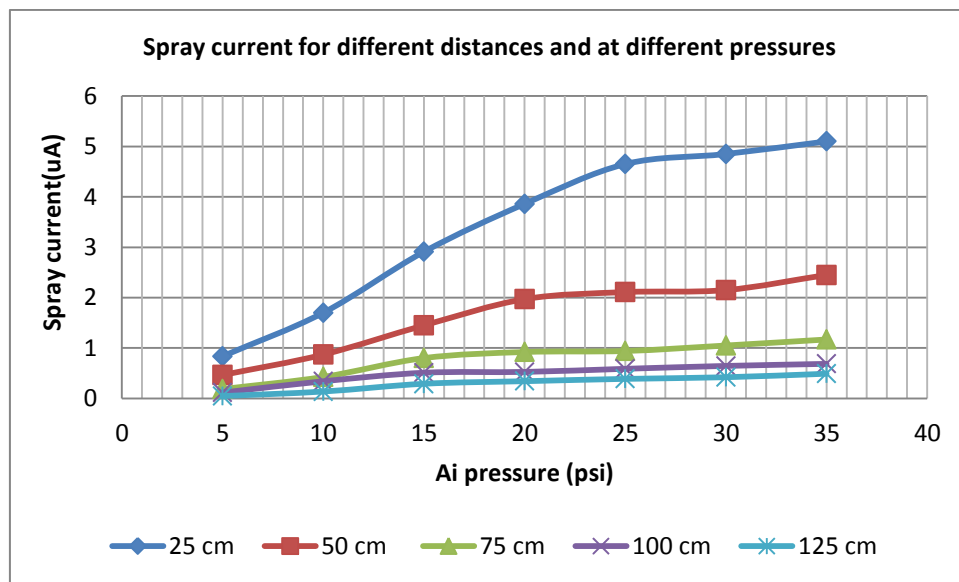
Figure 3.9: The values of spray current with different air pressure at different distances.

3.5.4. Measuring of the charge to mass ratio

The value of the charge to mass ratio is calculated by dividing the value of the spray current (measured in amps or Coulombs per second) by the mass flow rate value (kilograms per second), which represents the performance of the nozzle [49]:

Charge to mass ratio = spray current / mass flow rate.

$q = I/M$ ---------- (3.1)

where,

q = Charge to mass ratio(C/kg)

I = spray current (A) or (C/s)

M = Liquid mass flow rate (kg/s).

M = V *D----- (3.2)

where,

Mass flow rate = volume of flow rate * water density

V = water flow rate (m^3/s)

D = water density (kg/m^3)

The results obtained from the experiments indicated that the values of charge to mass ratio have a direct relationship with air pressure (see Figure 3.10 below). The reason for this is due to an increase in the flow rate when the air pressure increases, which results in the charge to mass ratio also increasing. This concurs with results reported by Frost and Law [13] and Marchant and Wilson [23][6]. Furthermore, according to findings presented by Mamidi *et al*, the charge to mass ratio increases with increases in both air pressure and the electrode distances [47]. However, the study outcomes do not agree with those obtained by Maski and Durairaj, as these researchers elicited that the rate of increasing spray chargeability with decreasing liquid flow rate was higher in the lower flow rates than for, the higher ones [40].
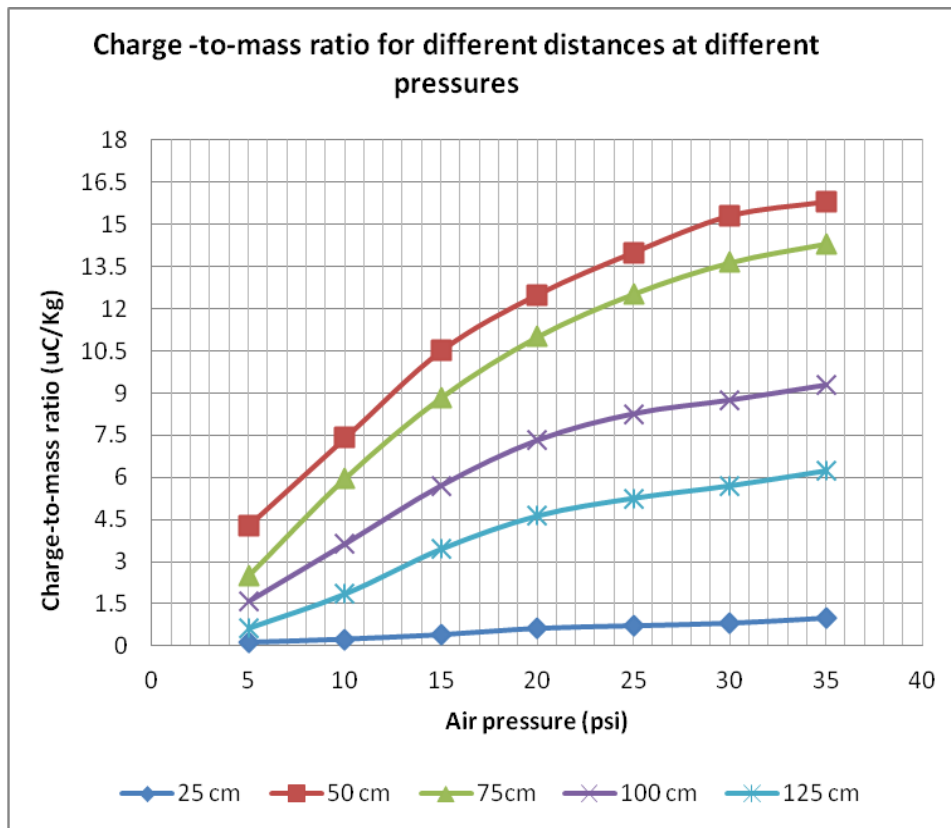
Figure 3.10: The relationships between charge to mass ratio, nozzle air pressure and nozzle-target distance.

At the same time, the charge to mass ratio is found to have a negative relationship with the nozzle target distances (see Figure 3.10), which is due to increase in the drift of the nozzle spray as the distance increases. This means that the amount of the charge to mass ratio that reaches the back of the target is low. This result is consistent with that reported by Zhao *et al*. [35] and [63]. In general, the value of the charge to mass ratio ranges from 1 to 16 µC/kg across the tested distances.

3.5.5. Space charge

3.5.5.1. Space charge définition

Space charge is defined as the charge density that exists in free air. Specifically, it refers to an excess electric charge that is treated as a continuum distributed over a region of space (either a volume or an area) rather than being of a distinct point-like form. Space charge usually only occurs in dielectric media (including a vacuum), because in a conductive medium the charge tends to be rapidly neutralized or screened. The sign of the space charge can be either negative or positive. In an aerosol, if the charge of two particles is the same they exhibit mutual repulsion, and if they are opposite, they attract each other. The net result is integration

across the whole cloud of particles is an internal electric field, ultimately resulting in deposition onto solid surfaces [95].

3.5.5.2. Factors affecting the space charge density

The space charge generated due to the charged droplet cloud change both the electric field distribution and the trajectories of the droplets. Its value depends on factors such as the liquid flow rate, nozzle-to-target distance, spray angle and droplet charge. For example, with a fully developed spray, the spray cloud expands in all directions owing to the space charge field. During conduction charging, the space charge field from the transport region serves to counteract the charging field near the electrode. Whilst with induction charging, the space charge field from the transport region strengthens the electric field near the electrode, thus leading to more droplets being attracted to the charging electrode, resulting in electrical leakage to the electrode or discharge through the air [35].

3.5.5.3. Measuring of the space charge density

The formula used to calculate the value of space charge proposed by Castle *et al* [10]involves dividing the spray current value by the air flow value as below:

$\rho = I /Q$ (3.3)

where,

ρ = Space charge density (C/m3)

I = Induction current (A)

Q = entrapment air flow rate (m^3/s).

The results for space charge density are presented in Figure 3.11 below. These show that the space charge increases when the air pressure increases and when the nozzle-target distances are reduced. The minimum values range from 0.5 to 2.5 at 5 psi and the maximum from 6 to 24.5 $\mu C/m^3$ at 35 psi. These findings are within the range of the electrostatic nozzle results reported by Law [11].
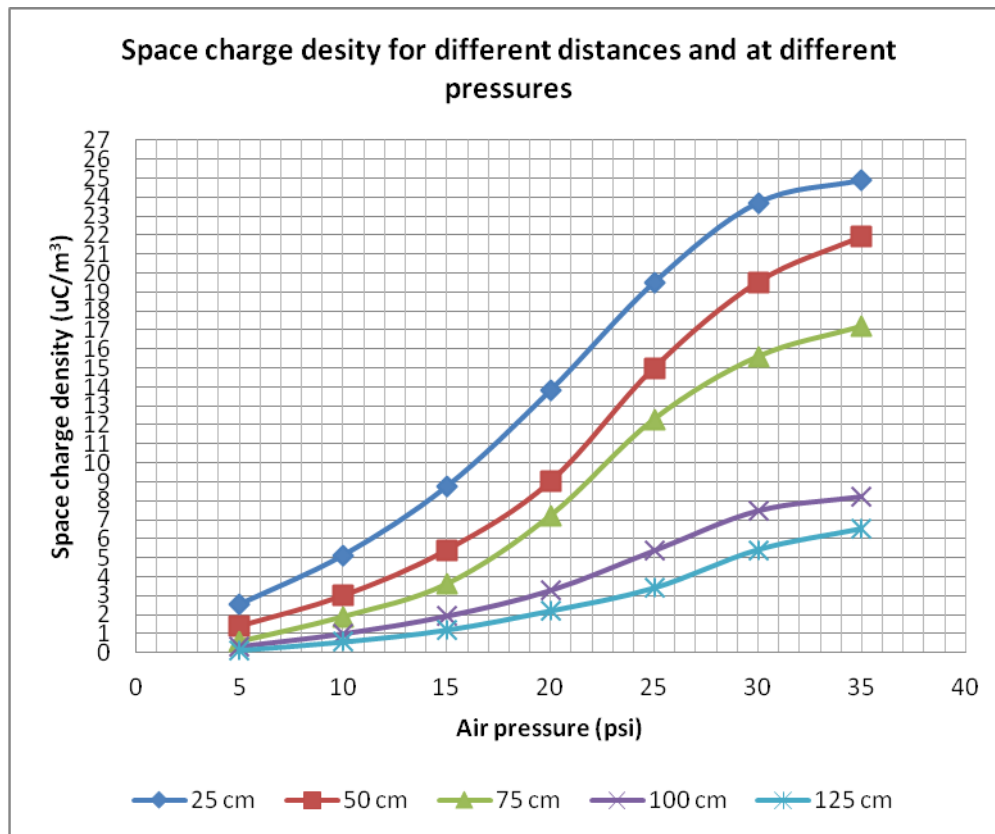
Figure 3.11: The values of the space charge density for different distances and air pressure.

3.6. Measuring the droplet size

3.6.1. Using a high-speed camera with the MATLAB software

Given different water flow rate is produced at each level of air pressure used, the nature of the droplet size distribution will also change. To create the desired droplet size distribution, the optimal nozzle air pressure needs to be found and in this study, as aforementioned, the induction nozzle was operated at twelve levels ranging from 5 to 60 psi using 5 psi increments. A high-speed camera was used to capture the process of the nozzle spray in relation to the distribution of the droplets. In addition, as previously explained, a strobe light was attached inside the Faraday chamber to enhance the capturing of pictures and a program run through MATLAB provided the image processing for their analysis. At the same time, water sensitive paper was attached to the top and bottom surfaces of the leaves so as to capture the droplets that had fallen onto them. The reason for using two methods was to see whether the outcomes were the same or at least very similar. The results of the droplet size

distribution for all the levels collected from the Matlab program are presented in Figure 2.12 below.
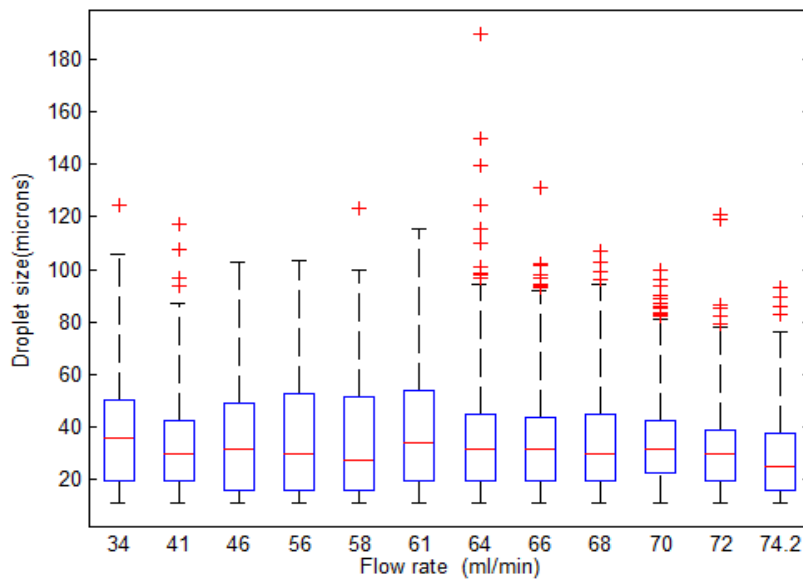
Figure 3.12: The relationship between droplet size distribution and nozzle flow rate.

The different size of boxes presented in Figure 3.12 indicates the different number of droplets and VMD produced at each level of the nozzle flow rate. The best result occurs when these two parameters converge and then the red line is located in the middle of a small box. According to the diagram, three boxes can be selected. These are when the nozzle is operating at a water flow rate of 61, 64 and 72 ml/s, respectively. The first two pressure values are in fairly good agreement with the recommendations provided by the designer of this nozzle [11], i.e. these produce the desirable droplet size distribution. Despite the nozzle being able to achieve the study aims at 72ml/s, this value was ignored owing to the high energy it would require. In addition, the electrostatic nozzle when operated at 55 psi will miss some parts of the plants.

In order to check the distribution of the droplets for each level of the flow rate, in Figures 3.13 to 3.24, the percentage of droplet size is plotted as well as their accumulated percentages. In these Figures, the droplet size distribution for all the levels of air pressure used is for one burst of spray. The size of droplet starts to increase and then is reduced again, but the VMD included at each level of air pressure is different. The best level is that which produces high numbers of the desirable droplet size and with the electrostatic nozzle this is ~35 µVMD.
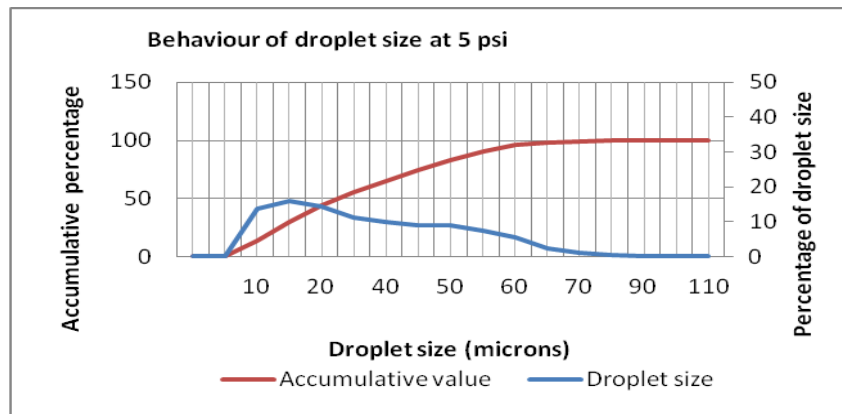
Figure 3.13: The droplet size distribution at 5 psi (or when the flowrate is equalled 34ml/s).
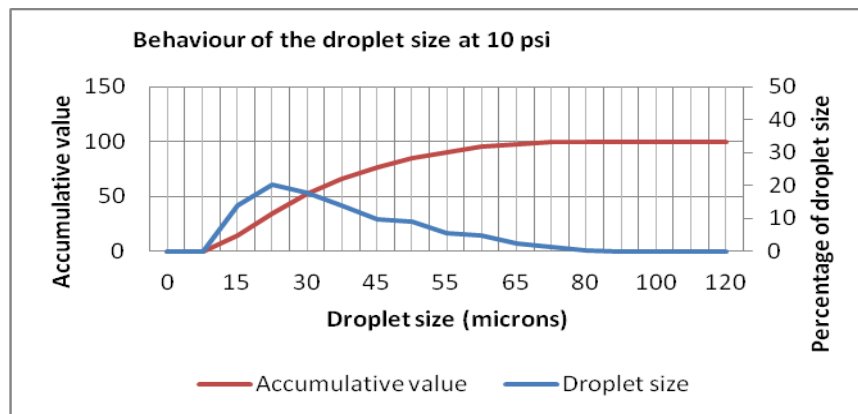
Figure 3.14: The droplet size distribution at 10 psi (or when the flowrate is equalled 41ml/s).
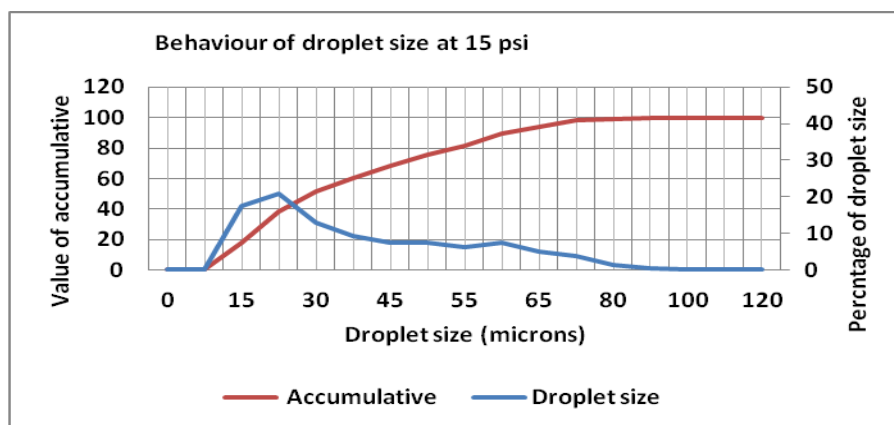
Figure 3.15: The droplet size distribution at15 psi (or when the flowrate is equalled 46ml/s).
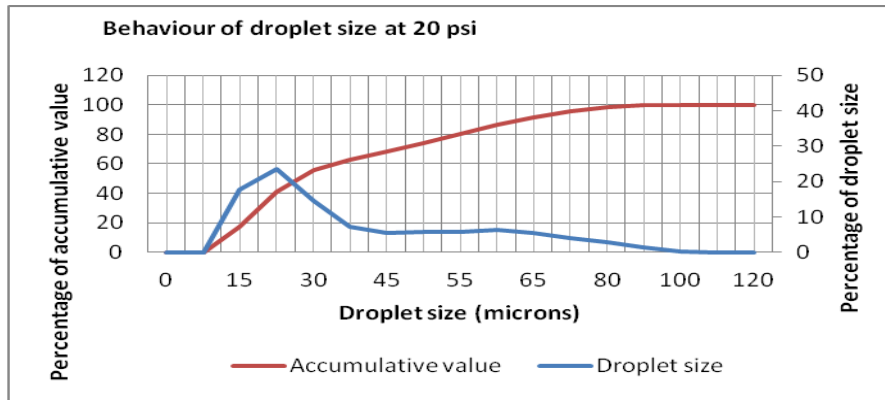
Figure 3.16: The droplet size distribution at 20 psi (or when the flowrate is equalled 56ml/s).
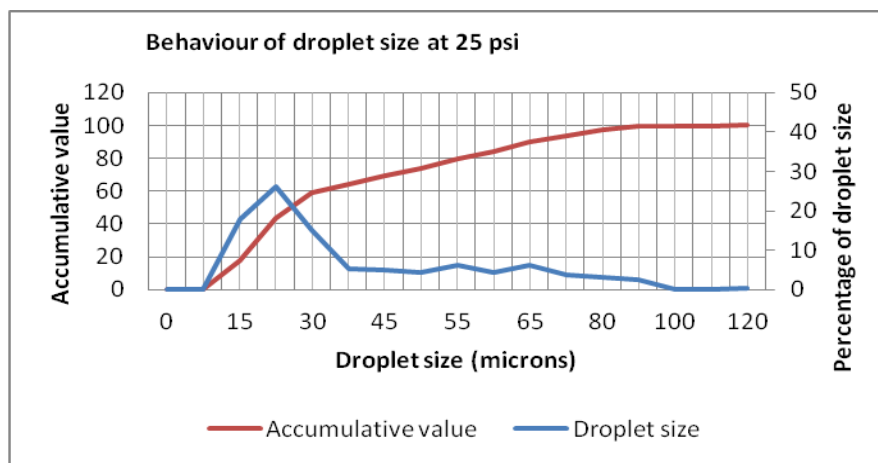
Figure 3.17: The droplet size distribution at 25 psi (or when the flowrate is equalled 58ml/s).
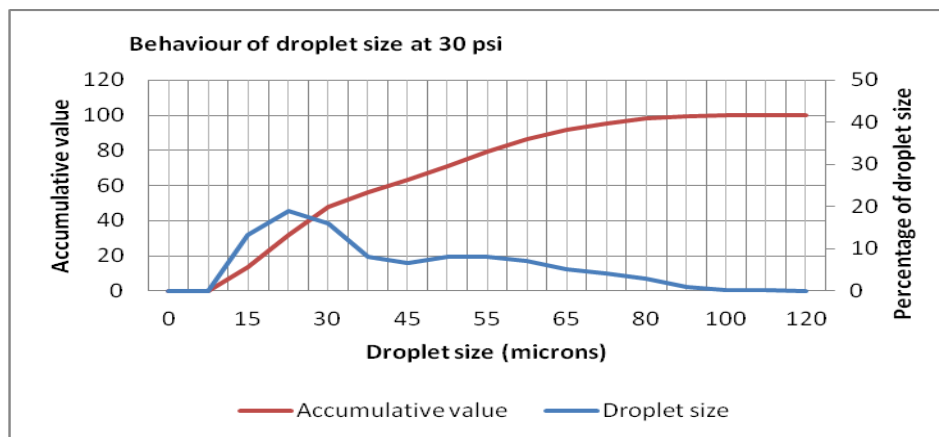
Figure 3.18: The droplet size distribution at 30 psi (or when the flowrate is equalled 61ml/s).
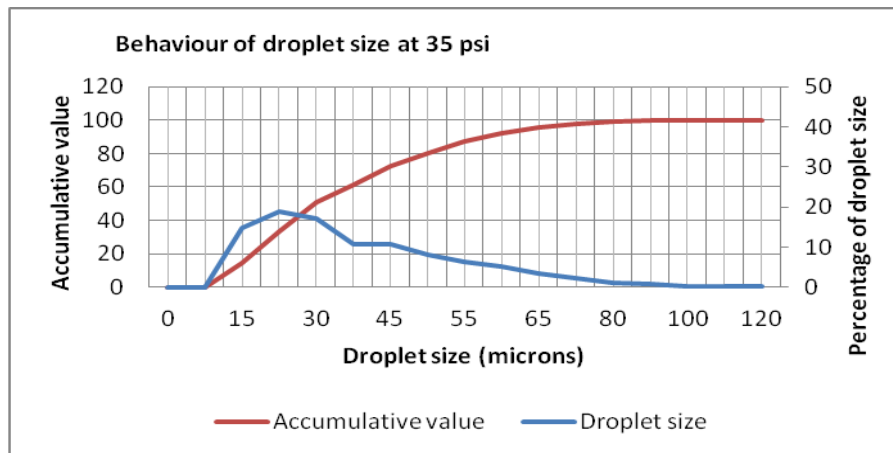
Figure 3.19: The droplet size distribution at 35 psi (or when the flowrate is equalled 64ml/s).
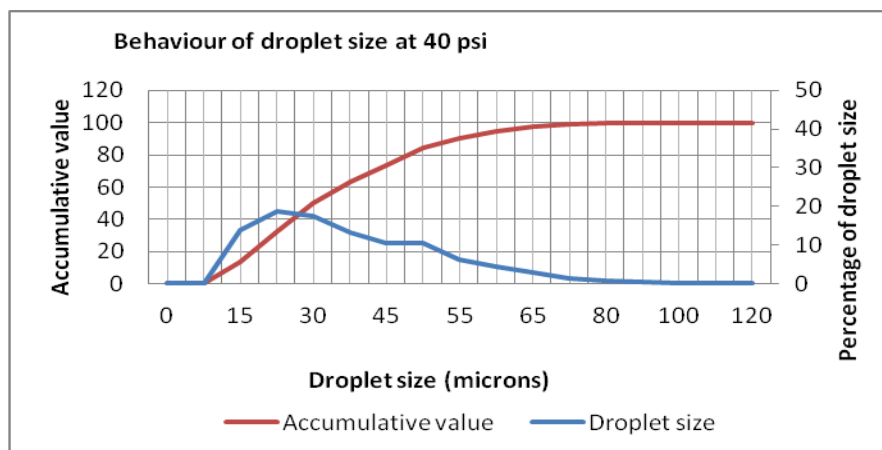
Figure 3.20: The droplet size distribution at 40 psi (or when the flowrate is equalled 66ml/s).
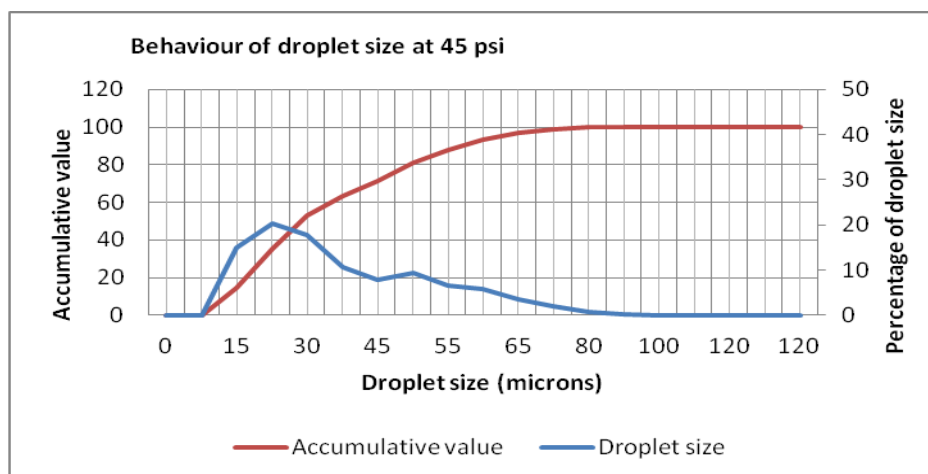
Figure 3.21: The droplet size distribution at 45 psi (or when the flowrate is equalled 68ml/s).
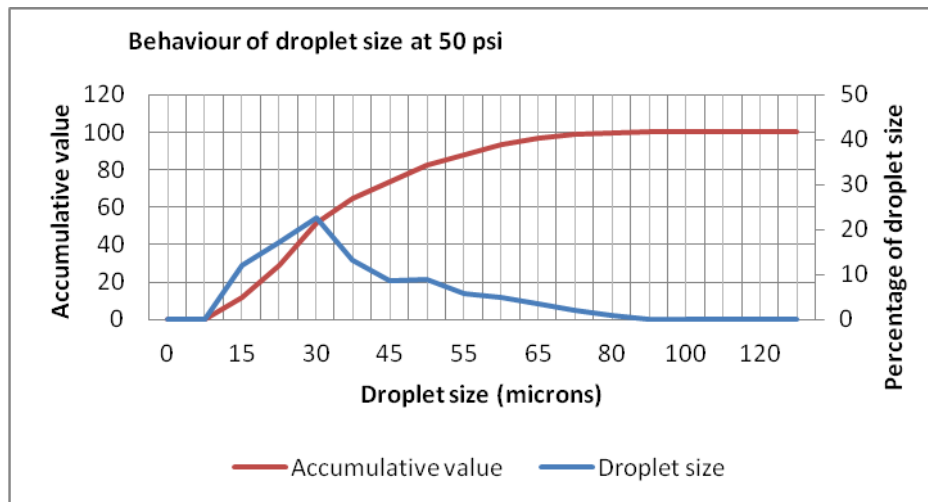
Figure 3.22: The droplet size distribution at 50 psi (or when the flowrate is equalled 70ml/s).
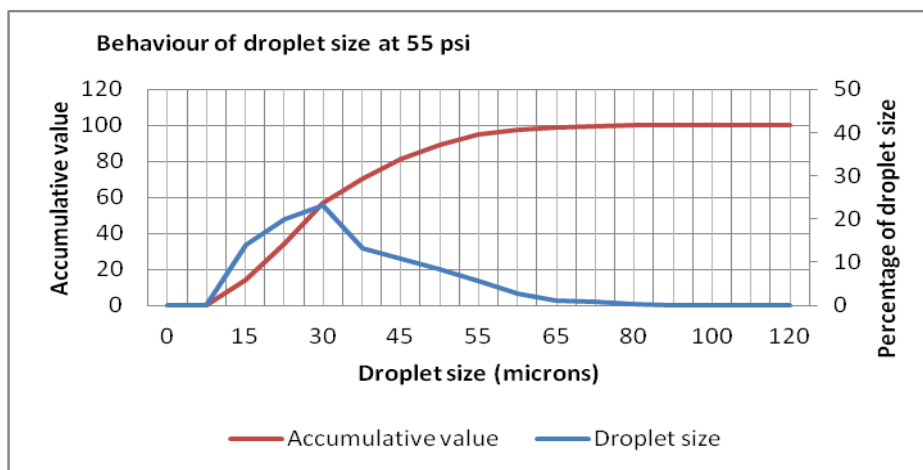
Figure 3.23: The droplet size distribution at 55 psi (or when the flowrate is equalled 72ml/s).
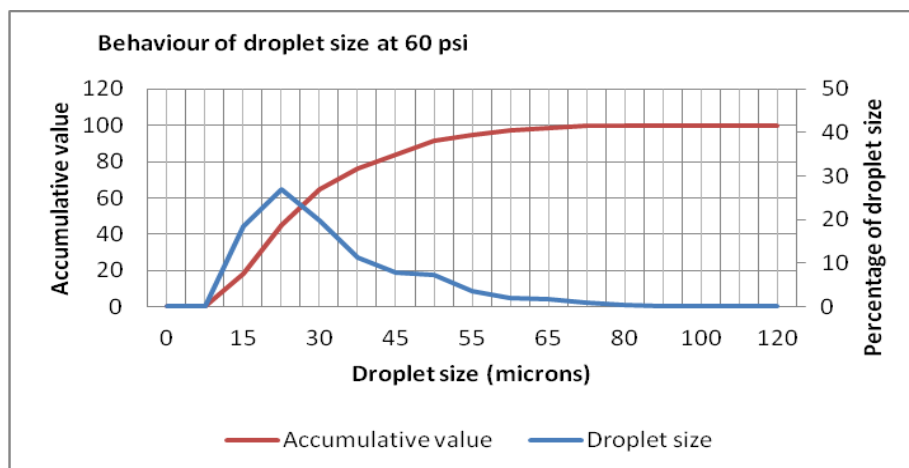
Figure 3.24: The droplet size distribution at 60 psi (or when the flowrate is equalled 74.2ml/s).

In order to get an overall Figure for each level of psi, the averages of the droplet size distribution were calculated and plotted as shown in Figure 3.25. From this it would appear

that for the electrostatic nozzle an air pressure ranging from 30 psi to 35 psi will produce the desirable droplet size.
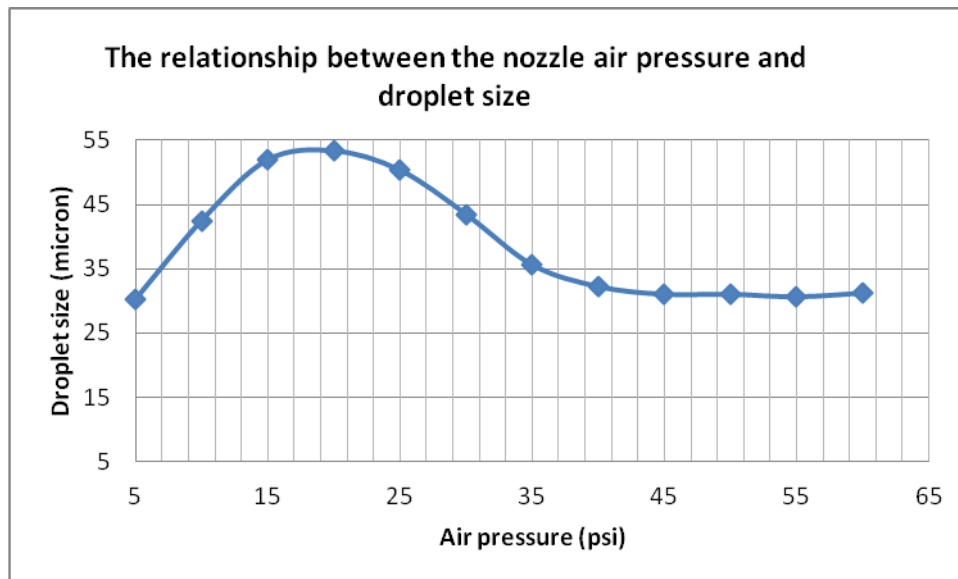
Figure 3.25: The averaged droplet size with air pressure.

3.6.2. Using water sensitive paper and Image J

Water sensitive paper was attached on the top and bottom a surface of the plant leaves (see Figure 3.26 below).

Figure 3.26: Artificial plants inside the Faraday pail with water sensitive paper on the top and bottom surfaces of the leaves (1,2,3, and 4).

The two reasons for using the paper were to measure the coverage area and droplet size for both with and without charging. These results were then compared with those collected from the Matlab image program. The papers were left in the laboratory for one day so as to become completely dry prior to their analysis. Then, a digital microscope USB camera was used to take photos of the samples. The area captured by the digital USB was 0.5mm^2 or 640x480 pixels, 1.2 MB. Image J software was used to analyse the results and the processing of this program is described next.

3.6.2.1 Image J procedure

After sending a microscopic picture to the Image J program from the option open file, the measuring tool in the taskbar was selected to measure the droplet size in the picture. The set scale option in the list in the analysis window was used to select the type of the unit and to measure the droplet size. The measuring tool involved drawing a line that was the diameter of the droplet over it on the magnified photo, which was displayed on the computer screen. This was automatically saved in a table located within the program and all the results were recorded using the type of unit selected [96].

Figure 3.27 shows the pictures taken to capture the top and bottom surface droplet size and distribution for both with and without charging. The results obtained from the analysis of the samples indicate that the coverage area with charged droplets is greater than for the uncharged condition. Moreover, the amount of coverage area is in a ratio 3 to 1 for charged and uncharged sprays, respectively. Regarding the other side (underside), the coverage area achieved is in the ratio 2 to 1 for the charged and uncharged surfaces, respectively (see Figure 3.28).
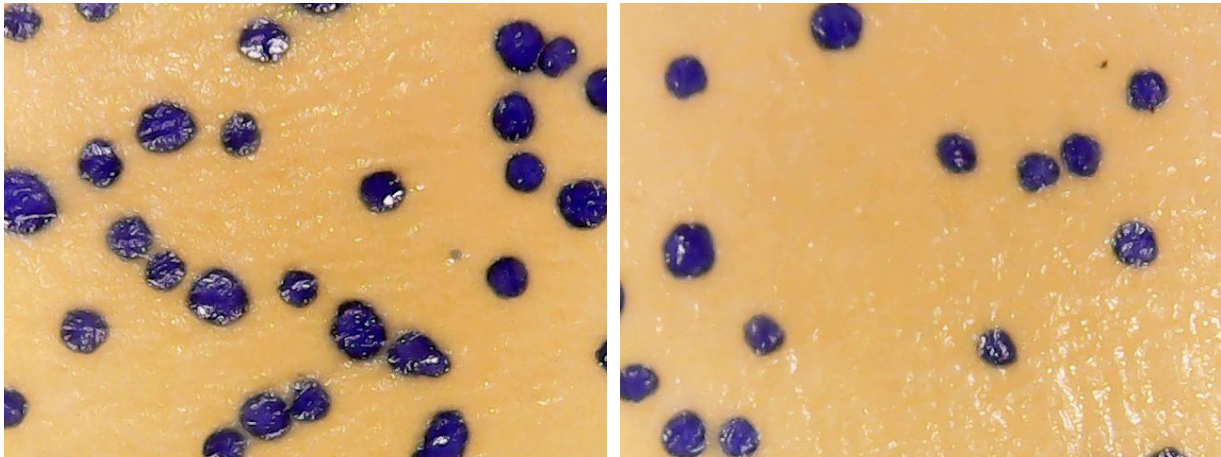
Figure 3.27: Microscope pictures for the top surface with (left) and without charging (right).
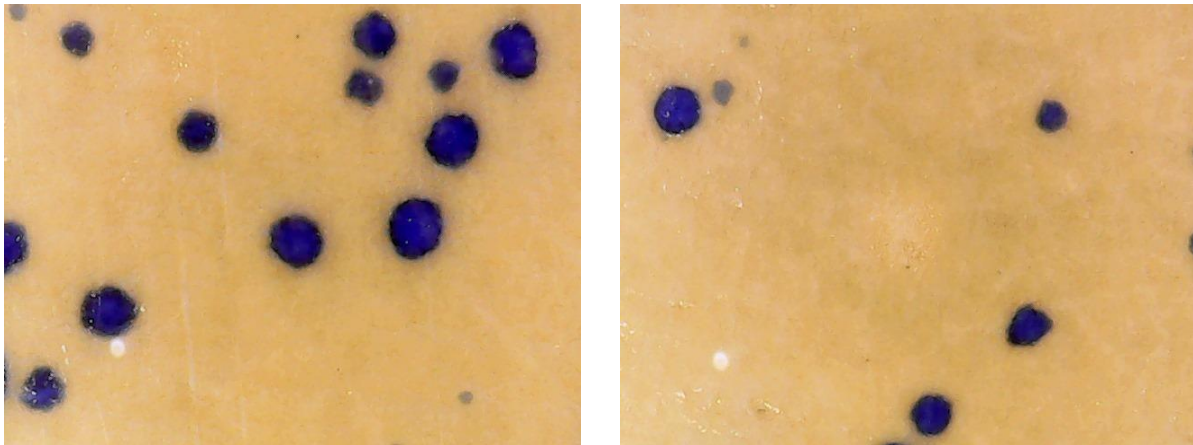
Figure 3.28: Microscope picture for the bottom surface with (left) and without charging (right).

As the nozzle used the induction charging method in these experiments, the electric field created was controlled by the distribution of the nozzle atomization and increased the deposition when compared to without an induction voltage. In fact, it emerged that the electric field lines allow for good coverage of all the surfaces of the intended targets, evidence of which is provided by the pictures taken with the high-speed camera, some of which are presented below (see Figure 3.29).
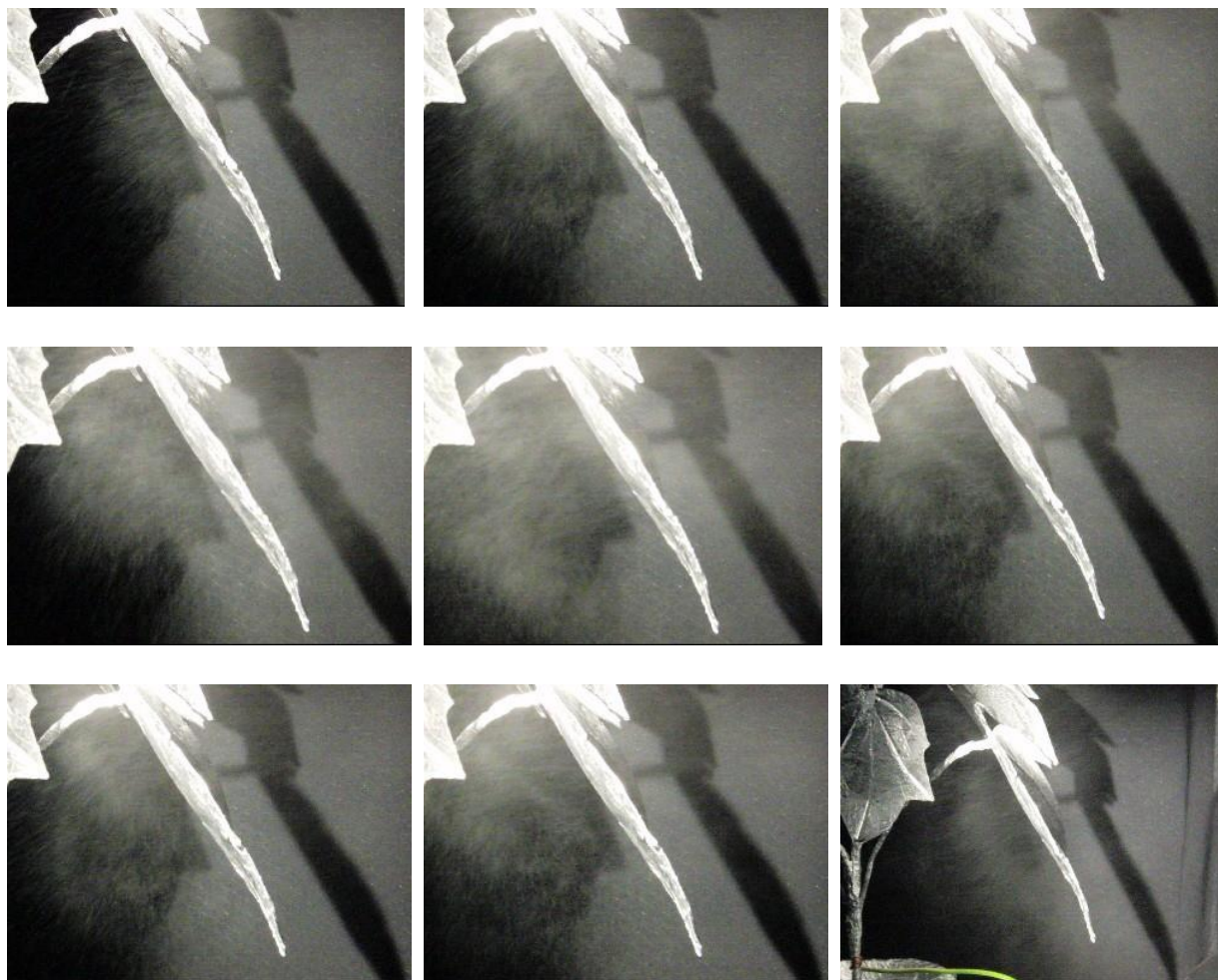
Figure 3.29: Pictures showing that induction charging increases deposition on the bottom surface of the leaf.

3.6.3 Droplet size measurement

Table 3.1: Water sensitive paper results for droplet size.

Droplet area (si^2)	Droplet size (size measurementthat	Actual droplet size after correction by dividing by 1.7 (F*).	Average value
1,736.089	47	27	
4,304.202	74	43	
1,736.181	47	27	
3,906.182	70	41	
4,774.243	77	45	
3,038.181	62	36	
3,906.242	70	41	
1,302.061	40	23	
2,170.101	52	30	34.6
1,736.081	47	27	
1,302.061	40	23	
2,604.121	57	33	
2,170.129	52	30	
1,736.081	47	27	
2,604.121	57	33	
3,472.162	66	38	
3,038.173	62	36	
3,038.148	62	36	
4,774.323	77	45	
3,472.162	66	38	
3,038.142	62	36	
4,340.259	74	43	
3,906.233	70	41	

F* = is the factor for expansion of the droplets on the water sensitive paper, which is equal 1.7.

To measure the droplet size on the water sensitive paper, Image j software was used and the results obtained are shown in table 3.30. Droplet spread factor correction has to be applied to obtain the right diameter of the airborne droplet. To this end, it is taken that the water sensitive paper magnifies the droplet size by a factor of 1.7 as recommended by the paper makers Q-Instruments [97]. The results indicate that the VMD produced is 34 to 35 μm, which match with that obtained from the image processing of the Matlab software (see Figures 3.12 and 3.25). Moreover, the results are in good agreement with the features of the electrostatic nozzle mentioned [11].

3.6.4 Summary

The set-up of the laboratory experiments aimed at studying the properties of the chosen electrostatic spraying nozzle have been presented in this chapter along with the results. The principles of electrostatic spray application were established, and outcomes from testing the

nozzle are to be drawn upon when designing the new induction nozzle to be manufactured in this project. The factors tested in this chapter have included nozzle water flow rate, nozzle air flow rate, space charge density, spray current, charge to mass ratio, coverage area and the droplet size distribution. The results obtained from the experiment are consistent with those of the electrostatic nozzle designed by Law in terms of the different desirable parameters. In addition, the results regarding the measurement of droplet size obtained from Matlab image processing and those collected by using Image J, match.

CHAPTER FOUR: NEW NOZZLE DESIGN AND MANUFACTURE

4.1. Introduction

In this chapter, the experiments conducted using the fan hydraulic nozzle so as to be able to convert it into the more efficient form is explained. Subsequently, the steps taken using a COMSOL simulation to establish the features of the new induction nozzle are presented. Finally, all the stages of SOLIDWORKS and 3D printing used to build the new induction nozzle are provided.

4.2. Spray system description

A new nozzle was required that would have the correct properties for efficient spraying of cotton plants in Iraq, given the weather conditions, types of pests et., a explained in chapter 1. The system had to have the ability to move forward and backward so as to be at the distance required between the nozzle and the target before treatment is applied. It consists of a small mobile robot with the new induction nozzle attached to it. The reason for using such a robot is because it can move along rows in a field planted with cotton scanning the plants for insects. The induction nozzle employs electrostatic forces so as to be able to cover the front and back surfaces of the target. In addition, this method provides high coverage area on the target as well as less drifts and soil contamination. Also, this nozzle had to have smart features and a pulse type of operation so as to reduce the amount of pesticides used and hence, save the money as well as reduce pollution. This system has sensor devices in order to achieve this task. Specifically, a CCD camera, microcontroller with sensors is used to measure the distances between the nozzle and the target as well as setting the time for scanning the plant. The nozzle structure is explained next.

4.3. Nozzle Design

A commercial fan hydraulic spray nozzle (FHSN) was used to generate the required spray and a pair of induction nozzles were designed to control the spray in terms of spray angle and droplet size. Two stages were involved. The first one is to characterise the spray properties and second one is to optimize the induction electrode dimensions. The first stage was performed through a set of controlled experiments, and the results were fed into the second stage. This was executed using COMSOL multi-physics software to develop an FEM model of an induction FHSN, and a number of simulations were performed to find the best set of

induction electrode parameters. In the following two subsections, these two stages of the design process are explained in detail.

4.3.1. Selection and study of the nozzle properties

The commercial Fan Hydraulic Spray Nozzle (FHSN) [98] used in this project is the TEE jet -TO80015E from (Tee Jet Technologies), which operates at a pressure of between 3 and 4 bars and has spraying capacity of 0.59 l/min (see Figure 4.1).

Figure 4.1: The fan hydraulic nozzle.

The reasons for choosing this nozzle are due to its theoretical and practical properties. Regarding the former, it needs a low air pressure, is easy to use, is cheap, has a small size and is commercially available in the market. While the practical properties are that the nozzle flow rate and the sizes droplet produced are a good match with the Iraqi weather and with the aims of this study. However, order to achieve these aims of increasing the coverage area on the target as well as reducing drift and soil contamination, it was necessary to convert the fan hydraulic spray nozzle (FHSN) into an induction hydraulic nozzle (IHSN). This conversion required changing certain properties of the FHSN to obtain the IHSN and the experimental procedures for achieving this are described below.

First, the spray properties (dimensions of the liquid film spray plume and drop size distribution) of the chosen commercial fan spray nozzle (FHSN) had to be determined. Figure 4.2 illustrates the experimental setup used to study the liquid film shape and the dimensions.
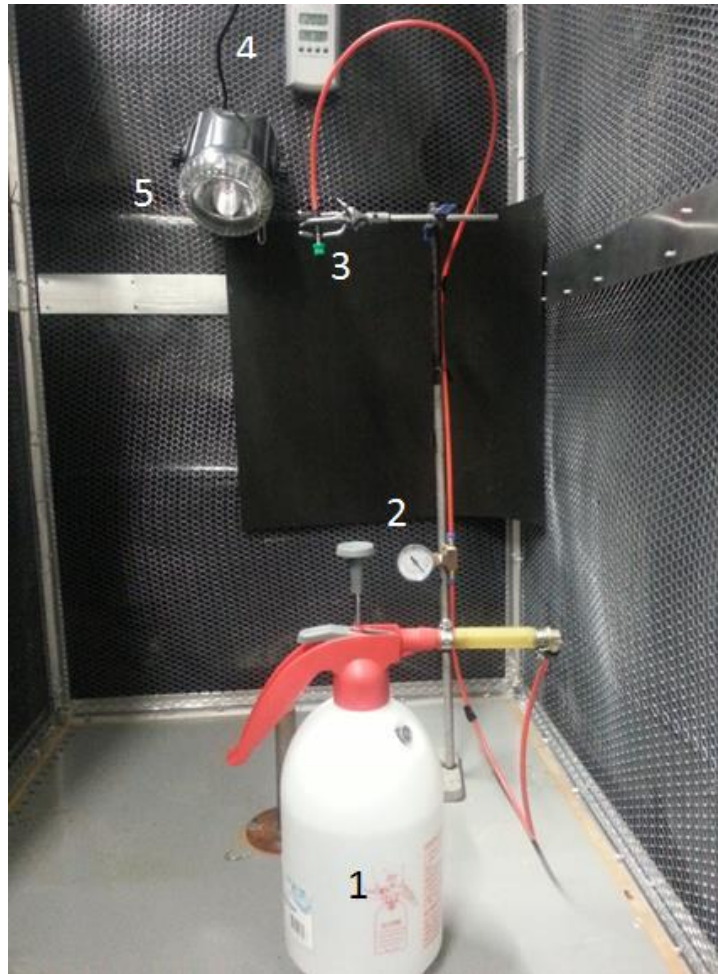
Figure 4.2: Experimental set-up for the fan hydraulic nozzle: Water bottle (1), air pressure gauge (2), (FHSN), measuring of relative humidity and temperature (4) and strobe light (5).

The experiment was conducted in laboratory conditions of 40% humidity and a temperature of 20 ^{0}C according to the reading of device attached inside the Faraday cage. The set up included a fan hydraulic spray nozzle (FSHN) connected to a water bottle by a 6 mm diameter plastic tube to maintain the water supply via the air pressure gauge, which was used to monitor the level of air pressure. In addition, a strobe light was used to capture pictures of distribution the droplets and their size after the nozzle liquid atomization. The shape of the thin film water spray captured off the atomization liquid is shown in Figure 4.3.
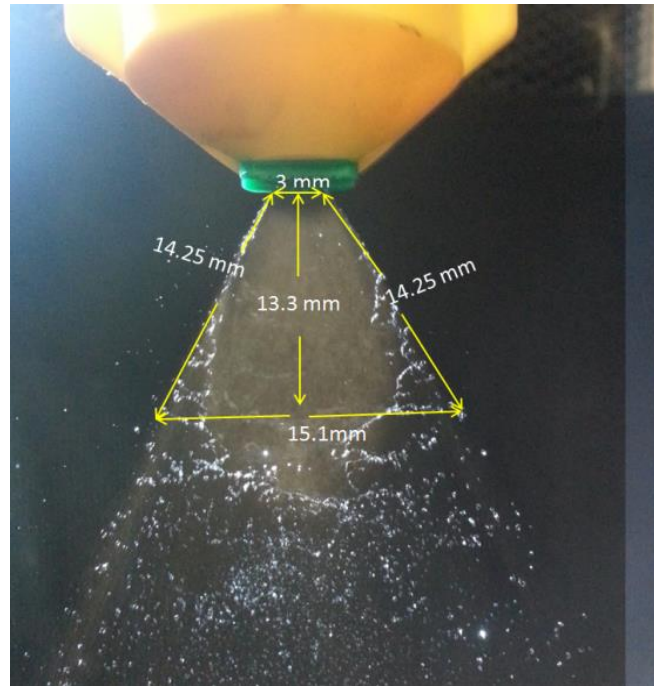
Figure 4.3: A thin film spray from the fan hydraulic nozzle.

The spray formed a diverging thin film which had a diverging semi cone shape with a vertical angle of 21.30° and Image J software was used to measure the liquid film dimensions, as explained in chapter 3[96].

4.3.2. Design of the induction spray

The second stage of design process was to devise a pair of induction electrodes in conjunction with the FHSN so that the spray could be controlled more effectively. That is, the spray dimensions (length, width and thickness) and electrode positioning were determined from this part of the design process. An FEM was developed using COMSOL multi-physics software, and a number of simulations were performed for various settings of the electrode parameters in order to achieve the aims described above. The underlying conceptualization regarding the design of the nozzle for the project is illustrated in Figure 4.4.
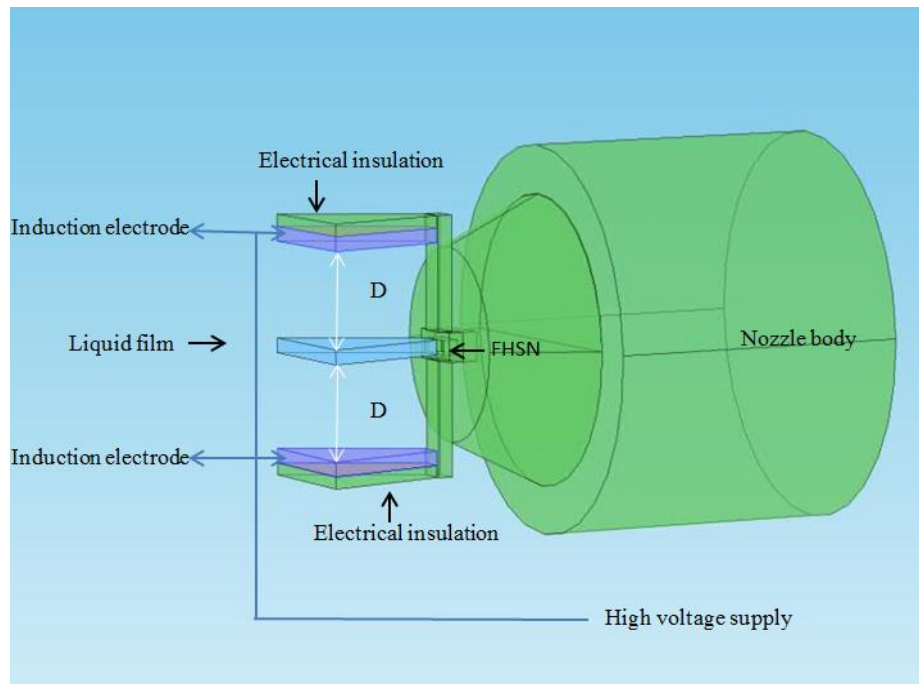
Figure 4.4: The proposed induction nozzle.

As shown in Figure 4.4, two nozzle electrodes are placed parallel to the thin film spray and separated by a distance D (known as the 'nozzle distance'), which is to be determined. By applying a high voltage (to be determined), the thin film spray can be split into tiny droplets, and the spraying angle can be controlled. The FEM COMSOL model was used to find the optimum nozzle electrode distance and high voltage for producing the desired properties of the spray. In addition, the induction electrodes were insulated using plastic to avoid any discharge to an external body, so too was the nozzle body in order to avoid any pesticide spray reaching the internal structure of the sprayer.

4.4. COMSOL simulation

The most accurate approach for solving electric field problems is using numerical techniques to find approximate solutions.

COMSOL metaphysics is used in this research because of the following features:

1-The software provides a method to solve electric field problems;

2- It allows for modelling actual phenomena that can occur when operating in an electric field;

3- It takes into account the relevant and provides results very quickly, thus saving time and money, when compared to other design methods.

4.4.1. COMSOL simulation

A finite element FEM model using commercial software (COMSOL multiphasic software) was employed to study and compare the electric fields generated between the electrode of the induction nozzle and liquid film of the nozzle spray for two cases [99]. In the first, different distances between the electrode of the nozzle and the liquid film of the nozzle spray were tested, from which the best position of the nozzle electrode was selected. This occurs when there is no contact between the nozzle and the liquid film as well as there being enough chargeability on the latter. Twenty levels of distances were deployed, and the increment between each was one millimeter. The second case pertained to using different levels of induction voltage in order to select the best, which refers to level that achieved enough chargeability without electric breakdown. The levels of the induction voltage used were 400 volts, 500 volts, 750 volts and 1000 volts.

The COMSOL shown in figure 4.5 explains how simulation of the induction nozzle was built. For this simulation, the type of model selected to design the nozzle was 3D and physics used was electrostatics in AC/DC field. Moreover, this simulation was stationary. The first activity is to make decisions about the geometry of the model design. The four parts constituting the nozzle model were the nozzle body, nozzle electrodes, and the covers of the nozzle electrodes and the liquid spray of nozzle spray. For the nozzle body, two geometrical shapes were selected, namely, cylinders and cone, while for the nozzle electrodes and the liquid film a trapezoid was chosen.
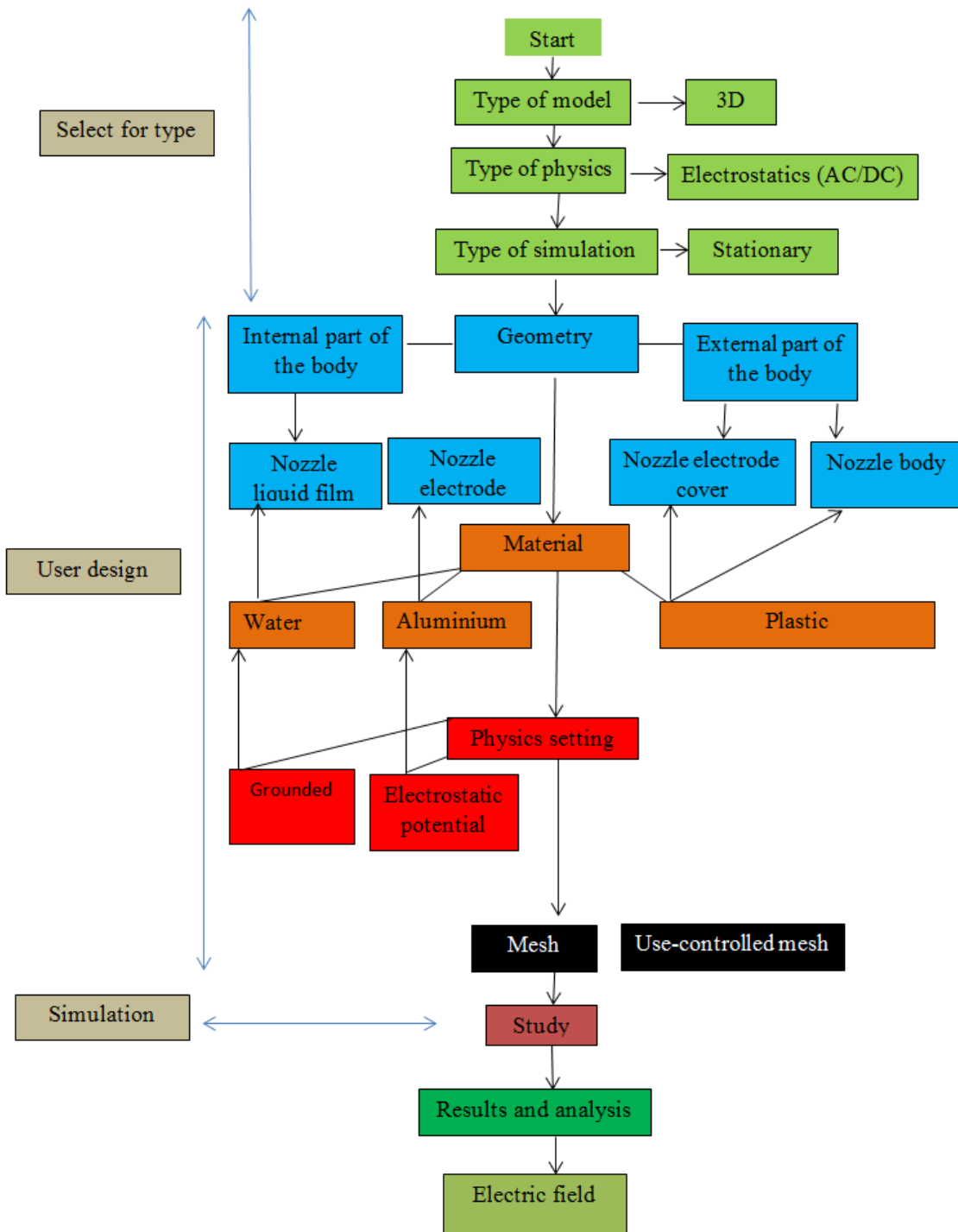
Figure 4.5: Flow chart of the development of the COMSOL model of the induction hydraulic spray nozzle (IHSN).

The next step was identifying the types of materials to be used in building the whole nozzle. Acrylic plastic was chosen to represent the nozzle body and the covers of the two electrodes of the induction nozzle, whilst water was used to represent the liquid spray of the nozzle sprayer. Finally, aluminum was used for the electrodes of induction nozzle (see Figure 4.6).
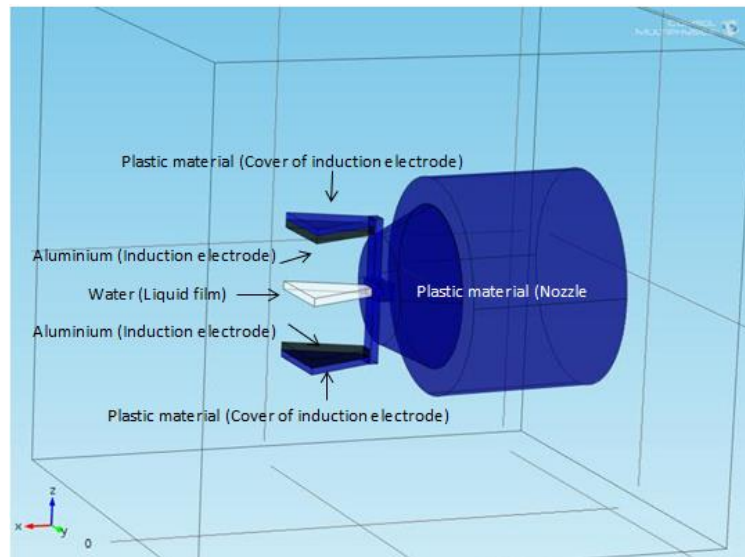
Figure 4.6: The COMSOL IHSN model showing the 3D geometry and material choices.

Regarding the physics of the experimental set step, the electronic elements were as follows. The whole body and the two covers of the nozzle electrodes had zero volts as they comprised insulation materials. Whilst the liquid film had ground value was connect to the nozzle body, which is of grounded value. Finally, the electrodes of induction nozzle gave electric potential due to their connection with the electrode attached to the high voltage supply. Figure 4.7 explains this physics as distributed throughout the nozzle model.
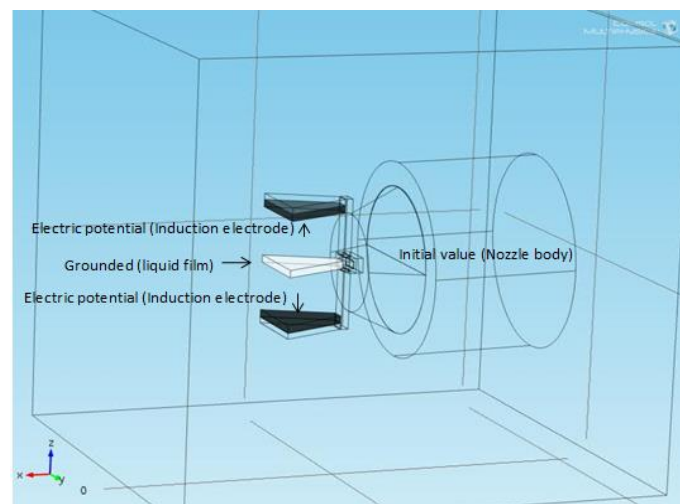
Figure 4.7: The COMSOL IHSN model showing the physics aspects.

In order to achieve a high chargeability value on surface of the liquid film, different values of induction voltages and different distances of the nozzle electrodes needed to be tried out. Seven levels of induction voltage were used for the simulations in ascending order, these being 400, 500, 600, 700, 800, 900 and 1000 V. While the distance of nozzle electrode positions had twenty levels of 1 mm increments, starting at 1 mm and ending at 20 mm. The COMSOL simulation computed all combinations of these voltages and distances. After all

simulated environmental conditions had been assessed the type of mesh to be used in the construction of the nozzle was provided by the software. Figure 4.8 illustrates the type of mesh selected.
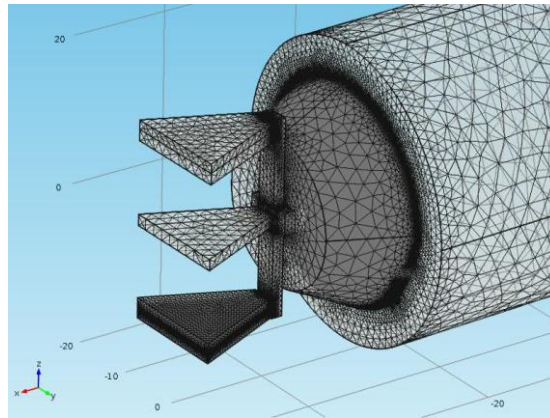
Figure 4.8: Mesh of the model.

The last step was computing the simulation in order to present and analyse the results, with the aim being to choose the design.

4.4.2. COMSOL simulation results

The results obtained from the COMSOL simulations of electric field values generated for all the cases described above are shown in Figure 4.9. From these outcomes, it can be seen that the value of the electric field was initially reduced when the distance between the electrodes of the nozzle and the liquid film was increased up until approximately 10 millimeters.
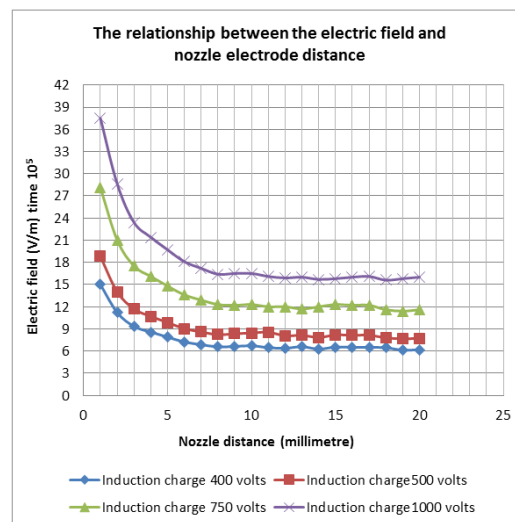
Figure 4.9: Association between electric field and nozzle electrode distance.

Subsequently, the value of electric field stabilised as the distance between the nozzle electrode and the liquid film was increased up to 20 mm, i.e. the maximum distance

employed in the experiment. The values of the surface charge density on the liquid film were calculated using the following equation;

$\rho = E * \varepsilon_0$ ----------- (4.1)

where,

ρ = surface charge density (C/m^2)

E = electric field (V/m),

ε_0 = permittivity of free space (8.8542 x10^{-12} F m^{-1}) or (8.8542 x10^{-12} C^2 N^{-1} m^{-2})

Figure 4.10 presents the surface charge densities that were calculated for all cases. From the results, it can be seen that the surface charge density exhibits the same behavior as the electric field. Moreover, the surface charge density remained relatively constant from approximately when the nozzle electrode distance was 10 mm up until 20 mm. The reason for this is due to the direct relationship between the two, as shown in formula 1 above.
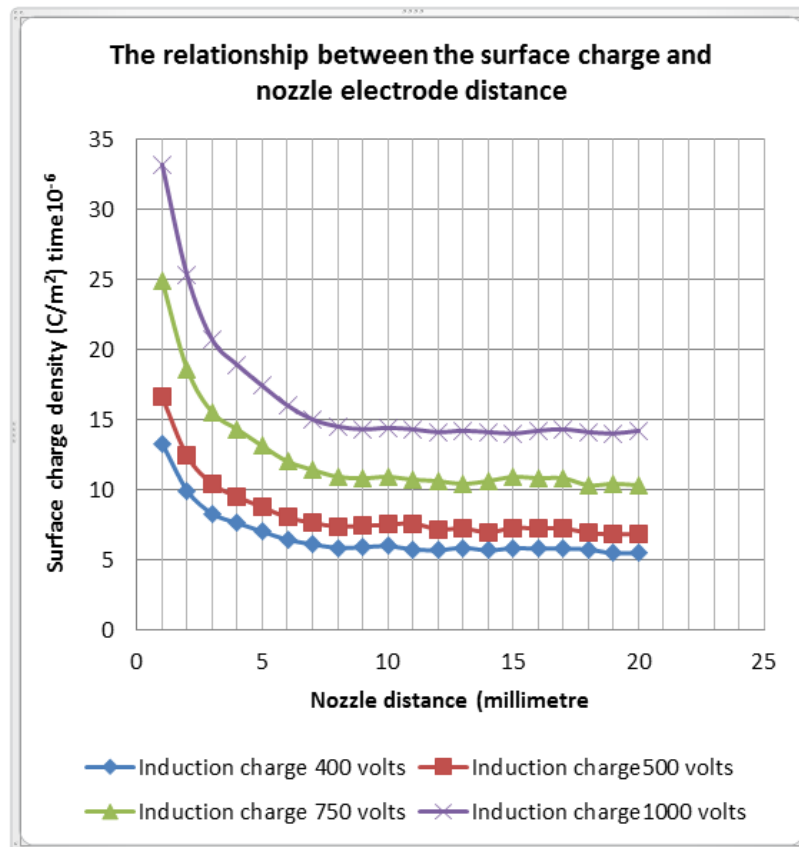
Figure 4.10: Association of surface charge density with the nozzle electrode position.

Given the results obtained for electric field and surface charge, the longer distances after 10 millimeters were ignored. The modified results of the electric field and surface charge density for up to 10 mm distance are presented in Figures 4.11 and 4.12, respectively.
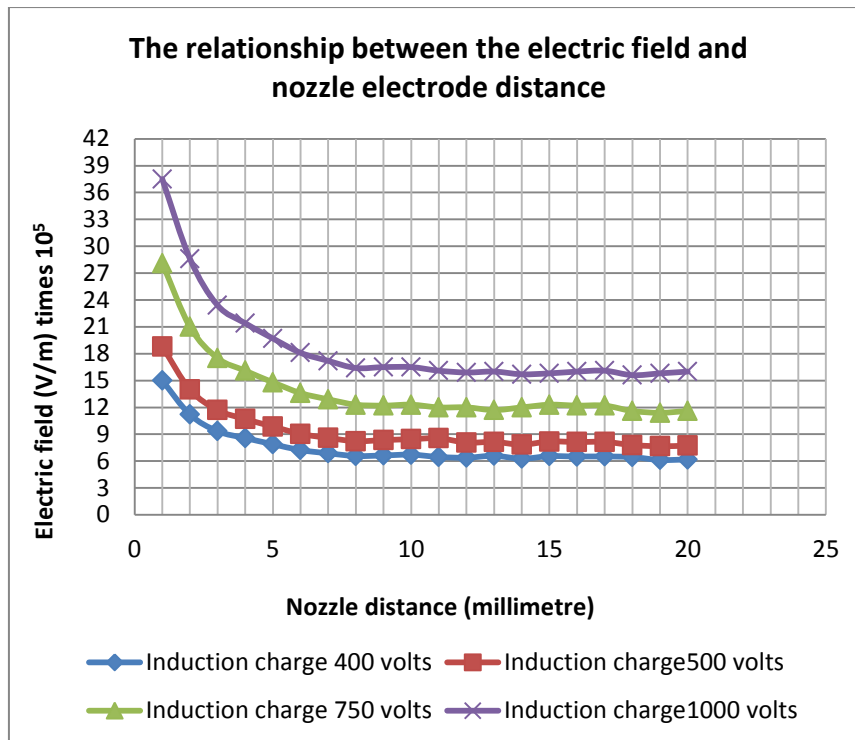
Figure 4.11: Association between the electric field values and nozzle electrode position.
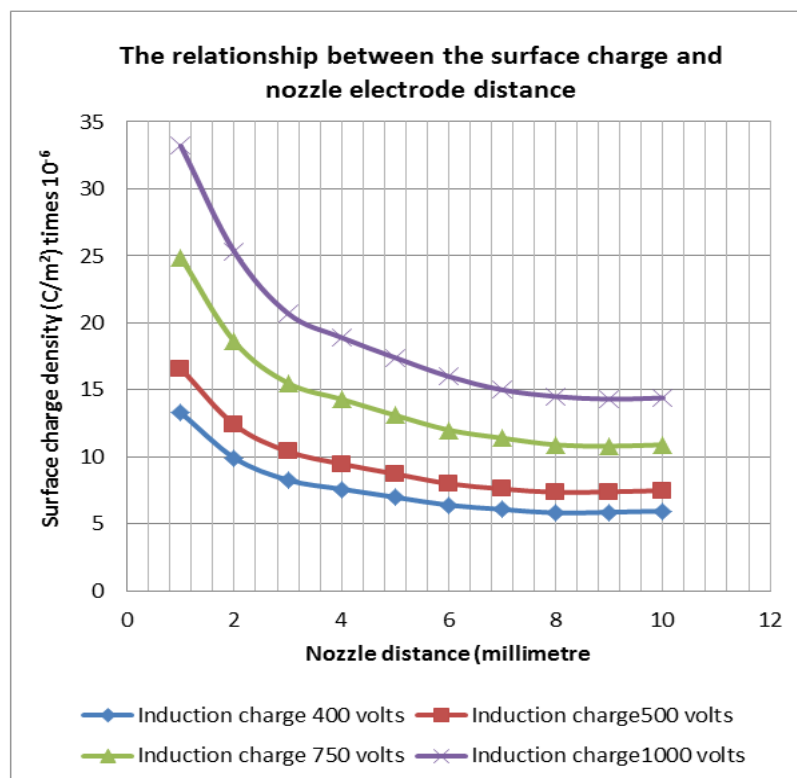
Figure 4.12: Association between the surface charge density values and nozzle electrode position.

As for the induction voltage levels, there appears to be a direct relationship between the levels of induction and the value of electric field created, as shown in Figures 4.9, 4.10, 4.11 and 4.12. Of the four levels used, that of 500 V seems to be the best as electric breakdown

occurs for the two higher values, namely, 750 and 1000 volts, whilst 400 volts cannot deliver sufficient chargeability. In sum, according to the results of the COMSOL simulation, two electrostatic parameters have been identified, with first being that the position of nozzle electrode has to be 10 millimeters away from the liquid film. This is because with this size gap no contact between the electrode of the nozzle and the liquid film of the nozzle spray is ensured. The second parameter is that the level of the induction voltage must be 500 volts as this gives sufficient chargeability, whilst avoiding the electric field break that happens at higher values.

Depending on these two factors as recommended by the COMSOL simulation and the value of the surface charge density calculated, the shape and the features of the induction nozzle created for this study are as shown in Figure 4.13.
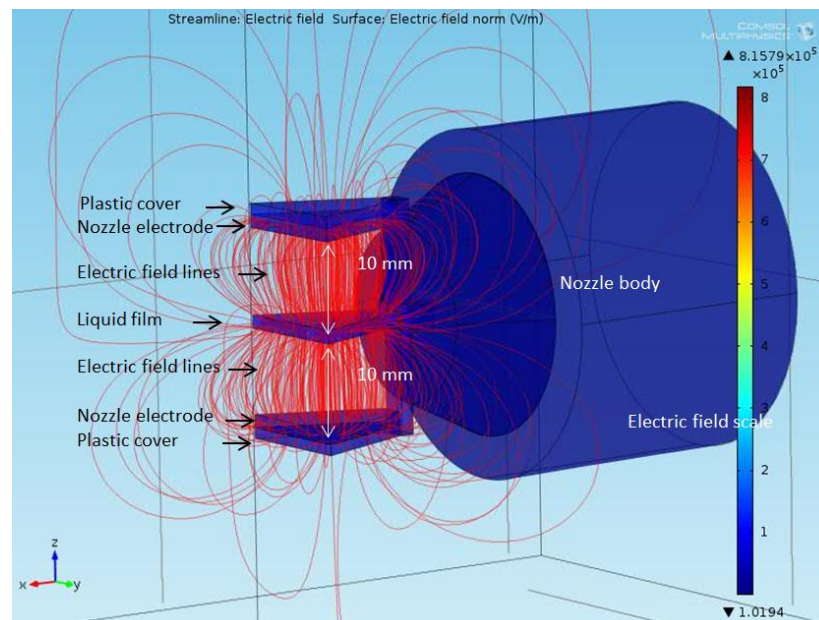
Figure 4.13: The last simulation for designing the induction nozzle.

4.4.3. Nozzle manufacture

Having established all the features for the induction nozzle used in this study, it was necessary to identify suitable software to draw the nozzle design and given the high ability of the SOLIDWORKS software in drawing, it was chosen for this purpose. A brief description of this software and how used it to design the nozzle is provided below.

4.4.3.1. SOLIDWORKS

SOLIDWORKS 3D is an integrated drawing software program that provides design manufacturing solutions. It provides product and manufacturing information (PMI) directly in 3D, bypassing time-consuming 2D processes, and eliminating potential problems. It helps

users define, organize, and publish 3D PMI, including 3D model data in industry-standard file formats (such as SOLIDWORKS files, eDrawings®, and 3D PDF). It guides the manufacturing process directly in 3D, helping to streamline production, cuts cycle time, reduce errors, and complies with industry standards. In addition, SOLIDWORKS software provides users with an intuitive 3D development environment that helps maximize the productivity of the available design and engineering resources to create better products faster and more cost-effectively [94].

Using this software, two parts of the induction nozzle were drawn. The first consisted of the shape of the liquid film, shape of the nozzle electrode and the shape of the plastic cover for the electrodes. The shapes these sections have to have are shown in Figure 4.14. The reasons for having these parts of the nozzle are as follows. First, the nozzle electrode design has to cover completely the spray liquid film and so they both have the same shape. Second, the plastic cover has to cover the nozzle electrode completely in order to prevent any liquid reaching the nozzle electrode and hence, discharge occurring.
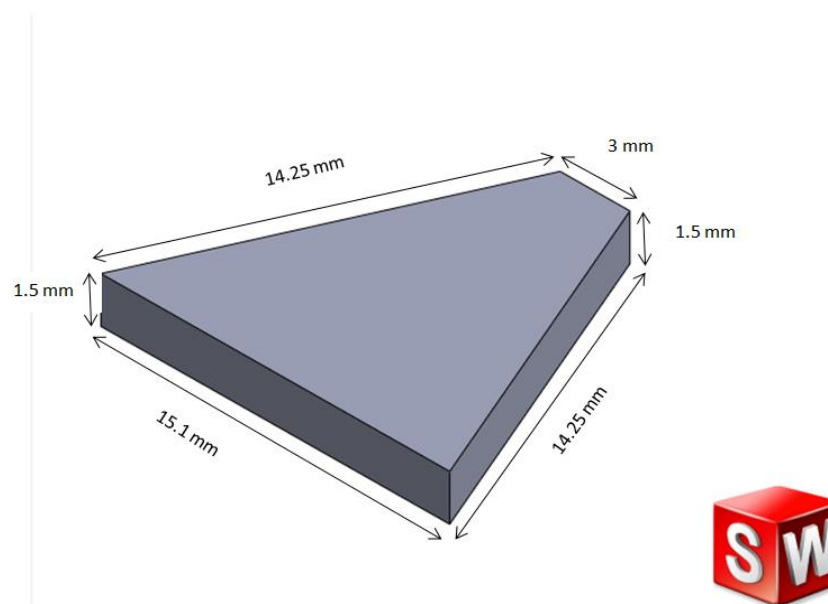
Figure 4.14: The shape of part one.

The second section pertains to the external cover connected to all the parts of the section one as one unit, which depends on the distances that there must be between these parts. Figure 4.15 shows the shape of the section two that the software generates.
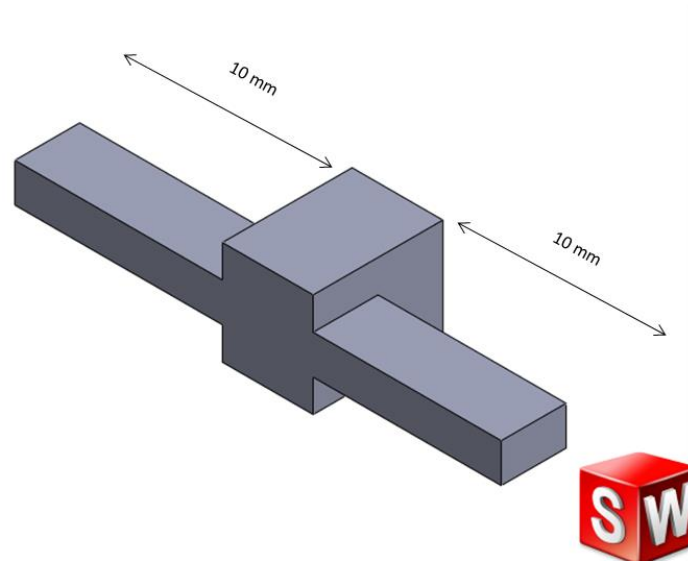
Figure 4.15: The shape of the part from section two.

The final shape of the induction nozzle after connecting the two sections one and two is shown in Figure 4.16.
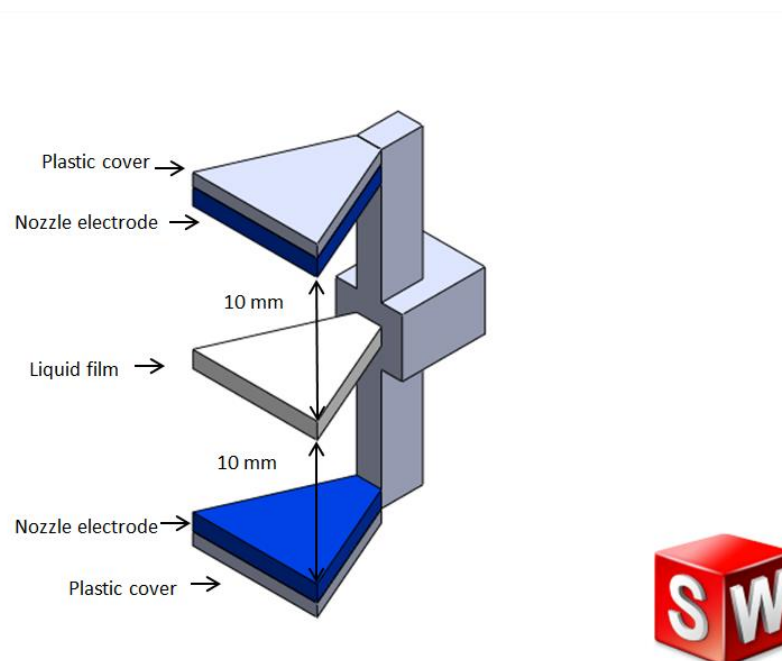
Figure 4.16: The final shape of the induction nozzle as drawn by SOLIDWORKS software.

4.4.3.2. Building the induction nozzle

After completing the drawing of the nozzle according to the required properties, the SOLIDWORKS software file was transferred to the 3D printer system to build the parts of the nozzle. 3D Printing does not just produce a prototype but rather, manufactures the real object and hence, the actual nozzle was produced by it [100]. Figure 4.17 shows both the 3D printer file diagram of the nozzle and the completed plastic printout.
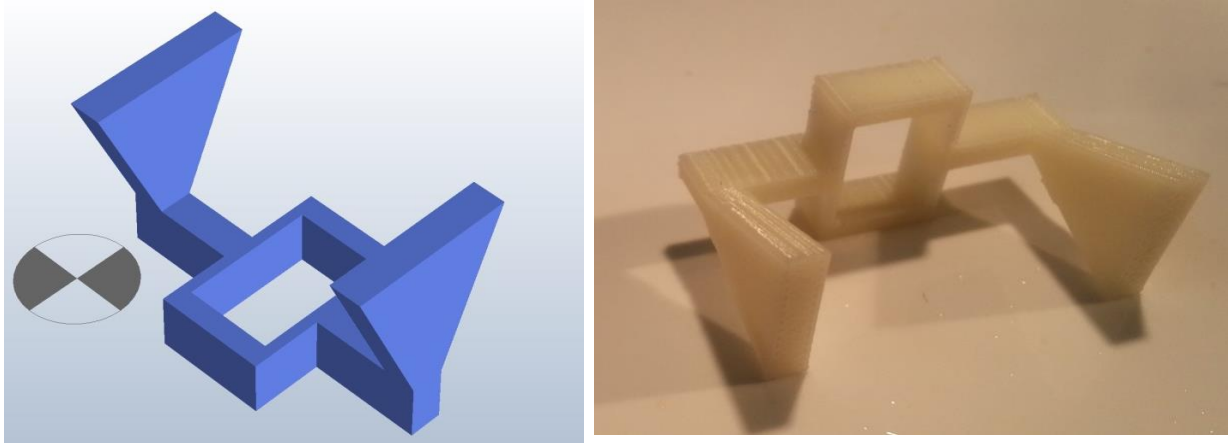
Figure 4.17: 3D Printer file (left) and the plastic section after printing (right).

The last part to make was the electrode of the nozzle, which had to be manufactured from material with good conductivity as it is to be connected with the high voltage supply to provide induction voltage. Consequently, this made from aluminum with the same dimensions of the liquid film and the plastic cover for the nozzle electrode as presented above. Figure 4.18 illustrates how this nozzle is connected to the wire of the induction voltage, and the sharp metal edges of the electrodes were filed down in order to avoid electric discharge before using the nozzle.
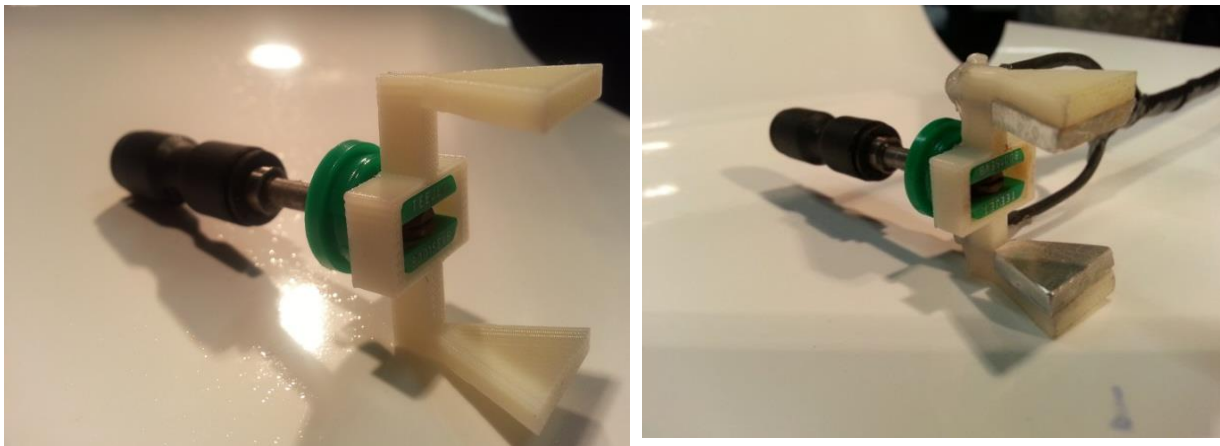
Figure 4.18: How the plastic section and nozzle electrode are connected to the fan hydraulic nozzle (FHSN).

4.5 Summary

The process of designing the new induction nozzle has been described in two sections. The first investigated the properties of liquid atomization in laboratory experiments. Moreover, there was comprehensive explanation of the steps of the COMSOL simulation that was used to design the new induction nozzle. The second section covered the steps involved with the nozzle building using the SOLIDWORK software and a 3D printer. The COMSOL simulation pictures to explain the simulation steps, and photographs of the final shape of the induction nozzle have also been provided in this chapter.

CHAPTER FIVE: MINI ROBOT BASED SMART ELECTROSTATIC CROP SPRAYING SYSTEM

5.1. Introduction

This chapter describes all the stages used to assemble the mini mobile robot and the systems that support the actions of the new electrostatic system. In addition, explanations are provided for the choices made in relation to the components of the robot aimed at ensuring optimal performance of the crop spraying system.

5.2. The key characteristics that need to be considered for the robot design

Certain factors had to be taken into account when conceptualizing the electrostatic system, these being: the type of the nozzle, the nature of the plant and its cultivation as well as the robot itself. A brief explanation for each is provided below.

5.2.1. The nozzle selection: One of the study aims is searching for the insects and focusing the treatment on their location. This required an especial nozzle with smart behavior that can make decisions according to the results obtained from the plant's environment. Given this requirement, hardware and software, including a CCD camera and other sensors devices were necessary for guiding the nozzle operation. Moreover, all of these elements needed combining into one unit that could be operated a under controlled system.

5.2.2. Nature of the plant: The second factor pertains to the nature cultivation of the cotton plant, for in Iraq, cotton is always planted in lines 50 to 60 cm apart. Thus, in order to search effectively for pests, the mobile system needs to be of the right dimensions to be able to move freely amongst the rows of plants and maneuver the nozzle in such a way that it does not damage plants and yet, does find its target.

5.2.3. Robot design: The robot design had to be suitable for achieving the goals within a commercially viable cost.

5.3. General information

From the literature review, it can be said with confidence that electrostatic assisted crop spraying is an efficient way to improve plant coverage and to reduce wasted chemicals as well as soil pollution. Specifically in accordance with the aims of the current research, it was deemed appropriate to introduce smart automated crop spraying device using a mobile robot

to achieve these goals. The design would ensure that instead of targeting the whole plant during pest control operation, only the insects would be sought out and once identified, where necessary, small bursts of pesticide spray would exterminate them, thereby minimizing pesticide consumption and soil contamination.

To put this concept in action and demonstrate its feasibility, first, based on the literature and previous experimentation outcomes, the smart mobile robot spraying system components required were chosen. Specifically, in this regard, the mechanical components comprising the mobile platform and the robotic arm along with their associated drive motors were selected according to the following criteria: well defined kinematic analysis, effective load handling characteristics, a gripper reach required to handle average cotton plants and good manufacturer support. Having taken these into account, the TTRK-KT tracked electric vehicle from Lynxmotion™ and an AL05D robotic arm were selected, being also deemed to have the characteristics to cover the basic requirements of the proposed design, which requires moving a pesticide spraying system around a cotton plant field. In particular, the plant height and soil characteristics call for a tracked vehicle to be used rather than one that is wheel based.

The AL05D robot arm can lift loads of up to 285 grams without any modification to the motor system. The estimated load on the gripper in the new design is about 130 gm, which includes the camera, the distance detector and the electrostatic spray nozzle assembly. This means that the arm can run for long periods without the risk of overloading its drive components. The maximum height reached by the AL05D arm is 48.26 cm on top of the height of the robot arm base of 7.899 cm and the tracked vehicle platform to ground clearance of 3.221 cm, which results in a 59.38 cm total maximum height reached with respect to ground level. This height is sufficient to manage cotton plants at the time they become most susceptible to cotton insect infestation [101].The information used in this section was obtained from AL0D5 and TTRK-KT data sheets (see appendix A) [102]. The second section covers the drive requirements of the mechanical system in addition to the intelligence that is required and this is explained in Section 5.4.

5.4: Assembling the mechanical parts of the system.

The AL0D5 and the TTRK-KT arrived in a completely unassembled kit form (CKD) and required an extensive construction process. Specifically, The AL0D5 robotic arm kit contained all parts required to assemble the complete robot manipulator, consisting of all

metal parts, several plastic parts made of laser-cut Lexan, and four drive servo motors. Figure 5.1 shows the unassembled parts of the robotic manipulator.
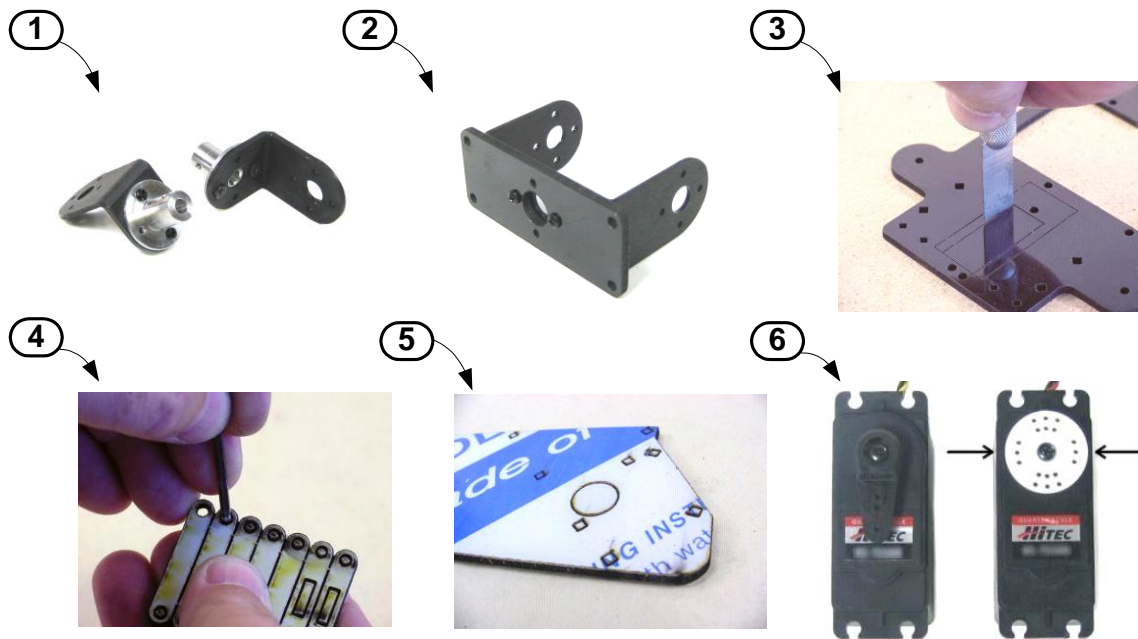
Figure 5.1: Pictures of some unassembled components of the AL05D robotic arm: 1-elbow to wrist link parts, 2- shoulder to elbow link parts, 3, 4, 5- laser-cut Lexan robot assembly parts, 6- servo drive motor of the robot manipulator joints.

The assembly process involved putting together several metallic and plastic parts along with laying out the wiring required to operate the servo motors that govern the manipulator joints' movements according to the instructions provided by the robotic arm kit manufacturer [103]. The assembly time was about six hours, which included connecting the robot motor wiring to the drive electronics board. Figure 5.2 shows some of the steps in the assembly process for the robotic manipulator.
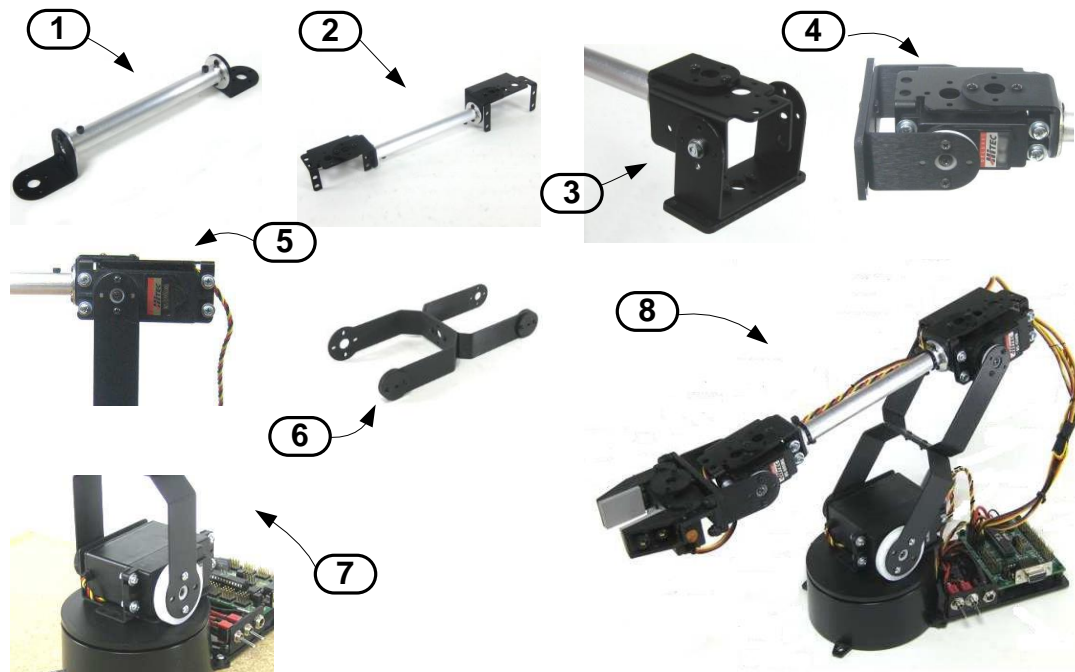
Figure 5.2: The assembly of the robot manipulator : 1-2-3-4-5- the assembly of the wrist –elbow link with its drive servo motor, 6-7- the assembled elbow – shoulder link on the manipulator platform, 8- the fully assembled robotic manipulator arm along with its drive electronics.

The TTRK-KT tracked electric vehicle kit contained all the necessary parts required to assemble the mobile platform as to be able to accommodate the robotic manipulator along with its associated electronic circuits necessary for the smart electrostatic crop spraying robot. Figure 5.3 shows some of the basic parts that the tracked electric vehicle was assembled from.
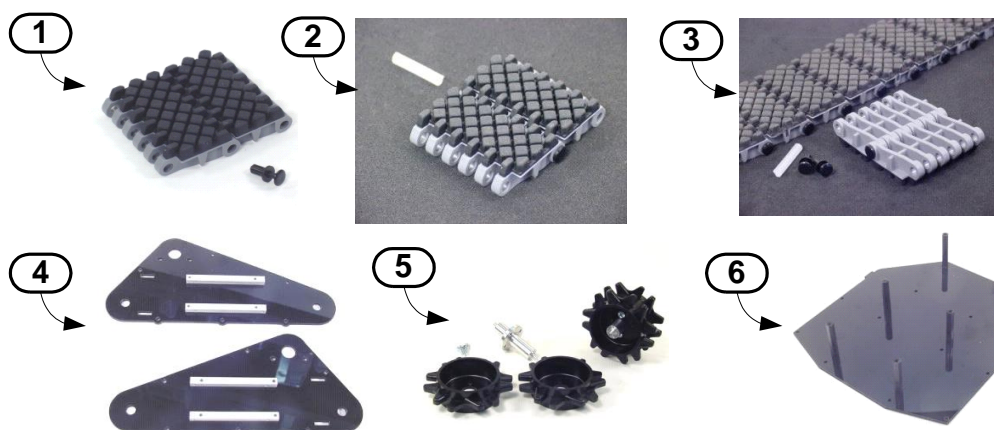
Figure 5.3: Some of the unassembled parts of the TTRK-KT mobile platform: 1- track segment, 2- two track segments joine, 3- assembled track, 4- Lexan track drive housing, 5- track drive sprockets, 6- the lexan platform of the tracked vehicle.

The assembly process of the tracked mobile platform for accommodating the assembled robotic manipulator and system electronics involved putting together several metallic and plastic parts along with mounting and wiring the two drive DC motors required to operate the tracked vehicle. The assembly followed the procedure provided by the tracked vehicle kit manufacturer [104] and took about four hours. Figure 5.4 shows some of the steps in the assembly process of the tracked vehicle.
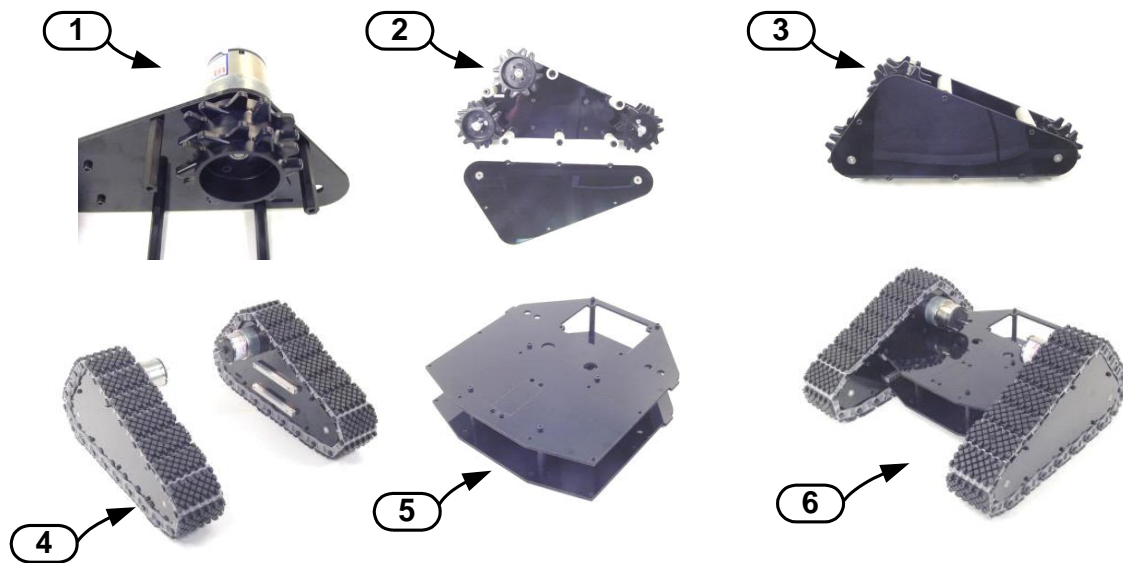
Figure 5.4: Assembling the TTRK-KT tracked vehicle: 1-assembling drive motor and sprocket to track frame, 2-putting together idle sprockets for the track frame, 3-Track frame cover bolted to frame, 4-The fully assembled right and left track, 5-tracked vehicle platform fitting,. 6- the completely assembled tracked vehicle.

The last stage in the assembly process is to put the tracked vehicle and robotic manipulator together. The tracked vehicle platform had pre drilled holes in the Lexan surface plate that could be used to bolt down the manipulator onto it. The resulting mechanical structure formed the basis of the experimental smart electrostatic crop sprayer and Figure 5.5 shows the fully assembled system. Table 5.1 shows the dimensions and specifications of the assembled unit.
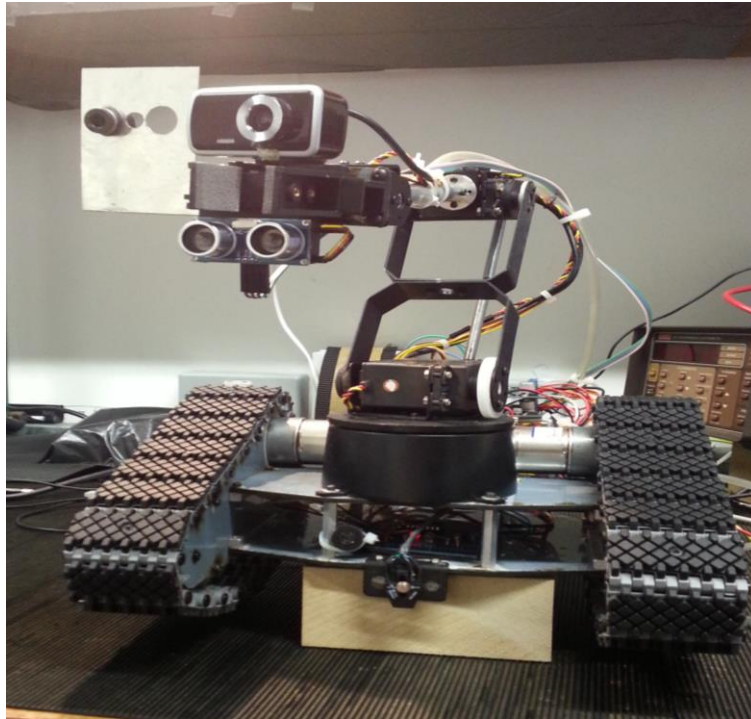
Figure 5.5: The fully assembled mechanical structure of the smart spray system.

Table 5.1 Dimensions and specifications of the mobile robot manipulator

Part Description	Dimension	Range of Angular Motion
Shoulder to elbow	14.605 cm	180º
Elbow to wrist	18.7325 cm	180º
Wrist to tip of gripper	8.5725 cm	180º
Manipulator base height	7.899 cm	180º
Tracked vehicle platform height	3.221 cm	N.A.
Total reach height	59.38 cm	N.A.
Median forward reach	26.035 cm	N.A.

5.5: Selecting the drive electronics, sensing elements and the computing system

This section discusses the required sensing and computational elements needed to create smart spraying system using the assembled mobile robot platform. As explained above, the smart mobile spraying system is required to move along the cotton plant field rows and inspect each plant for insects on the leaves. The insect that attacks cotton plants most devastatingly, as explained in the introductory chapter, is a moth called *'spodoptera littorals'*. The smart mobile spray robot identifies these using image processing techniques by capturing the image of the plant using a digital camera and then analysing it for insect signature, one plant after another. Upon detecting the existence of an insect, the smart spraying system targets it by aligning the spraying nozzle with this location and setting the distance between the spray nozzle and it to between 20 and 25 cm. Finally, a short burst of pesticide is sprayed onto the target, thereby ensuring minimal pesticide usage, yet successful pest infestation control.

The computing system for performing this task needs to have extensive data processing capacity in addition to large I/O operations so as to supply the necessary intelligence. It was therefore decided to split the computing system into a master computer, that is, an IBM compatible laptop computer with multi-core processor to execute the data analysis and to allocate processing tasks to a slave computer in the form of motion and I/O commands from the master computer. This slave computer was chosen from the Arduino family in order to minimize the need to develop the required hardware circuitry to achieve the required tasks. Specifically, the Arduino Mega 2560 was chosen as it has a large number of I/O lines and peripheral devices capable of accommodating any expansion needing to be introduced to the designed system in the future.

The drive electronics for the AL05D were included with the robot arm kit, namely, the SSC-32 board, which is based on a microcontroller from the Atmel AVR family, whilst for the TTRK-KT tracked vehicle; these electronics had to be selected. Considering which, these should be capable of driving the motors on the tracked vehicle platform and are type GHM-02 DC motors with a spur reduction gear rated at 12 Volts with a maximum drive current of 2A. The Cytron MD-10 DC motor drive shield board for Arduino-based systems was selected for the system as it provides the drive capabilities for tracked vehicle DC motors as well as its ease of interfacing with one of the Arduino based microcontroller system family. Finally, the distance detection unit chosen was the Cytron SRF-06 ultrasonic distance measurement unit.

In addition to these elements, there are some self-made units, including a voltage regulator that gives an output of 6 Volts from the main power source, a 12 Volt lead-acid battery. Another circuit was designed to drive the solenoid valve that operates the spraying nozzle and a final unit to detect plant positions signified by a marker placed on the ground was also devised. Figure 5.6 illustrates the block diagram of the system.
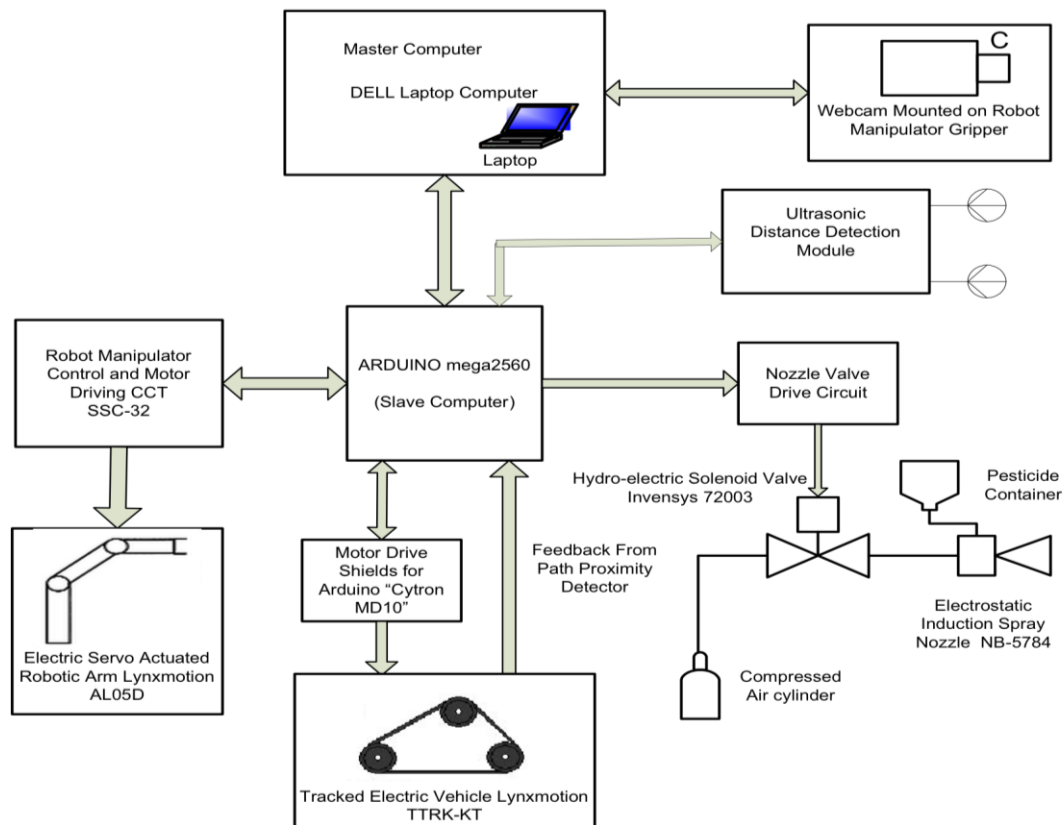
Figure 5.6: Block diagram of the smart spraying robot system.

The next section contains a description for the blocks shown in Figure 5.6 that represent the hardware of the smart spraying system.

5.6. Description of system hardware

In this section, a detailed description of the electronic hardware used in building the smart robot spraying system is provided.

5.6.1. Slave computer board

The first block to be described is the slave computer board that communicates with the main computing unit the "laptop PC" and controls the operation of the mobile spraying robot. As

explained above, this is the Arduino mega 2560 and this board accommodates an ATmega328 microcontroller along with all the required hardware to deliver the required computing function. The ATmega328 is a low-power CMOS 8-bit microcontroller based on the AVR enhanced RISC architecture. By executing powerful instructions in a single clock cycle, this microcontroller achieves throughputs approaching 1 MIPS per MHz, thus allowing the system designed to optimize power consumption versus processing speed. The AVR core combines a rich instruction set with 32 general purpose working registers, all of which are directly connected to the Arithmetic Logic Unit (ALU), thereby allowing two independent registers to be accessed in one single instruction executed in one clock cycle. The resulting architecture is more code efficient while achieving throughputs up to ten times faster than conventional CISC microcontrollers. The ATmega 328 provides the following features: 4K/8Kbytes of in-system programmable flash with read-while-write capabilities, 256/512/512/1Kbytes EEPROM, 512/1K/1K/2Kbytes SRAM, 23 general purpose I/O lines, 32 general purpose working registers, three flexible timer/counters with compare modes, internal and external interrupts, a serial programmable USART, a byte-oriented 2-wire serial interface, an SPI serial port, a 6-channel 10-bit ADC (8 channels in TQFP and QFN/MLF packages), a programmable watchdog timer with internal oscillator and five software selectable power saving modes. Regarding which, the idle mode stops the CPU while allowing the SRAM, timer/counters, USART, 2-wire serial interface, SPI port, and interrupt system to continue functioning. The power-down mode saves the register contents but freezes the oscillator, thus disabling all other chip functions until the next interrupt or hardware reset. In the power-save mode, the asynchronous timer continues to run, thus allowing the user to maintain a timer base while the rest of the device is sleeping. The ADC noise reduction mode stops the CPU and all I/O modules except the asynchronous timer and ADC so as to minimize switching noise during ADC conversions. Finally, in standby mode, the crystal/resonator oscillator is running while the rest of the device is sleeping, which allows for very fast start-up combined with low power consumption. The 16 MHz crystal oscillator module is designed to handle off-chip crystals that have a frequency of 16 MHz, the output of which is fed to the system. As an alternative to using crystals, an externally generated 16 MHz clock source as input to the on-chip 16 MHz oscillator could be used. Figure 5.7 shows the Arduino Mega 2560 microcontroller board [105].
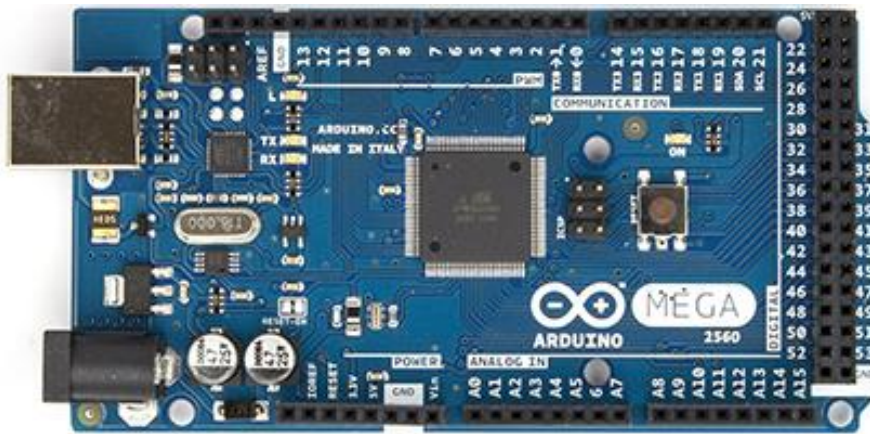
Figure 5.7: the Arduino Mega 2560 Computer board [105].

This device communicates with the main computer, i.e. the laptop PC through a USB interface that is mapped as an additional serial port to the PC.

5.6.2. The tracked vehicle motor drive board.

This board is connected through the Arduino bus system to the tracked vehicle motor drive circuit boards, namely, the Cytron MD-10 DC motor drive shields, two of which are used to control the left and right track drive motors. Figure 5.8 shows this circuit board.

Figure 5.8: The Cytron MD-10 DC motor drive shield [106].

This shield is designed for controlling a high-current brushed DC motor up to 10A continuously, and it is compatible with Arduino main boards. It uses full solid state components, which results in faster response time and eliminates the wear and tear of the mechanical relays. It has stackable side headers, which allows for more Arduino shields to be stacked on top of it as in the case of the mobile spraying robot system, where two of these boards are implemented. This shield circuit provides speed and direction control via the Arduino computer board and the I/O assignment is programmed via hardware jumpers

located on the shield board, which preselects the I/O pins that will control the operation of the motors [106].

5.6.3: the ultrasonic distance measuring board HC-SR04

This circuit module, supplied by Cytron Technologies™, provides the necessary components to enable the smart robot spray system to detect the approximate distance from the spray nozzle to target on a cotton plant by emitting an ultrasonic pulse travelling at approximately 340 m/sec. Subsequently, it measures the transit time required by the ultrasonic pulse to travel back from module actuator to the target and back to the former. Figure 5.9 shows the HC-SR04 module [107].
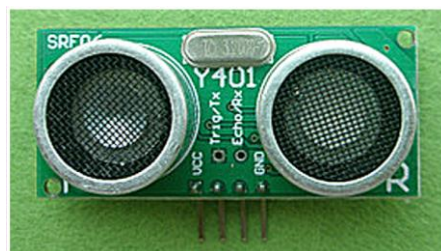
Figure 5.9: The HC-SR04 ultrasonic module for distance measurement supplied by Cytron Technologies™.

In addition to the mentioned hardware elements, the slave computer board has other tasks and circuitries that sense the position of the vehicle, control the operation of the solenoid valve that governs the spraying action and generate the required commands to be sent to the robot manipulator controller board, the SSC-32.

5.6.4: The robot manipulator controller board

The SSC-32 is a microcontroller board specifically designed to operate the AL05D robotic manipulator servo drives; it is a Hitec servo drive module [107]and Figure 5.10 shows this hardware element.
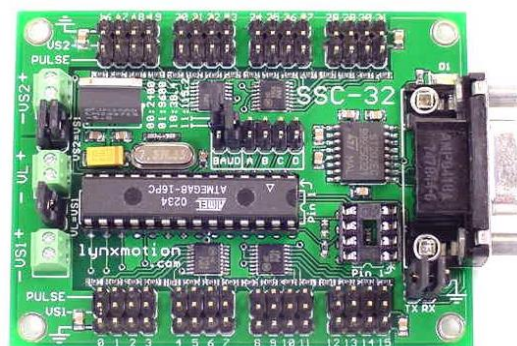
Figure 5.10: The SSC-32 robot arm control board.

This control board has its own firmware that enables it to communicate through a serial COM port with the controlling computing system so as to receive pre-designed motion commands that control the movement of the robot manipulator joints and acknowledge the fulfillment of each command. The serial communication baud rate is programmable and is RS-232C compatible. It can control up to 32 servos plugged in directly and is compatible with the Futaba and Hitec servo drive modules. It has a servo travel range of 180°, with a servo resolution of 1μ step of 0.09° and a servo speed resolution of 1μ step/second. It provides additional motion control that allows for the operation of all servo devices attached, in timed speed or in synchronized fashion or in a combination of these. A unique "Group Move" allows any combination of servos to begin and end motion at the same time, even if they have to move different distances, which allows for accurate positioning, and extremely smooth moves. Moreover, the servo's position or movement can be queried to provide feedback to the host computer, which permits complete control of all aspects of robot manipulator position monitoring by transferring a few values from the host controller.

5.6.5: Additional support circuits.

These circuits are required to complete the electronic hardware needed to operate the smart robotic pesticide spraying system and are as follows:

1. The voltage regulating unit: This circuit is required to deliver the 6 V potential required to operate the robotic manipulator servo drives and the SSC-32 controller board. The tracked vehicle operates directly from the 12 volts main battery that powers the whole system. The circuit is a series regulator built around the integrated regulator 78xx with a current boosting transistor to assist in delivering the required load current necessary to operate the robotic arm servo drivers, which can reach 2.6 A at full load. An LED is used to indicate the 6 V supply availability. The circuit board also accommodates a slow blow fuse for protection from short circuiting and overload. Figures 5.11 and 5.12 show the circuit diagrams for the voltage regulating unit and a picture of the assembled circuit respectively.
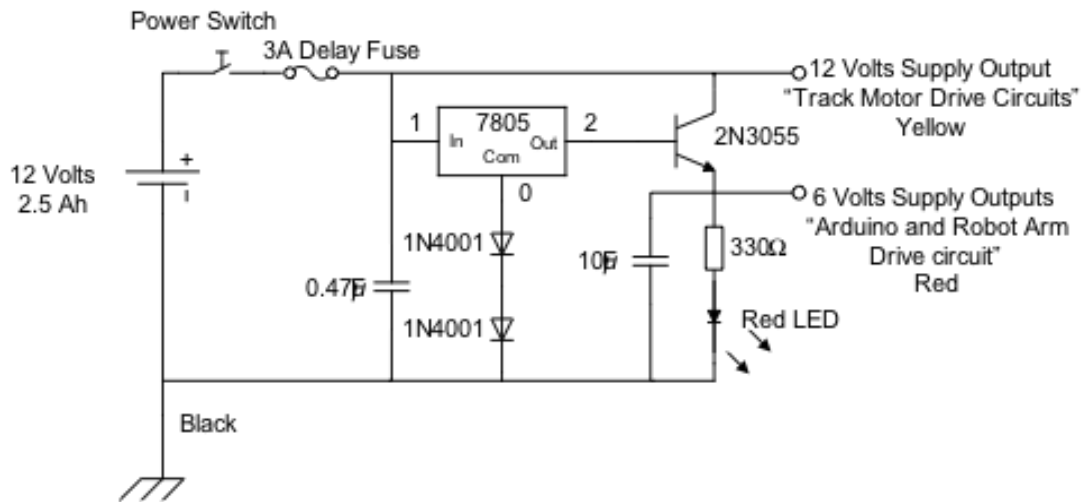
Figure 5.11: The voltage regulator circuit diagram.
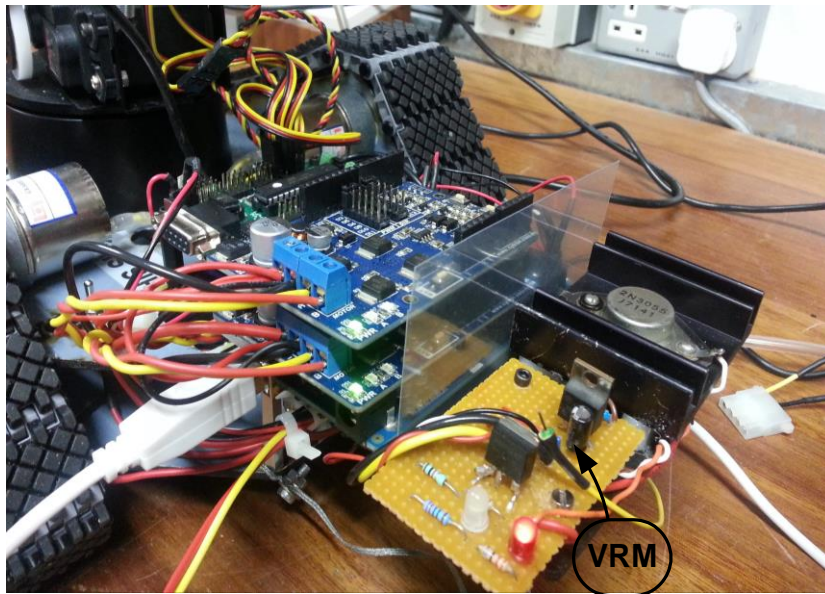
Figure 5.12: The constructed voltage regulator module (VRM).

2. The solenoid valve drive circuit: This circuit comprises one MOS FET switch with its associated snubbed circuit and other necessary passive components. This transistor can be turned fully on by a logic level signal of 3.3 V potential obtained directly from the slave microcomputer output port. An LED indicator is added to this circuit to visualize the valve operation function, and Figure 5.13 shows this circuit in detail. Figure 5.14 explains how to check the ability of the solenoid valve.
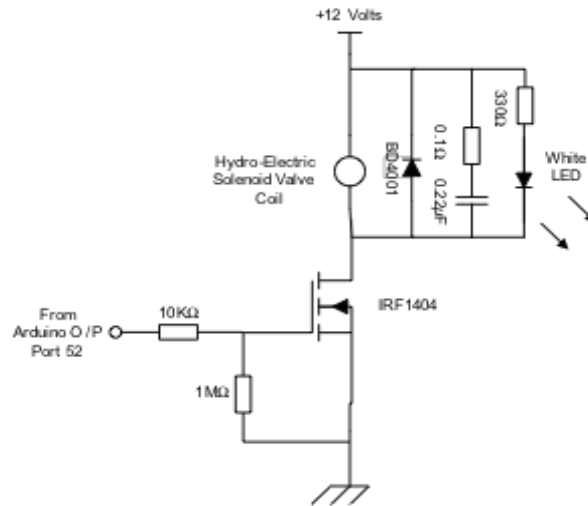
Figure 5.13: The solenoid valve drive circuit.
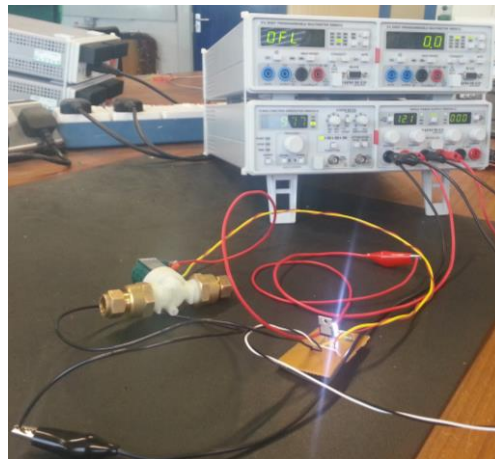
Figure 5.14: Picture of the solenoid valve and the constructed drive circuit.

3. The path mark detection circuit: This circuit is required to detect path labels indicating the positions of the cotton plants that require pest control by the direct pest spraying method. It consists of one reflective optocoupler along with bias passive components and resolving logic that uses the 4093 quad NAND gate with hysteresis to provide reliable detection of path marks. A switch is used to reconfigure circuit output so that it will generate positive logic output when detecting a white marker on a black background (switch at position one) or vice versa (switch at position 2). Figure 5.15 shows the circuit diagram of the path mark detector. Figure 5.16 explains the constructed circuit of the path mark detector.
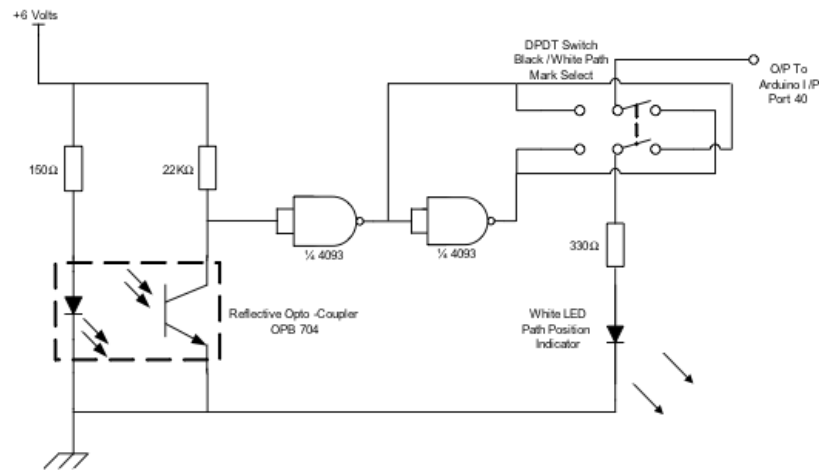
Figure 5.15: The circuit diagram of the path mark detector.
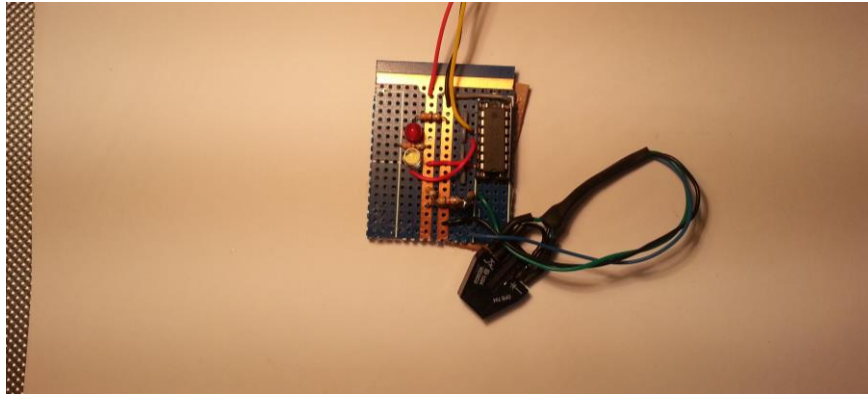
Figure 5.16: The constructed circuit of the path mark detector.

5.7: Description of system software.

In this section a detailed description of the software written to operate and control the smart robot spraying system is provided. This system software has two parts, with the first being written for the Arduino microcontroller and its main task is to receive motion commands and other control actions from the laptop computer, which it delivers to the robot arm controller, the drive circuits for the tracked vehicle electric motors and the spray nozzle valve control circuit. It also receives sensor signals and delivers feedback to the main computing system, i.e. the laptop computer. These programs were written using micro C. The other part of the software was written for a Matlab environment. It includes the motion control program module, the camera image capturing and detection program module, in addition to several other programming modules that are used to carry out other necessary functions, such as I/O operations and system resources management.

Most of the functions were processed in the laptop PC which is the main computing system and has high computational power and performance. The image processing and robot manipulator motion control data calculations were performed using inverse kinematics equations processed in the laptop PC using programs written for Matlab [108]. The main tasks executed by the slave computer are receiving motion control data for the robot manipulator and the tracked vehicle, receiving data from the path mark detector, and operating the solenoid control valve of the pesticide spraying unit. Motion data for the robotic manipulator are sent via the serial controller to the SSC-32 robot manipulator servo controller, while the solenoid valve control and tracked vehicle motion commands are directly executed inside the slave computer microcontroller, the ATmega328 on the Arduino Mega 2560 computer board, which is directly interfaced with the solenoid valve drive circuit and the motor drive control circuits in the Cytron MD-10 DC motor drive shield. The detected path marker signal is picked up by the input port of the slave computer and directly stops the tracked vehicle motion, whilst at the same time reporting the action to the main computer via the USB interface that operates as a serial communication port in the RS-232C protocol.

5.7.1: Slave computer software

This software has the primary task of receiving motion and spraying actuation commands and executing them accordingly. C language was used to write software for the slave computer and the Arduino integrated design environment, known as "Arduino studio", was used to compile user programs and load them onto the slave computer's flash memory. Figure 5.17 shows the user interface screen of the Arduino studio.
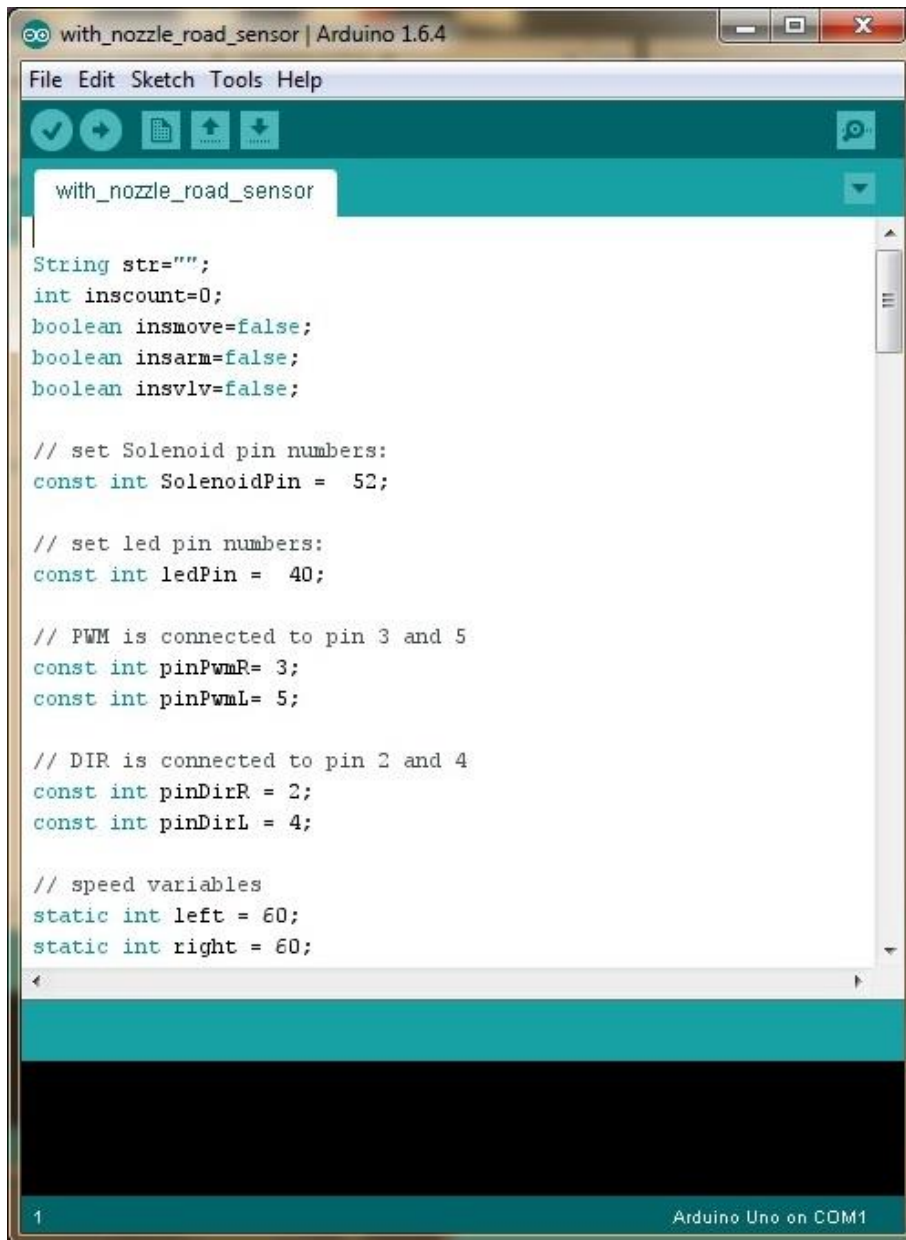
Figure 5.17: The Arduino studio integrated design environment.

The tasks required from the slave computer are as follows:

1. Communicating between the main computer and the servo controller, the SSC-32 of the robot manipulator ALS05D. It receives motion parameters calculated inside the main computer "the laptop PC", then organizes them in the form required by the firmware of the servo controller as shown below:

<ch> P <pw> S <spd>... # <ch> P <pw> S <spd> T <time><cr>

where:

<ch> = Channel number in decimals, 0 - 31

<pw> = Pulse width in microseconds, 500 - 2500

<spd> = Movement speed in us per second for one channel (optional)

<time> = Time in ms for the entire move, which affects all channels and has a 65,535 max reading

<cr> = Carriage return character, ASCII 13 (required to initiate action)

<esc> = Cancel the current command, ASCII 27

The angle of motion for any joint of the robotic manipulator is calculated inside the main computer and then transformed into the special form accepted by the servo controller. This follows the information supplied by the manufacturer of the servo actuator, namely Hightec Inc., whereby these servos are of the pulse proportional type. The signal required to drive the servo device consists of positive pulses ranging from 0.9 to 2.1ms long, repeated 50 times a second (every 20ms). The servo positions its output shaft in proportion to the width of the pulse, but most servos have more than 90° of mechanical range and often can rotate 180°. However, it should be noted that some servos can be damaged when commanded past their mechanical limitations, but the SSC-32 can drive the servos throughout their extended range. A position value of 500 corresponds to 0.50ms pulse, and one of 2,500 corresponds to a 2.50ms, with a one unit change in position value producing a 1μs change in pulse width. The positioning resolution is 0.09°/unit (180°/2000). These values are necessary to translate the required angle of motion to the numerical value accepted by the SSC-32, which in turn translates it into the pulse width signal needed to drive the servo element to the desired position. As an example, the following string is sent from the slave computer to the SSC-32:

 "#5 P1600 S750 <cr>"

This string, when sent to the SSC-32, will move the servo on channel 5 to position 1600. It will move from its current position at a rate of 750 μSteps per second until it reaches its commanded destination. For a better understanding of the speed

arrangement, consider that 1000 µsteps of travel will result in around 90° of rotation and hence, a speed value of 100 µsteps per second means the servo will take 10 seconds to move 90°. Alternately, a speed value of 2,000 µsteps per second equates to 500ms to move the robot joint 90° from its zero position. Figure 5.18 shows the relation between the pulse width sent to the servo device from the SSC-32 and the resulting motion in degrees.
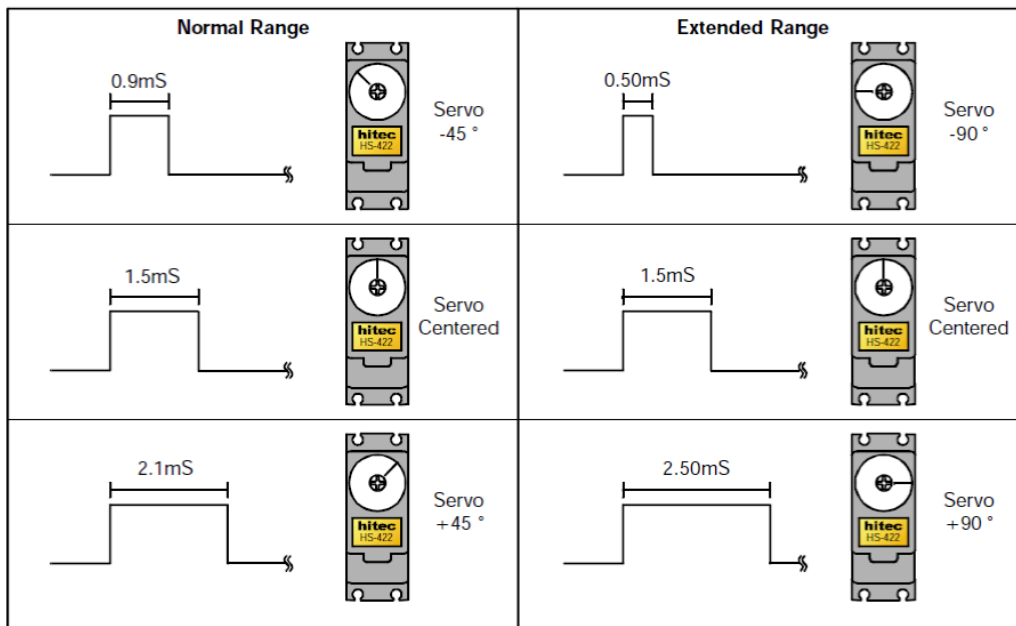
Figure 5.18: The relation between the pulse width signal sent to the servo device and the resulting angle of motion.

2. Controlling the motion of the tracked vehicle: Upon receiving a tracked vehicle motion command from the master computer, the slave computer sets the two DC motor drive shields and the two Cytron MD-10 boards to supply the drive motors of the vehicle with the necessary power to move the whole system through the field. The vehicle keeps on moving until the slave computer receives a signal from the path marker detector, the output of which is linked to one of the slave computer's input ports (pin 40 "PG1" on the slave computer board). At this point, the slave computer stops the tracked vehicle and signals to the master computer that a new plant has been reached so another insect search operation should commence.

3. Measuring the approximate distance from the spray nozzle to the target: The slave computer controls the operation of the Cytron HC-SR04 ultrasonic distance measuring unit that operates on a pulse transit time principle to measure the distance to the target. After

receiving a request from the master computing device, the slave computer begins the distance from the nozzle to target measurement subroutine, which starts by initiating a timer module and turning the Trig pin on the HC-SR04 on and off (connected to I/O pin 33 "PC4", which is assigned as a digital output on the slave computer board) so as to send out a sound pulse. Then, how long until the Echo pin (pin 9 "PH6" on the slave computer board which is assigned as a digital input pin) receives the echo is monitored. The timer is then stopped and the distance calculation is executed, with the result being sent to the master computer to calculate the motion commands that will set the distance between the target and the spray nozzle to the desired value.

4. Operating the solenoid valve controlling the spraying action: After the master computer image detection program detects the presence of an insect on the leaves of the plant and after zeroing on the target, the master sends the spray command to the slave. When the spray command is received, the latter sets the output port (pin 52 "PB1" on the slave computer board) that controls the solenoid valve drive circuit to logic high, thus turning the MOS switch device on for a predetermined period. Subsequently, the output is set low and if the plants on the right and left of vehicle position have been searched and dealt with, the slave computer returns the robotic arm to home position awaiting a further tracked vehicle motion command from the master computer to proceed to the next plant or if the end of the row has been reached, the vehicle stops.

5.7.2: Master computer software

Most of the intricate functions of the smart mobile spraying robot are accomplished inside the master computer using Matlab as the programming platform.

The main tasks required of the smart mobile spraying robot system are:

- Searching cotton plants for insect infestation

- Exterminating insects by direct spraying of pesticide on them

    To accomplish these tasks, the system is equipped with a camera attached to the gripper of the robotic manipulator along with the spraying nozzle. The gripper motor is used to steer the camera and spraying nozzle during the course of searching the cotton plant for insect infestation.

The software specially written to accomplish the required tasks will run on the master computer and from the outset was designed to consist of a main program and five subprograms so as to simplify the development of the whole system program. The main program starts by calling the subprogram to obtain camera information (getCameraInfo). The camera used is a standard USB interfaced VGA resolution webcam that was chosen for ease of operation and being light in weight. After determining the camera specifications, operation modes, and video formats, the execution returns to the main program, where it starts by sending the initialization parameters that set the robotic manipulator in the home position. Then, these parameters are sent to the slave computer by calling the master-slave communication program (conout), which sends the prepared data to the former computer via the serial interface through a USB port that operates as a COM port. Subsequently, the main program sends a command to the slave computer to start moving the tracked vehicle by calling the subprogram (ismoving). The slave computer stops the vehicle upon reaching the first marker in the field, which indicates that the robot is now in the vicinity of a plant in a row inside the cotton field. The slave computer sends a signal back to the main computer indicating a marker has been reached and again, the program execution returns to the main program. At this moment, the main program sets the motion parameters to the robotic manipulator to start scanning the plant on the right of the vehicle, while looking beneath the plant leaves and then calls the subprogram (movearm).

The camera is activated during the scan and captures frames at a rate of five per second, which is slow enough to give time for the detection process. Each frame captured is analyzed to detect insect presence. In this feasibility study, it is assumed that the insect is colored red and the minimum size of it on the captured frame is equal to or greater than 300 pixels. Any red area on the captured frame that is smaller than this is neglected so as to reduce the probability of false insect detection. The process of detecting an insect involves identifying red objects in a captured picture frame. For each frame, the program subtracts the red component from the grayscale image to extract the red components in the image. Then, a median filter is used to filter out noise in the image, subsequent to which, it is digitized to binary values with respect to a threshold value (0.18 is used) and any object of a smaller size is ignored (object smaller than 300 pixels). All resulting objects are labeled, with the centroid of each being extracted and then, the boundaries of the objects are determined for those detected. Once the pixel centers of each object have been determined, the program selects the one with the largest area and calls the subprogram (bugfocus), which will calculate the

manipulator movements required to move the arm so as to put the detected object at the center of the captured frame.

When this operation has finished, the targeted object is put at the center of the picture frame, thus situating it at the center of the spray nozzle target area. At this point, the main program calls the slave computer to execute the target distance measuring subroutine and the latter returns the measured distance to the former. The execution returns to the (bugfocus) subprogram to move toward or from the target so as to set the distance between the target and spray nozzle to about 20 to 25 cm. Afterwards, the operation returns to the main program, which sends a command to the slave computer to energize the solenoid of the valve that starts the spraying action and this takes about 0.6 to 0.7 seconds to finish.

If this operation finishes, or if no insect is found on the lower side of the cotton plant leaves, the main program sends another path to the slave computer to start moving the robotic manipulator in a fashion that will cover the upper side of the leaves and the process repeats. If the scanning action on the plant on the right side of the vehicle has finished, the main program sets another set of motion parameters to the slave computer to start scanning the plant on the left side of it in exactly the same manner as before. After finishing this process, the main program commands the slave computer to start moving the tracked vehicle, which will move until reaching the next marker and the process repeats. When all plants in the row have been searched (the number of which is set to 20 in the experimental stage), the main program commands the slave computer to stop the vehicle and return the robotic manipulator to its home position, where it awaits another round of operation initiated by the user running the program again. The flowchart in Figure 5.19 shows how the smart mobile spray robot control program operates.
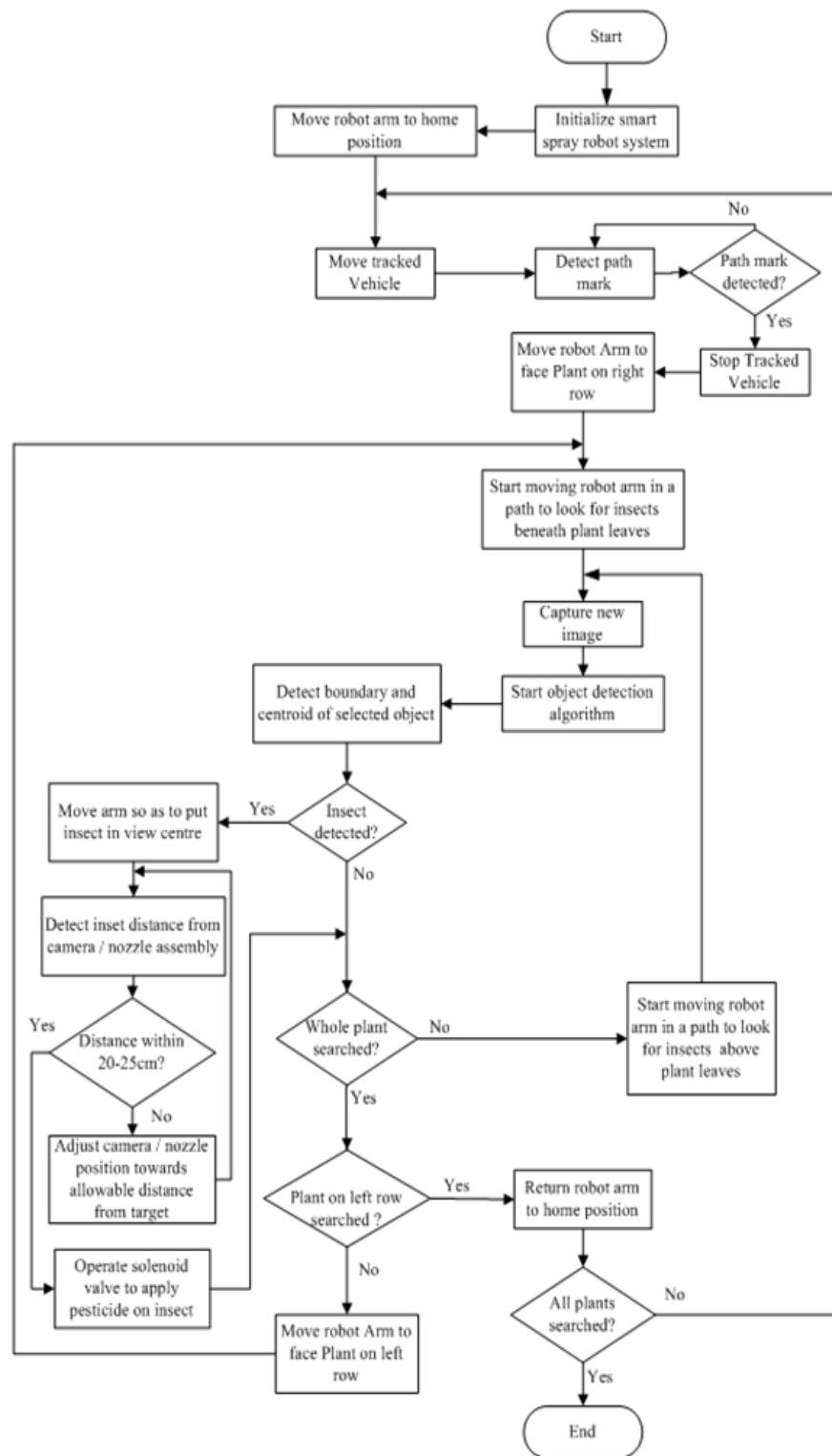
Figure 5.19: Flowchart of the smart mobile spray robot program.

5.8: Summary

In this chapter, a description was given regarding the selection and assembly process of the smart spraying robot system. Also included was an explanation of the electronic circuits required for the operation of the smart spraying system along with additional circuits designed for various purposes such as driving a 6 V source from the 12 V battery, the electro-hydraulic solenoid drive circuit and others. Finally, detailed description for the system software has been provided along with a flowchart that explains the operation of the designed smart spraying robot.

CHAPTER SIX: THE NEW ELECTROSTATIC INDUCTION SYSTEM

6.1. Introduction

This chapter explains the experiments conducted to test the ability of the newly designed mini mobile robot and the induction nozzle. The first of these experiments started with testing the mobile robot, with many tests being conducted on it to check for movement and stability. The purpose of these experiments was to check the ability of the robot to test different targets of different shapes such as 2D and 3D and when the targets were organised in groups or were presented individually. The second set of experiments was geared towards checking the new induction nozzle design. Regarding which, the experimental setup is explained and other experiments that were conducted to assess the suitability of the induction nozzle are described. Its performance can be determined by measuring electrostatic parameters, such as: the flow rate, spray current, charge to mass ratio, spray coverage area and soil contamination in situations when the nozzle operates with and without charging. All of these experiments are presented in this chapter.

6.2. Testing the robot systemization in movement case

To check the robot systemization, inducted to test the ability of the newly designed mini mobile robot and the induction nozzle. The first of these experiments started with testing the mobile robot, with many tests being conducted on it to check for mained the computer codes for image processing and other codes that facilitated the movement of the robot. See Figure 6.1.

Figure 6.1: How the PL is attached to the robot system (1) and how the robot system moves towards the artificial plants (2).

The purpose of this was to check the robot systemization ability during movement. Artificial cotton plants were located on the right and on the left sides of robot system pathway. Attached to these plants were a variety of shaped targets which were positioned on their leaves and on other areas. A white tape line was fixed in the middle of the corridor for guiding the robot system. The robot system started scanning and searching for targets on the plants, as shown in Figure 6.2.
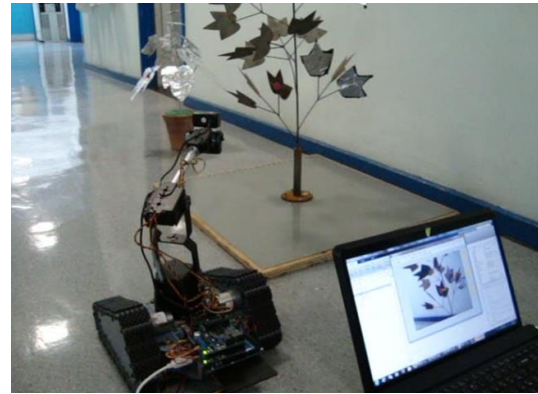
Figure 6.2: The robot system during the process of plant scanning.

The sensor that stops the movement of the robot system and starts the scan was attached to the bottom of the system, while the other one that is used to measure the nozzle to target

distance was attached to the manipulator arm. These two sensors and the sensor for the CCD camera as well as the new induction nozzle were all attached to the mobile robot. Figure 6.3 shows all the attachments.
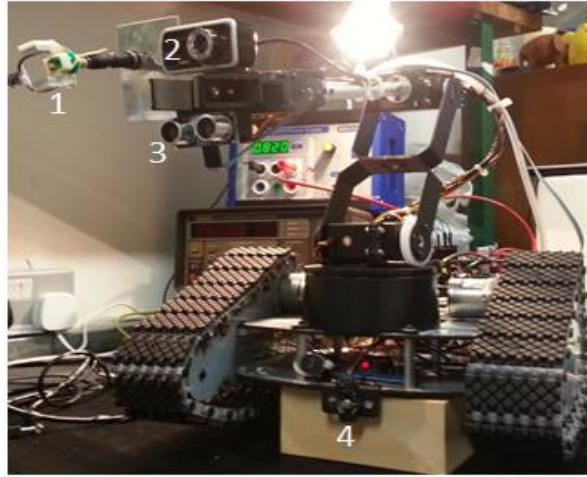
Figure 6.3: The robot system with the attachments: induction nozzle (1) CCD camera (2) sensor for plant distances (3) sensor for plant lines (4).

During the testing of the robot system for both movement and stationary status, the images captured by the mobile robot were saved in special file in the software program as evidence of its ability to deal with the targets for all the cases presented in the experiments. Figures 6.4, 6.5, 6.6, 6.7 and 6.8 include some of these images that demonstrate the ability of the mobile robot to deal with the targets. These images were captured for the targets on artificial plants with differently coloured leaves and on real plants with different numbers of targets.
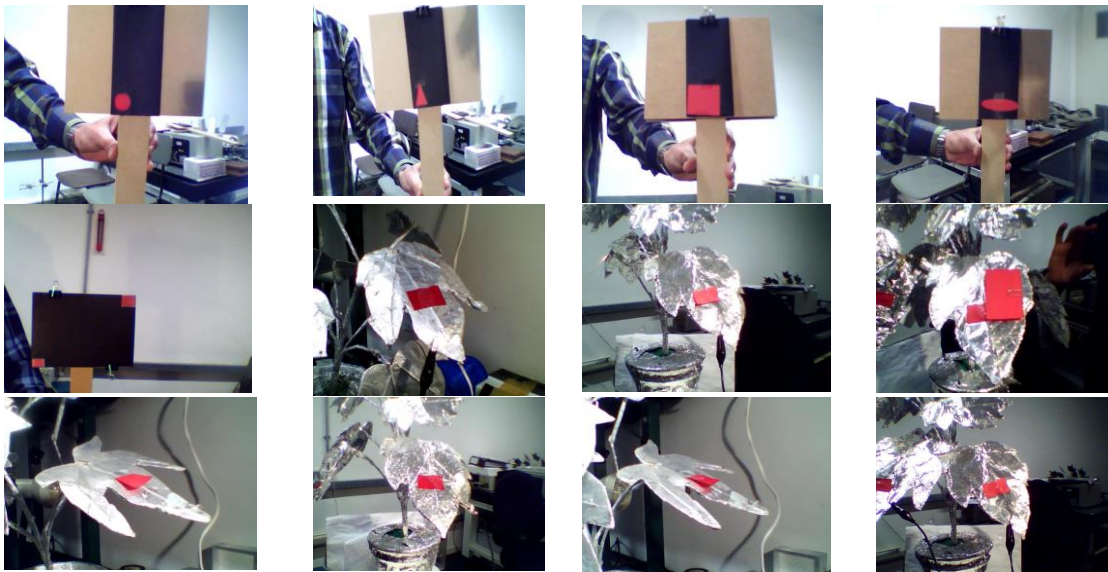
Figure 6.4: The robot mobile images for the artificial plants when the attached targets have a 2D shape.
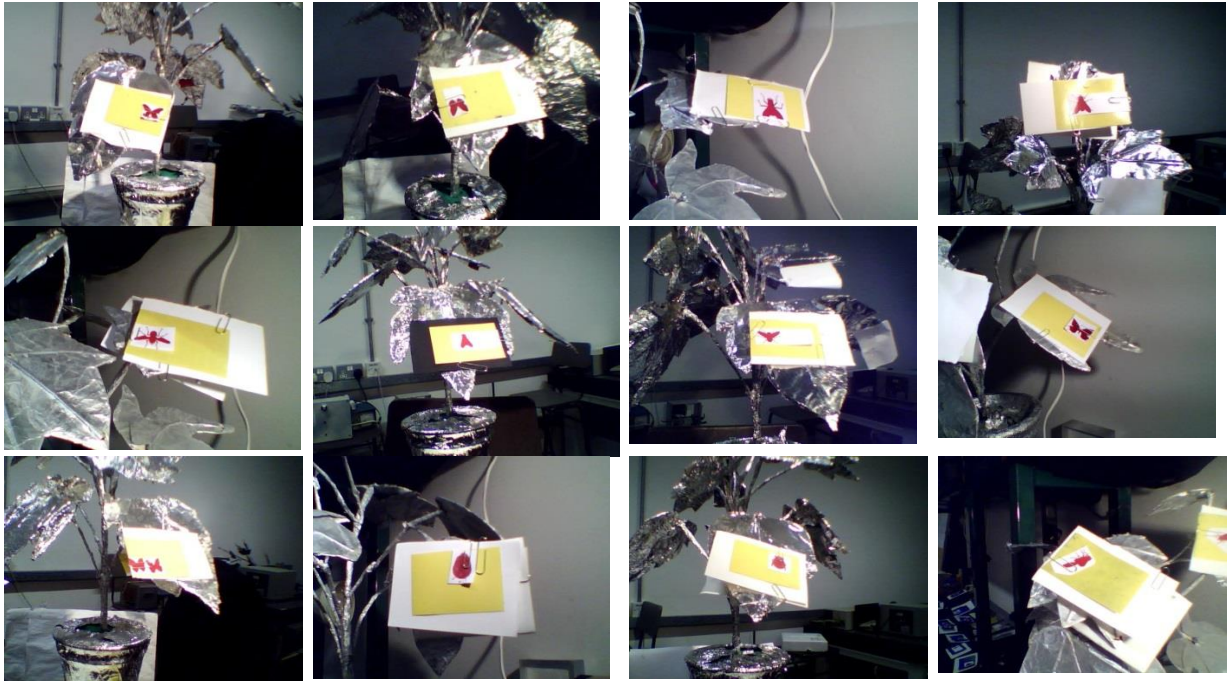
Figure 6.5: The robot mobile images for the artificial plants when different shapes of insect pictures are attached.

Figure 6.6: The mobile robot images for the real plants.

Figure 6.7: The mobile robot images for the colored artificial plants; the leaves attached to the targets have a 3D shape.
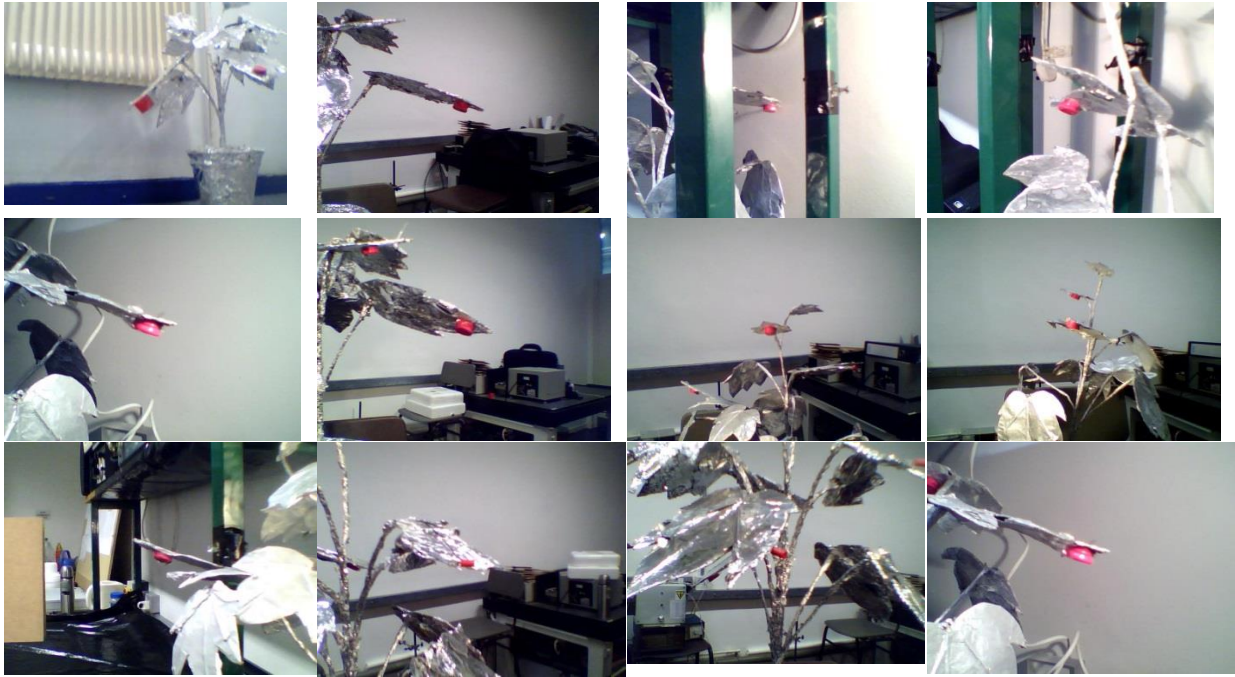
Figure 6.8: The mobile robot images for the artificial plants; leaves attached to the targets have a 3D shape.

6.3. Testing the performance of the electrostatic spray nozzle

To check the efficiency of the new electrostatic spray nozzle design, some experiments were conducted in the laboratory on artificial plants as well as other 2D and 3D targets. The experimental setup is illustrated in Figure 6.9 and it comprised the following. Two artificial cotton plants were located on both the right and left sides of the electrostatic system with WSPs attached to both the front and back of their leaves. The artificial plants were used to represent real cotton plants and the WSP was used to make sure that the nozzle spray reached the intended area of the targets. This is indicated when the WSP changes from yellow to blue. In addition, these papers were used to determine electrostatic parameters, such as the coverage area on the front and back surfaces of a leaf and the droplet size, with and without charging being applied. The induction nozzle was connected to a water bottle in order to supply water via an air pressure gauge and a solenoid valve determined the pressure used. A high voltage supply was connected to the electrode of the induction nozzle to supply the voltage, which could be various different levels. The reason for having a range of voltage levels was to enable the selection of the best one for achieving a high surface charge density on the surface of the liquid film before electric breakup occurs. An electrometer device, model 617, was connected to the plant leaves in order to measure the spray current on the

intended targets. A personal computer with a Matlab program for image processing and the other programs described in chapter 5 was connected to the mobile robot system to guide it to the intended location. In addition to the induction nozzle on the robot, a CCD camera was used to record the plant scanning that allowed for the insects on the plant to be recognised once their images were processed. Furthermore, as described above Figure 6.3, there were the two types of sensors that were used to control the electrostatic system. The first one of which was attached to the bottom of the system stops it and starts plant scanning, while the second measures the target to nozzle distance. All the experiments were conducted under laboratory conditions.

Figure 6.9: The components of the experimental setup: artificial cotton plant with the targets (1), electrometer (2), induction nozzle (3), high voltage supply (4), CCD camera (5), sensor for measuring nozzle to target distances (6), robot (7), sensor for searching plants lines (8), water bottle (9), air pressure gauge (10), solenoid valve (11), personal computer (12) and, artificial plant (13).

6.3.1. Calculation of the charge to mass ratio

The definition and the formula of this value for the electrostatic spraying system were presented in Chapter 3. To measure this value, spray current and mass flow rate calculations are needed.

6.3.1.1. Flowrate measurements

Preliminary experiments of the nozzle were operated for several time periods, namely, 50, 100, 150, 250, 400, 500, 600 and 700ms. A special program was included in the general

software used to control these time periods. In order to measure the nozzle water flow rate a small plastic bag was fixed to the induction nozzle to accumulate the nozzle spray, as shown in Figure 6.10 (left). In addition, an aluminum tray placed underneath the artificial plant was used for the collection of the volume of the spray reaching the tray and a volumetric flask was used to measure this, as indicated in Figure 6.10 (right). The efficiency of the spray nozzle was measured by calculating the ratio between the volume reaching the ground surface and the total spray volume i.e. the lower the ratio, the better the spraying efficiency.
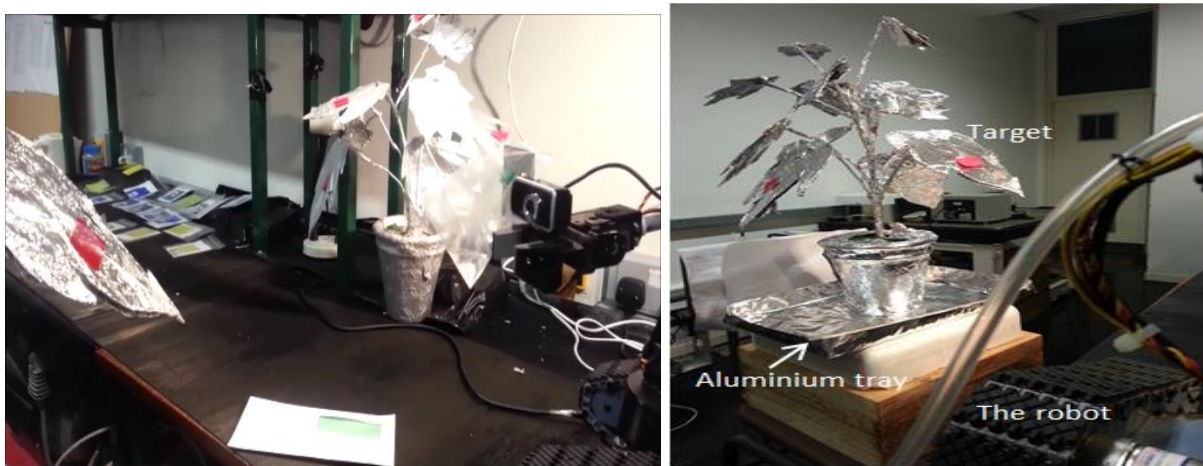
Figure 6.10: The flow rate (left) and volume of drift (right) measurements.

A normalized method was used to present the results regarding the water flow rate, drift volume and the ratio of drift to nozzle flow rate. This was justified on the basis of organising the results in a consistent style, which made it easier to make comparison among them. As can be seen in the graph in Figure 6.11, the ratio of waste to applied water flow rate reduces for longer pulse periods and further experiments were performed to find the optimum pulse parameters by taking into account other factors, such as leaf coverage as well as the waste. A time period of 600 ms gave the best results out of all those tested as well as achieving high coverage with the least tray to volume ratio.
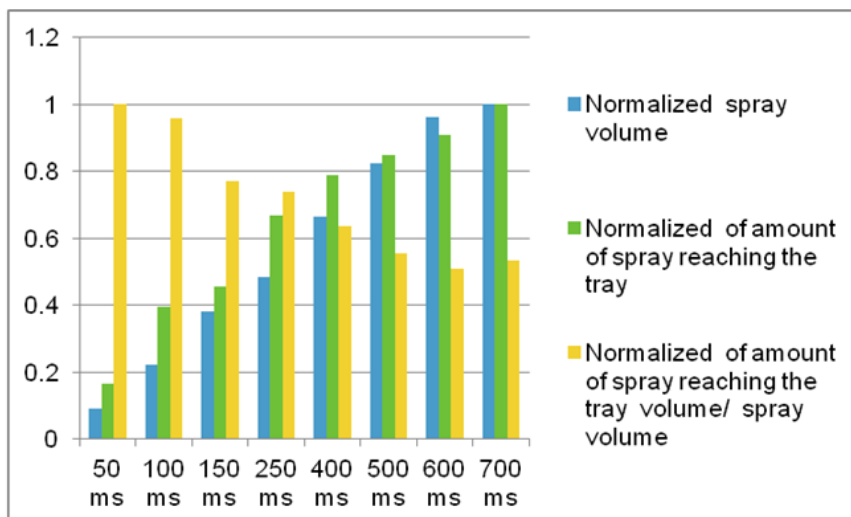
Figure 6.11: The normalized values for the spray reaching the target (equivalent to soil contamination)

In addition, when investigated further, a time period of 600 ms gave the least soil contamination underneath a plant, as shown in Figure 6.12.
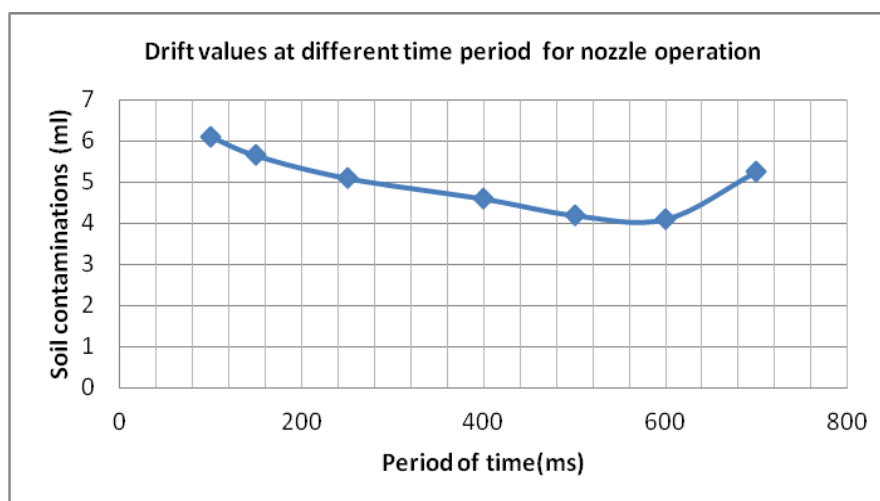
Figure 6.12: The soil contamination values for all time periods.

6.3.1.2. Experimental setup used to measure the spray current

Figure 6.13 portrays the experimental setup used to measure the spray current of the induction hydraulic spray nozzle (IHSN) on the plant leaves. The electrometer was connected directly to the plant leaves in order to record the spray current value on the target.

Figure 6.13: The experimental setup for measuring the spray current on the artificial plant: induction nozzle (1), high voltage supply (2), electrometer (3), electrometer nippers with the target (4, 6) and artificial plants (5 and 7).

In order to achieve high surface charge density on the surface of the spray droplets, high induction voltage levels were applied: 400, 500, 600, 700, 800, 900 and 1000 V. So as to make sure that the level of voltage connected perfectly with the electrode of the nozzle, it was necessary to check the voltage on its surface. Figure 6.9 shows the procedure for checking the induction voltage values on the electrode surface of the nozzle. A high voltage probe positioned between the surface of the electrode of the nozzle and multimeter recorded the real value level of voltage on the surface. The multimeter reading had to be multiplied by the constant of the high voltage probe, which was one thousand (1000) so as to give the actual voltage value on the electrode surface, as shown in the pictures in Figure 6.14.

Figure 6.14: The procedure used to check the nozzle electrode voltage: high voltage prop (1), induction nozzle (2) multimeter (3) and high voltage supply (4).

The time period 600ms was used to operate the induction nozzle with all the levels of the induction voltages mentioned above. The purpose of this was to measure the spray current on the target at each level in a range from 400 to 1000 volts. The results obtained from these experiments are presented in Figure 6.10.

It appears that, initially, a positive relationship is found between increasing the induction voltage and the value of the spray current on the plant target. These results are in good agreement with the outcomes reported in previous research [38] [47] [35]. However, after reaching the 800 volts level the spray current values on the target begin to drop when the induction voltages are increased. The reason for this could be attributed to the discharge phenomenon that causes the reduction in spray current [38]. This behavior of the spray current values indicates that the best voltage induction for achieving a high one on the target is 800 volts. This value seems mismatched with the results of COMSOL, which recommended 500 volts and there is gap between the two of 300 volts. The reasons for this difference can be summarized as follows:

1 It is not unusual to find differences between theoretical and experimental values;

2 Simulation results depend on theoretical assumptions and perfect conditions while field experiments face all the changing circumstances occurring in the real environment;

3 Laboratory experiments are affected by changes in external and internal conditions while in a simulation all the conditions are fixed.

The values of the charge to mass ratio were calculated according to the values of spray current and mass flow rate, as presented in Figure 6.15.
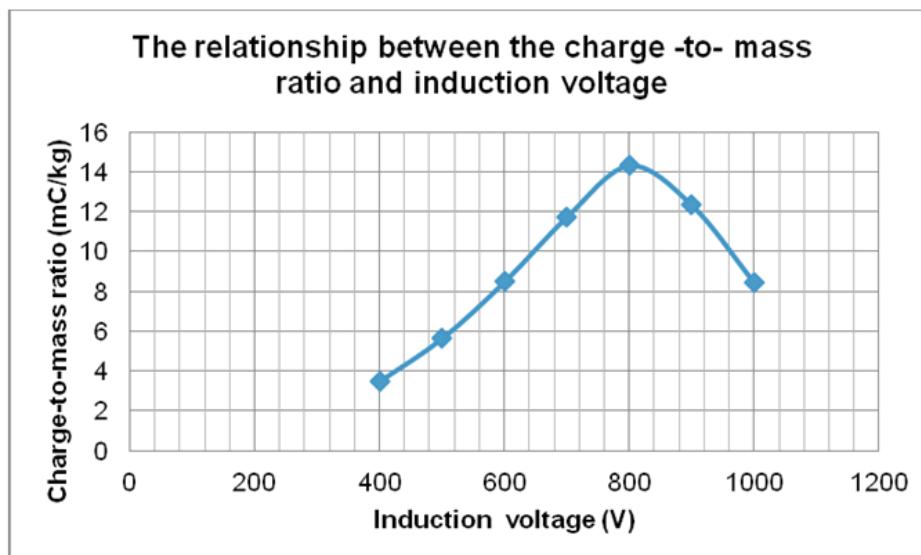
Figure 6.15: Values of the charge mass ratio for different induction voltages.

The above graph indicates that the charge to mass ratio values increases when the induction voltage is increased up to 800 V and then decreases for the last two levels. With increasing voltage levels, the amount of the chargeability on the induction nozzle liquid film also increases, a result that is consistent with the findings in earlier works [13][15][47]. The maximum value reached is 14.5 mC/kg when the induction nozzle is set at 800 volts. Then, the value is reduced to 12 and 10 mC/kg when the nozzle induction voltage is increased to 900 and 1000 volts, respectively. Two reasons might account for this reduced charge to mass ratio. The first can be attributed to the reduction in the value of the spray current for the two last two levels, as illustrated in Figure 6.10. The second explanation is that the value of the charge mass ratio becomes non-linear with increases in voltage due to ionization of the surrounding air in the charging region [56].

6.3.2. Measuring the spray angle

The value of the spray angle plays an important role when measuring the coverage area and the amount of drift [70]. In order to determine the spray angle of the novel induction nozzle, two actions needed to be taken. The first was to prepare an experimental setup in which to operate the nozzle under laboratory conditions, with and without charging. The second was to capture the atomization of the spray of the nozzle so as to measure the angles that formed under all conditions, i.e. with and without charging. The experimental setup preparation is shown in Figure 6.16. Inside the Faraday pail, the induction nozzle was attached to the metal holder and joined to the water holder via an air pressure gauge so as to provide tap water and

control the air pressure. A high voltage supply was used to control the voltages supplied to the nozzle and a temperature and humidity device was employed to monitor the environmental conditions. Finally, a high-speed camera and a strobe light were set up to capture the atomization of the liquid through the nozzle spray.
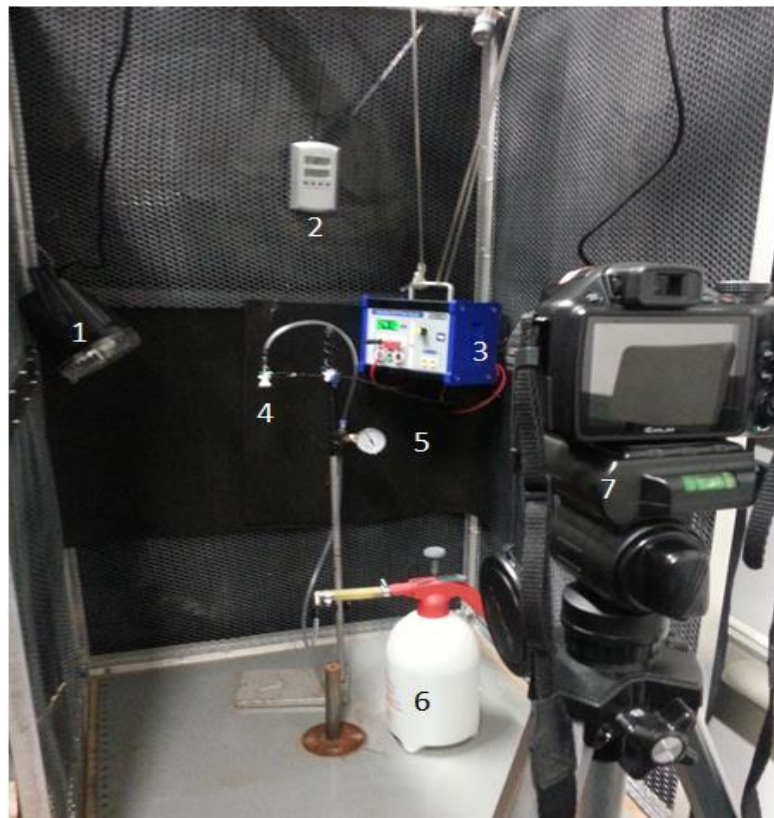
Figure 6.16: The experimental setup for measuring the nozzle spray angle: strobe light (1), temperature and humidity device (2), high voltage supply (3), induction nozzle (4), air pressure gauge (5), water bottle (6) and, high-speed camera (7).

Under the charging condition, the high voltage supply was connected to the electrode of the nozzle while the ground wire was connected to the nozzle body in order to complete the electrical circuit. A high voltage probe and multimeter were used to check the voltage levels on the surface of the nozzle electrode (see Figure 6.17). The voltage levels used were 400, 500, 600, 700, 800, 900 and 1000 V, being the same as those for measuring the spray current. The reason for applying this range of levels was to check their effect on the size of the spray angle.

Figure 6.17: Checking the induction voltage on the nozzle electrode. High voltage prop (1), multimeter (2), induction nozzle (3) and high voltage supply (4).

Pictures of the spray angle captured with and without charging are shown in Figure 6.18. Image J software was used to measure the dimensions of the nozzle spray atomization and then, by employing these results, to calculate the spray angle. The procedure for using Image J software was covered in Chapter 3.

Figure 6.18: Pictures of spray angle, with and without charging.

All the results of the values of the spray angle that were obtained from the calculation are presented in Figure 6.19.
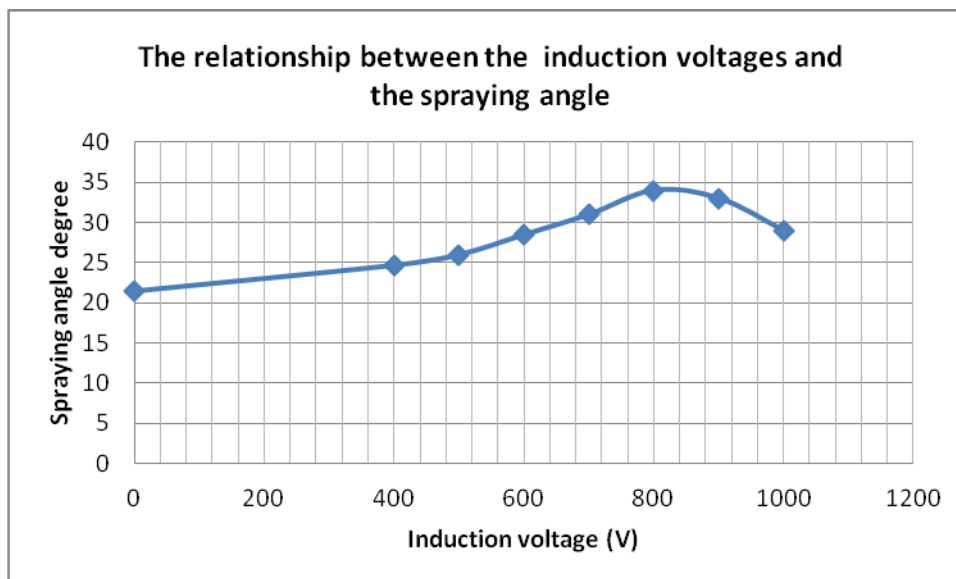
Figure 6.19: The trajectory of the spray angle values under charged and uncharged conditions.

In general, the results indicate that the spray angle increases when the levels of the induction voltage of the nozzle electrode is increased. Specifically, the spray angle starts at 21.5° for the nozzle operating without a charge and reaches 34° when the level of induction voltage equals 800 volts. The reason for this increase is attributed to the Coulomb repulsion phenomenon, which happens among the charged droplets that are generated from the atomization of the nozzle spray after acquiring unipolar charging. This increase in the nozzle spray increases the amount of charge to mass ratio on the intended targets, as seen in Figure 6.11 above. This result is firmly in agreement with the results of [18]. The reason for this is attributed to the small change in drop trajectory due to electrostatic forces, which could result in a large increase in deposit [18]. This outcome is also consistent with other results achieved by Jahannama *et al*, who explained that the droplet size distributions of horizontal sprays showed a significant difference between charged and uncharged scenarios [32]. In Figure 6.15, it is evident that the spray angle reduced from 32° to 28° when the induction voltage of the nozzle electrode was increased to 900 and 1,000 volts, respectively. This reduction might be attributed to the discharge phenomenon and the region in which there has been ionisation of the air, probably resulting in insufficient chargeability to reach the spray [56]. It can be

concluded that an induction voltage level of 800 volts is the best that can be used with the induction nozzle in terms of achieving the highest spray current.

6.3.4. Determination of coverage area

This parameter can indicate the efficiency of the method of application. The best method can be judged as that which gives a high coverage area on the intended target and relatively less drift to the environment or on the ground. For this reason coverage is used to compare the methods or ways of application. To test the ability of the novel induction nozzle to cover the target (insect), evaluation of the coverage area was deemed necessary. Figures 6.20 and 6.21 illustrate the preparation of the artificial plants and experimental setup. The front and back surfaces of the leaves of the plants were covered with WSP so as to facilitate calculation of the coverage area of both surfaces (front and back of the leaf). The other reason for using WSP was to capture the droplet size distribution, with and without charging.

Figure 6.20: The preparation of the artificial plants in relation to the targets.
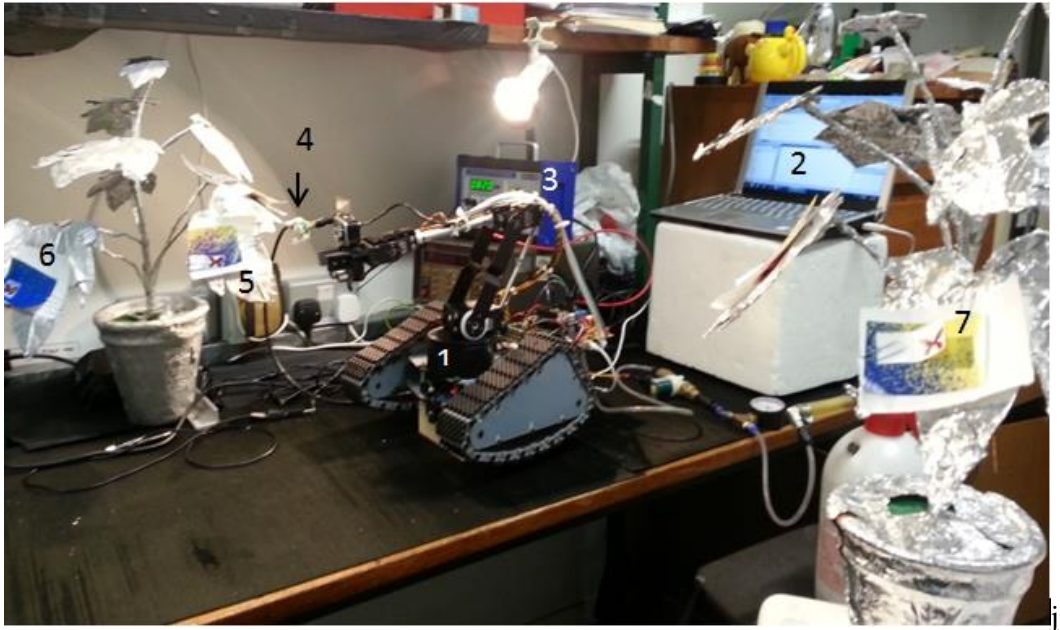
Figure 6.21: The experimental setup for controlling the insects and measuring the coverage area: robot (1); computer (2); high voltage supply (3); induction nozzle (4) and insect targets (5, 6 and 7).

The level of induction voltage used in these experiments was 800 volts as it was found to be the best in the experiments conducted previously. From Figure 6.22, it can be seen that the induction nozzle can deal with the targets when they are arranged individually or in groups with different positions. A change in the colour of the WSP from yellow to blue indicated the ability of the nozzle to deal with the intended target.

Figure 6.22: Induction nozzle dealing with the individual and group targets.

The values of depositions on the back surface of each leaf were captured both for with and without charging (see Figure 6.23).

Figure 6.23: The coverage area on the back of the leaf target under the charged (left) and uncharged condition (right).

Figure 6.24 shows the induction nozzle operating with different targets, before, during and after the procedure.

Figure 6.24: The induction nozzle working on the targets.

In order to compare the results of the samples that were collected, microscopic pictures were prepared from the samples and a digital microscopic device, the model HD colour CMOS Sensor, High-Speed DSP was used for this task. The unit area captured for all the samples was $0.5cm^2$ which is equivalent to 640x480 pixels. The images presented in Figure 6.25 below represent the nature of the coverage area under the charged condition. These pictures are for both the top and bottom surfaces of the leaves. Furthermore, Figure 6.26 presents the nature of the coverage without charging for the top and bottom surfaces of the leaves. The results obtained for these two cases indicate that the coverage area when charging is more

than when without. Moreover, the top surface has greater coverage than the bottom in both cases.
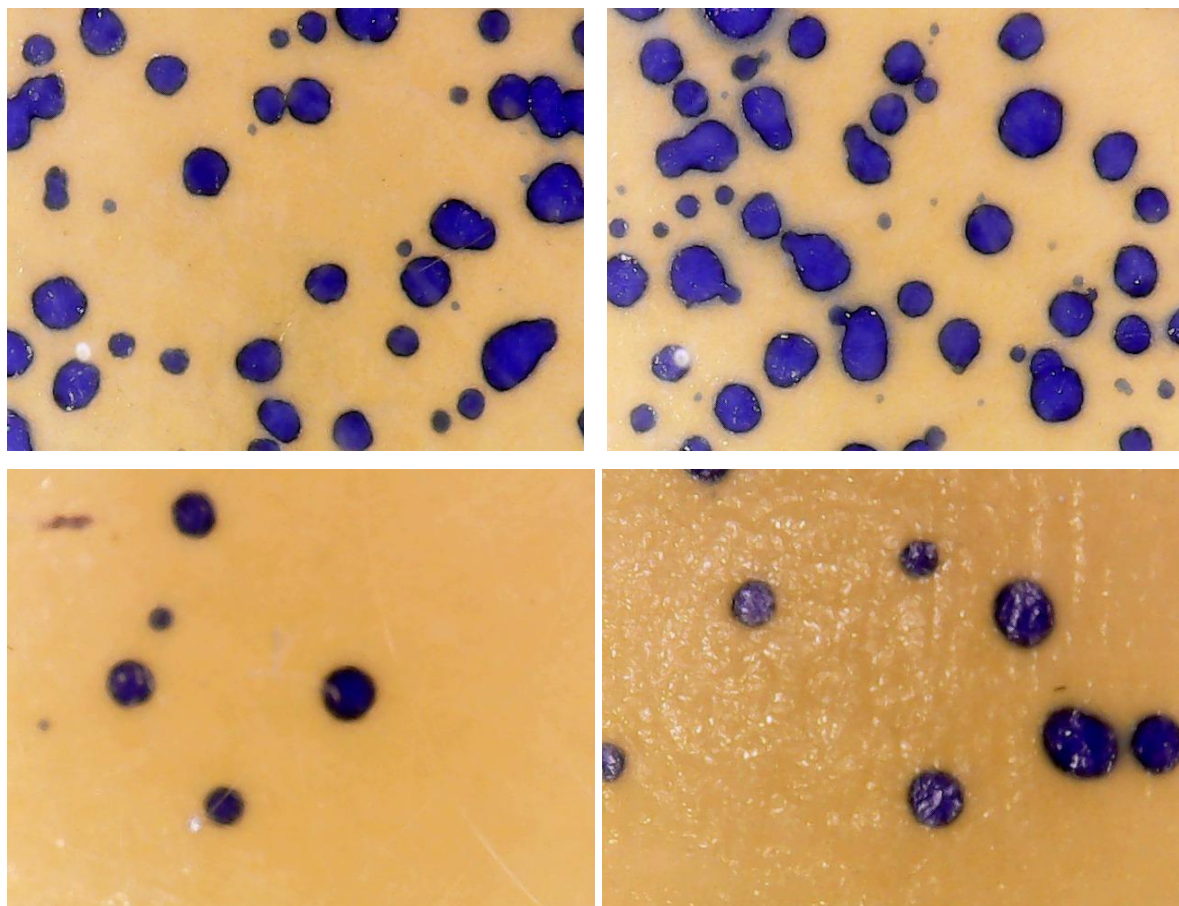
Figure 6.25: The coverage area under the charged condition on the top surface (top samples) and the charged condition on the back surface (bottom samples) of the leaves.
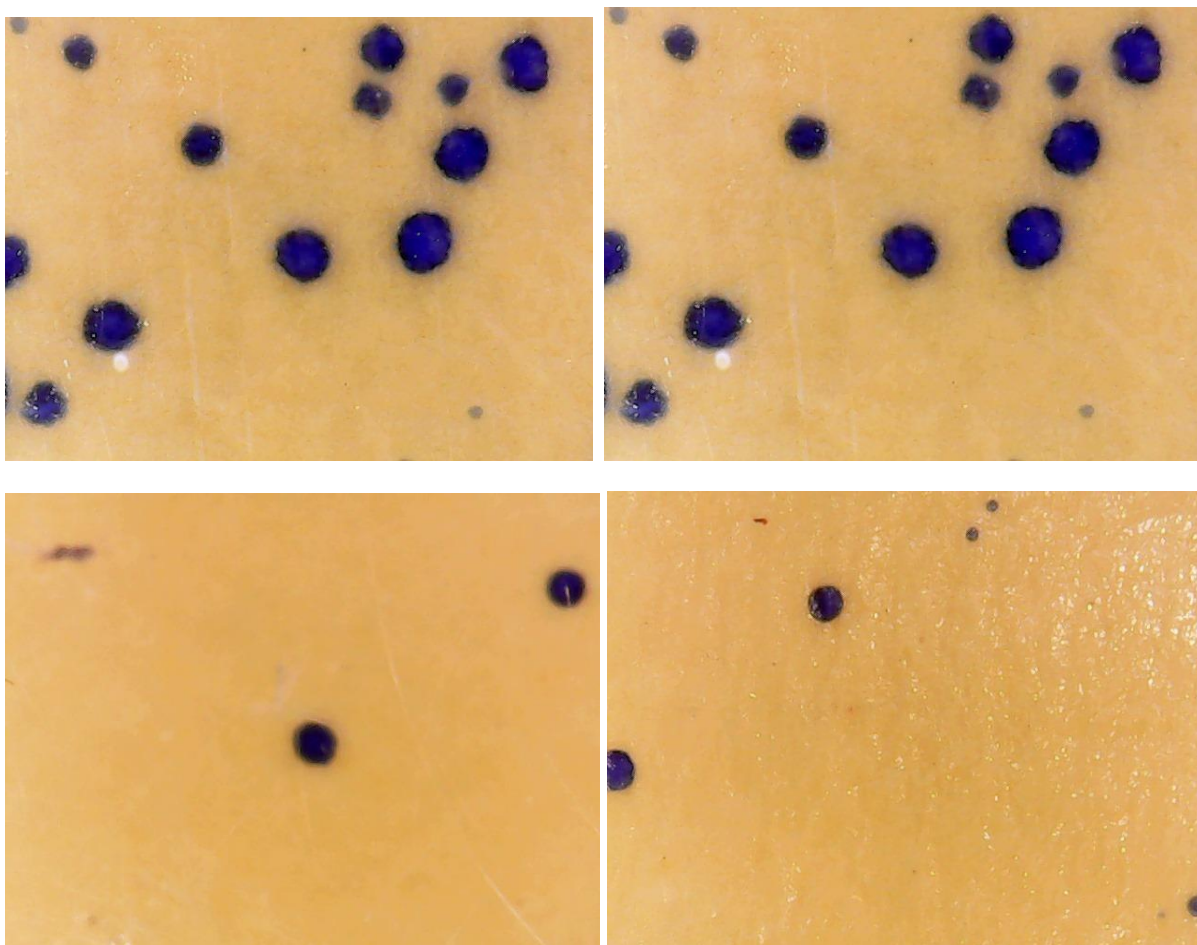
Figure 6.26: The coverage area for the uncharged condition on the front surface (top samples) and the uncharged condition on the back surface (bottom samples) of the leaves.

In order to measure the coverage area for the two cases, a simple program created with Matlab software was used. This program calculates the percentages of coverage area of all the droplets in one unit to the area of the original sample. The results obtained from this program for all the microscopic pictures were plotted and are presented in Figures 6.27, 6.28 and 6.29. These show that the areas of efficient coverage for the two cases, i.e. with and without charging as well as for the two leaf surfaces, front and back, are different. The percentage of coverage area for the front surface under the charging condition is three to fourfold more when compared to that for the same surface in the uncharged condition (see Figure 6.27). Moreover, in the charged condition on the back surface the value is two to three times more compared to the back surface under the uncharged condition (see Figure 6.28). These results are in good agreement with those of Maski and Durairaj, indicating that the adaxial (upper) surfaces received greater deposition than the abaxial (bottom) ones [41], also being consistent with findings by Chao *et al* [109]. In addition, the results that are obtained

from this study agree with the range of values obtained by Law 1980, which fell between 1.8 fold to seven-fold for the charged versus uncharged scenarios. Moreover, when comparing the charged value and the value of conventional deposition the range was 1.9 fold to 4.4 fold [12]. However, the results of the current study recorded greater increases than those reported by Cooper and Law [66], who recorded values of 1.5 and 1.8 fold increases when the current spray was positive and when it was negative, respectively [24].
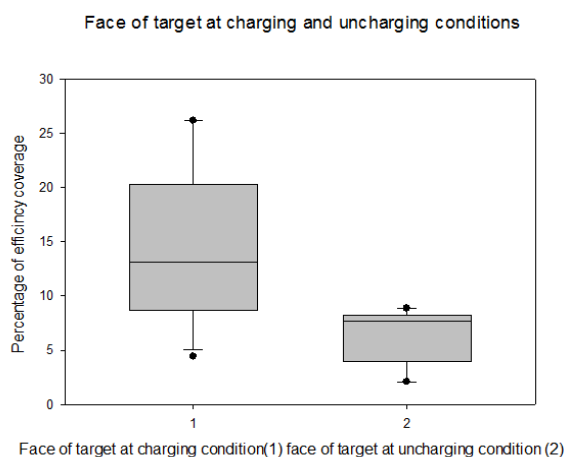
Figure 6.27: The coverage area of the front surface for the charged and uncharged conditions.
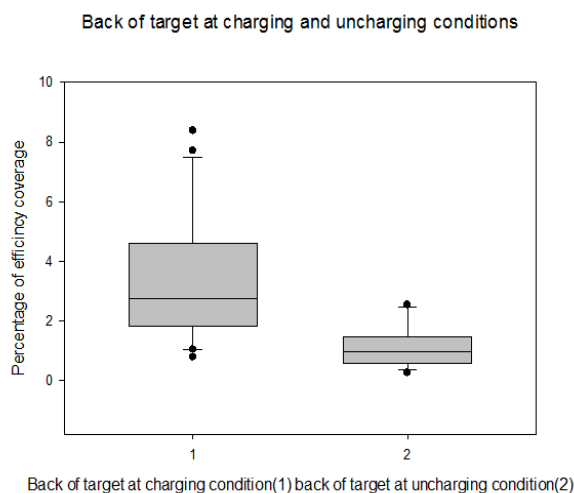
Figure 6.28: The coverage area of the back surface for the charged and uncharged conditions.

In general, the coverage area is reduced in the uncharged condition and the under surface receives less deposit than the upper regardless of whether the spray is charged or not (see Figure 6.29).
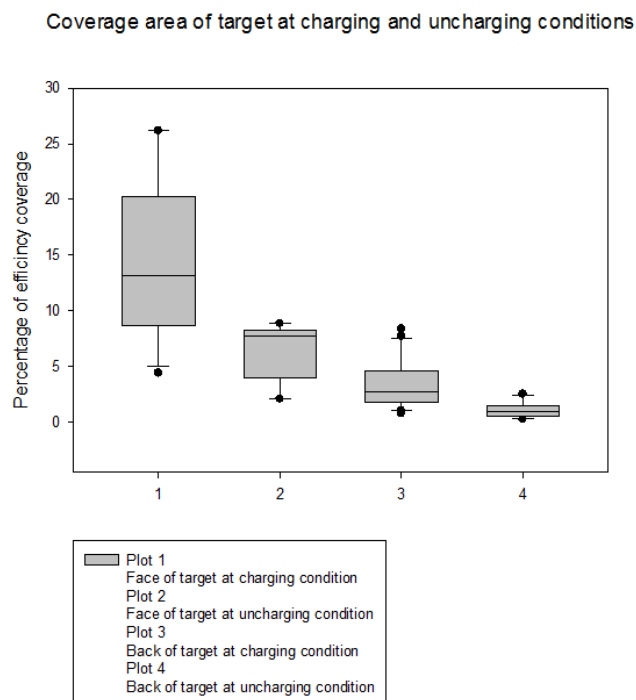
Figure 6.29: The coverage area for all the results.

6.3.5. Determination of soil contamination

For determining the amount of soil contamination, WSP was placed underneath the plant and on the ground. Figure 6.30 presents the condition of the WSPs collected from the charged and uncharged conditions.
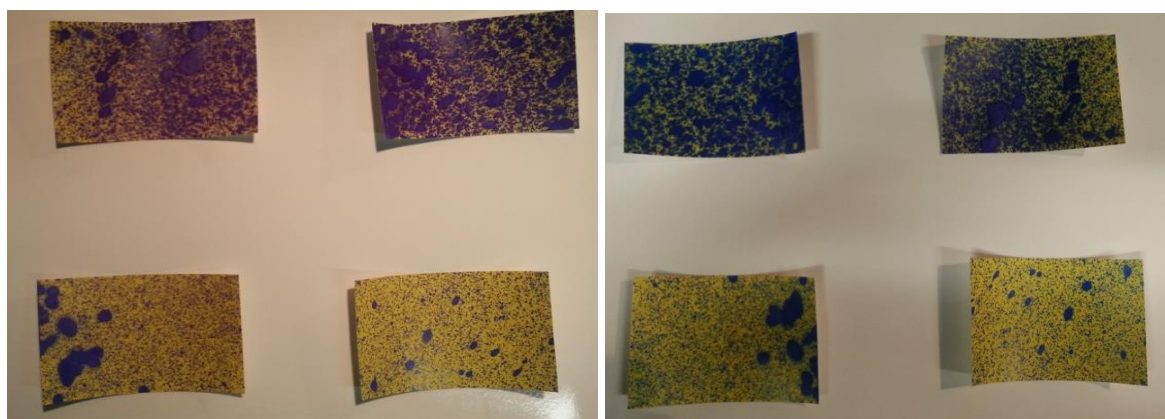
Figure 6.30: WSPs showing soil contamination for the uncharged condition (top samples) and charged condition (bottom samples).

To compare the results of these samples, microscopic pictures were required. In Figure 6.31 the samples obtained from soil contamination under the two cases of with and without charging are presented.
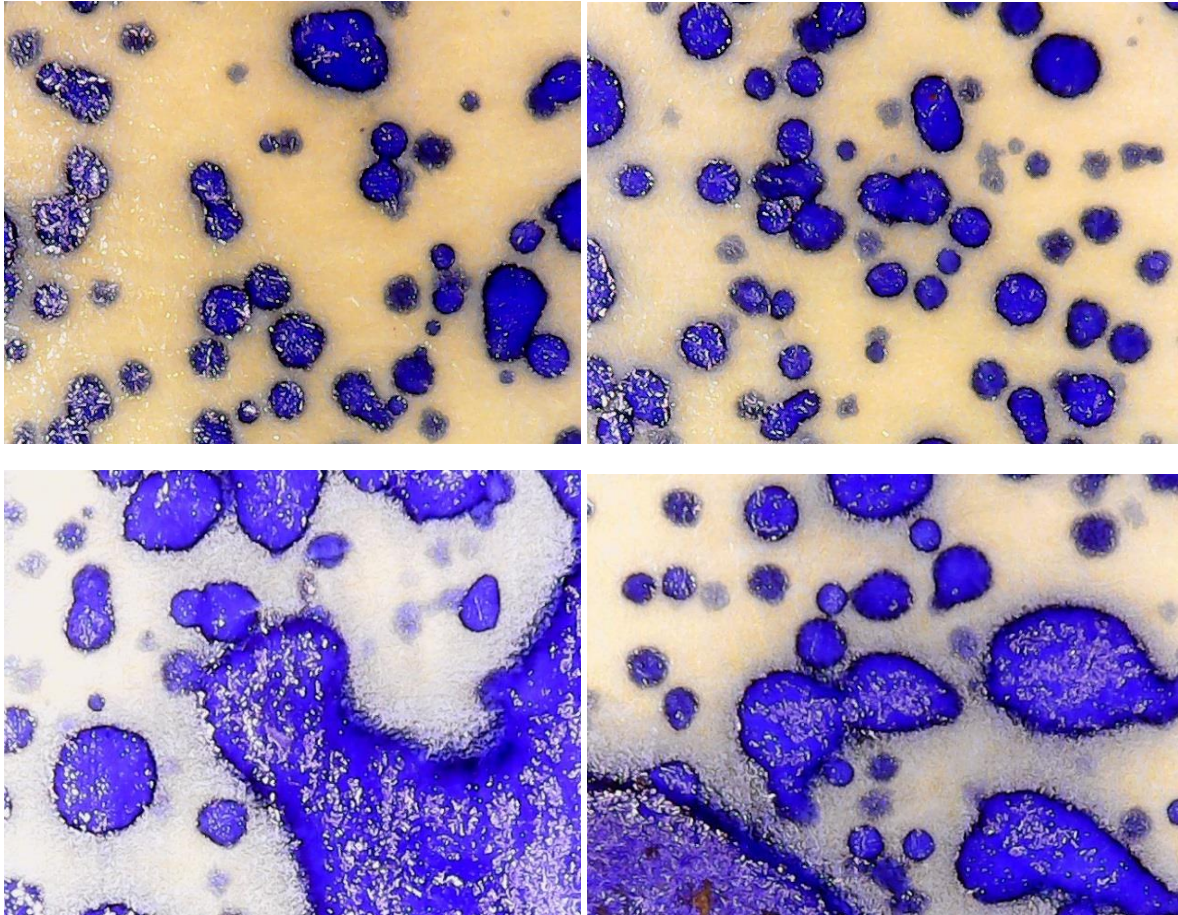
Figure 6.31: Soil contamination on the ground for the charged condition (top samples) and uncharged condition (bottom pictures).

The same program of Matlab software that was used to determine the target coverage area was deployed to ascertain the level of soil contamination and the results are presented in Figure 6.32. It appears that a reduction in soil contamination is achieved under the charged when compared with the uncharged condition. The value of this reduction ranges from two to four fold (see Figure 6.31). This result is in agreement with those stated by Inculet *et al* [14], Laryea and No [34] and Esehaghbeygi and *et al* [43]. The outcomes of their experiments confirmed that the charging method achieved high deposition values on the targets and reduced the amount of the drift and soil contamination in the air as well as on the ground [17], [34], [43], respectively.
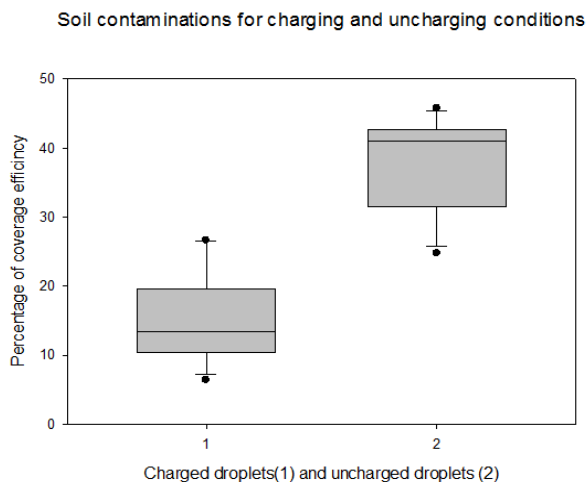
Figure 6.32: The value of soil contamination in the two cases: with and without charging.

6.4. Determination of the droplet size

The droplet sizes for both charged and uncharged droplets were measured by applying the Image J software procedure described above. The results indicate that the uncharged droplet sizes were larger than those for the charged droplets. The reason for this increase in size may be attributed to the two factors, first the spray angle, and second, the chargeability of the spray liquid. In the uncharged condition, the angle spray is smaller than that for the charged condition, as seen from the results presented in Figure 6.15 above. In this case, there are reduced opportunities for the nozzle liquid to atomize well and produce small sized droplets. Furthermore, the Coulomb repulsion of unipolarly charged droplets is absent in this case, which helps to create opportunities for two or more droplets to form one big droplet due to the coalescence phenomenon amongst the droplets. By contrast, under the charged condition, the spray angle is more than that for the uncharged state due to the space charge effect, as shown in Figure 6.19. The repellent phenomenon between the droplets will produce small droplets due to absence of the coalescing process. This result is identical to that obtained by Marchant *et al*, who reported that the diameter of the droplet decreases when the nozzle angle and pressure increase [56]. The sizes of the charged droplets produced in this study ranged between 200 and 300 μ, as illustrated in Figures 6.33 and 6.34.

Droplet size distribtion of charged droplet on the ground
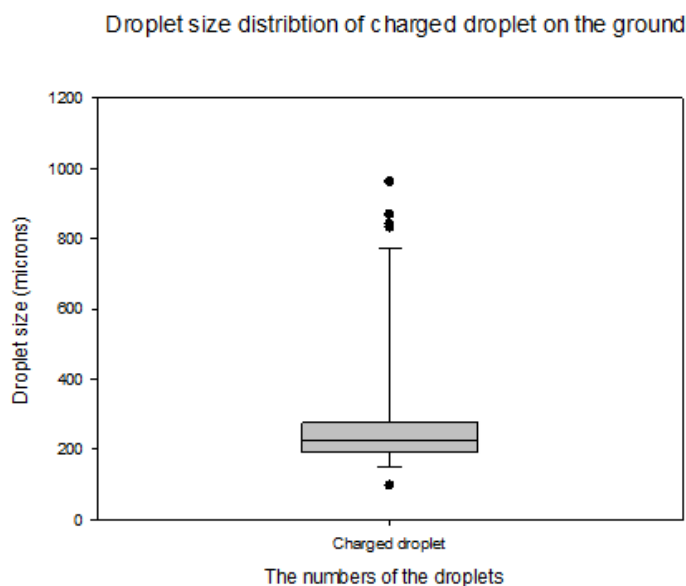
Figure 6.33: The sizes of charged droplets produced.

Droplet size distribtion of uncharged droplets on the ground
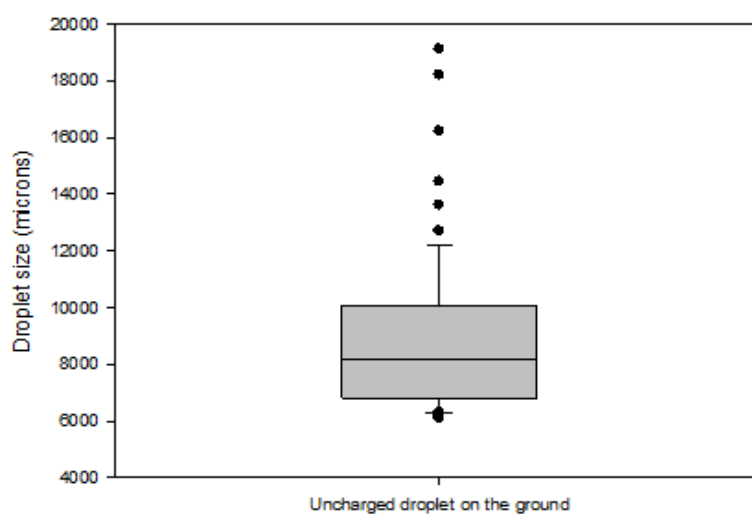
Figure 6.34: The sizes of the uncharged droplets on the ground.

The results of this study are in good agreement with the outcomes reported by Merchant and Green, who found differences in the droplet sizes between charged and uncharged systems, with the sizes of charged droplets produced ranging between 50 and 300 μ [16]. In addition, these results concur with those reported by Jahannama *et al* [32], whose work showed that the droplet size distributions of horizontal sprays had a significant difference for charged and uncharged cases [32]. Furthermore, the present results correspond with the outcomes reported

by Laryea and No [34] , which indicated that droplet size shows an increase in the VMD when voltage is applied [34] Moreover, there is agreement with Wilson's results, who found that droplet size can be affected by changing the operating voltage [61].

6.5. Summary

In this chapter, the abilities of the mobile robot system and the novel induction nozzle to deal with the targets and to achieve the goals of this study have been tested. The robot system has experimentally been proven to have robust static and mobile capabilities so as to be able to deal with the targets on the plant leaves as well as with different shapes, sizes and numbers. Furthermore, the capacities of the new induction nozzle have been tested with and without charging the spray. The results produced under the charged condition have achieved high values for spray current, charge to mass ratio, spray angle and coverage area, whilst reducing droplet size and soil contamination.

CHAPTER SEVEN: CONCLUSIONS AND FUTURE WORK

7.1. Conclusions:

 The work carried out for this thesis involved designing smart mobile robotic spraying system that would be used to corroborate the efficiency of smart spraying augmented by introducing electrostatic spray charging over conventional ones for better plant coverage, lesser wasted pesticide and lighter soil pollution.

An extensive study of the electrostatic system was carried out. The investigation was accompanied with thorough computer simulation and real world experimentation. The computer simulation was accomplished using the COMSOL™ version 4.4 software package running under the Windows 7 operating system. The simulation involved several targets with geometrical and non-geometrical shapes, different nozzle designs operating under different pressures while operating with and without applying electrostatic induction charging. Different levels of electrostatic charging along with different nozzle operating pressures were used to determine the optimal operating conditions that yield the best possible target or plant coverage and minimum waste. The application of electrostatic induction on pesticide spraying has greatly improved plant coverage and resulted in lesser amounts of wasted pesticide.

 Special experimentation gears and platforms were designed and implemented to carry out tests on nozzles in laboratory controlled conditions in order to obtain readouts from the specialized measuring equipment used with minimum possible error and interference from the surrounding environment. The experimentation was carried out on cotton plant models. Several experimentation setups were devised to ease test equipment operation under minimum man intervention so to minimize human error. Experimentation on industry standard electrostatic spray system (ESS) nozzles was carried out and detecting spray coverage was accomplished using water sensitive paper (WSP) along with using video capturing accompanied by optical spray visualization techniques involving the use of a strobe light and fluorescent dies.

 The large volume of data was obtained from the simulation and experimentation gave system designer the necessary experience and insight required to realise the end product namely the smart crop spraying system. To this end another type of nozzle was put examined, the fan hydraulic spray nozzle (FHSN). Supplementary simulation and experimentation were carried out on this nozzle type and the addition of electrostatic induction capabilities to it resulted in

an electrostatic induction spray nozzle (EISN) which is one of the prime parts of the designed smart spraying system.

Manufacturing the required additional parts required for the EISN involved using SOLIDWORKS software in designing parts of this nozzle which were subsequently manufactured using 3D printing.

The other requirements needed to attain the smart crop spraying system were the selection of the robotic platform and smart system that will carry out the intended tasks. The AL05D robotic manipulator and TTRK tracked platform form Lynxmotion™ were chosen as the mini mobile robot components required for the a feasibility study of the smart electrostatic crop spraying system. The selection was made because these devices were well supported by the manufacturer and were suitable for realizing the end product that was required to control pest infestation of cotton plants. Intelligence was added to the device by equipping the mobile robot with several sensing devices that included a CCD digital camera, a range detector, and a path mark detector. A Windows™ based mobile computer in addition to an ARDUINO™ based microcontroller system provided the computational power required by the smart electrostatic crop sprayer. They were arranged in a Master – Slave configuration with the main processing for image and motion being conducted inside the powerful master computer and programmed using Matlab™ software, whereas the execution of motion commands and the operation of the range and path mark detection units as well as operating the spray nozzle were performed inside the slave computer the Arduino mega2560. The slave computer software was written using C as the programming language.

The manufactured smart electrostatic spray system is capable of moving along cotton crop rows. The mobile spraying system repositions its camera in a motion pattern planned to scan the selected cotton plant for pest infestation on the upper and lower surfaces of the leaves. If a bug is detected, the spray nozzle is be aligned with the aid of the camera and the distance detector to put the spray nozzle in an ideal position to target the insect and spray a very short burst of pesticide directly onto the targeted insect.

The results obtained from the conducted experiments showed that using electrostatic induction has improved the resulting plant coverage by 3 to 4 fold and led a reduction in soil contamination of 2 to 4 fold.

The smart spraying system designed in this study still holds plenty of room for future performance improvement and further system development that will make capable of being adapted for other crops and applications.

7.2. Future Works Suggestions

The designed system has plenty of room for further improvement of its functioning and application. The following suggestions can be used as a guideline for future works.

1- Improving the performance of the spray nozzle by trying additional shapes and geometries for the induction electrodes with different materials that will ensure better liquid droplets charging and further minimize the possibility of contact between the nozzle charging electrodes and liquid film which will result in improved operational performance for the electrostatic charged spray nozzle.

2- Enhancing insect detection capabilities of the smart spraying system so as to reduce false detection by implementing a higher powered computing system capable of running a more sophisticated DSP algorithm that will improve insect detection. Using a higher resolution camera in addition to more powerful DSP image processing algorithms will result in better performance.

3- The designed system may be developed further to deal with several additional types of insects as well as to engaging with multiple targets simultaneously by adjusting the nozzle to target distance and varying the spraying period so as to provide the pesticide amount required to deal with larger insect numbers.

4- Selecting a robotic manipulator with additional degrees of freedom will result in a spraying system that will be capable of executing more complex search maneuvers thereby making the pest detection process more successful in detecting insects hiding in hard to reach places on the targeted plants.

References

[1] M. Yudelman, "Some Issues in Agricultural Development in Iraq," *Journal of Farm Economics,* vol. 40, pp. 78-88, 1958.

[2] M. Proto, S. Supino and O. Malandrino, "Cotton: a flow cycle to exploit," *Industrial Crops and Products,* vol. 11, pp. 173-178, 2000.

[3] T. Ahmad, "Field studies on sex pheromone trapping of cotton leafworm Spodoptera littoralls (Boisd.)(Lep., Noctuidae)," *J. Appl. Entomol.,* vol. 105, pp. 212-215, 1988.

[4] I. Bashour, M. Tolba and N. Saab, "Pesticides, fertilizers and food safety," in *Arab Environment: Future Challenges. Tolba, M., and Saab, N.(Ed.), Report of the Arab Forum for Environment and Development (AFED) and Technical Publications, Beirut, Lebanon,* 2008, pp. 137-145.

[5] S. Edward Law, "Agricultural electrostatic spray application: a review of significant research and development during the 20th century," *J. Electrostatics,* vol. 51, pp. 25-42, 2001.

[6] J. Grace and J. Marijnissen, "A review of liquid atomization by electrical means," *J. Aerosol Sci.,* vol. 25, pp. 1005-1019, 1994.

[7] Z. A. Huneiti, "Electrohydrodynamic atomisation of conducting liquid using an AC field superimposed on a DC field." 2000.

[8] S. E. Law, "Electrostatic pesticide spraying: concepts and practice," *Industry Applications, IEEE Transactions on,* pp. 160-168, 1983.

[9] A. Jaworek, "Micro-and nanoparticle production by electrospraying," *Powder Technol,* vol. 176, pp. 18-35, 2007.

[10] G. P. Castle and I. I. Inculet, "Space charge effects in orchard spraying," *Industry Applications, IEEE Transactions on,* pp. 476-480, 1983.

[11] S. E. Law, "Embedded-electrode electrostatic-induction spray-charging nozzle: theoretical and engineering design [in the overall process of electrostatic deposition of liquid pesticide droplets onto agricultural plants]." *Transactions of the ASAE [American Society of Agricultural Engineers],* vol. 21, 1978.

[12] S. Law, "Electrostatic deposition of pesticide spray onto foliar targets of varying morphology." *ASAE Paper,* 1980.

[13] A. Frost and S. Law, "Extended flow characteristics of the embedded-electrode spray-charging nozzle," *J. Agric. Eng. Res.,* vol. 26, pp. 79-86, 1981.

[14] I. Inculet, G. Castle, D. Menzies and R. Frank, "Deposition studies with a novel form of electrostatic crop sprayer," *J. Electrostatics,* vol. 10, pp. 65-72, 1981.

[15] S. E. Law and M. D. Lane, "Electrostatic deposition of pesticide sprays onto ionizing targets: charge-and mass-transfer analysis," *Industry Applications, IEEE Transactions on,* pp. 673-679, 1982.

[16] J. Marchant and R. Green, "An electrostatic charging system for hydraulic spray nozzles," *J. Agric. Eng. Res.,* vol. 27, pp. 309-319, 1982.

[17] Inculet,G.S. Castel and R.S. Vermey, "Electrostatic Spraying of Row Field Crops," vol. IAS84:37A, pp. 1058-1060, 1984.

[18] J. Lake and J. Marchant, "Wind tunnel experiments and a mathematical model of electrostatic spray deposition in barley," *J. Agric. Eng. Res.,* vol. 30, pp. 185-195, 1984.

[19] S. E. Law and H. D. Bowen, "Dual particle-specie concept for improved electrostatic deposition through space-charge field enhancement," *Industry Applications, IEEE Transactions on,* pp. 694-698, 1985.

[20] S. Law and S. Cooper, "Depositional characteristics of charged droplets applied by an orchard air-blast sprayer," *American Society of Agricultural Engineers,* 1985.

[21] D. Hadfield, "The modelling of charged spray deposition on artificial targets," *J. Agric. Eng. Res.,* vol. 36, pp. 45-56, 1987.

[22] S. E. Law, J. A. Marchant and A. G. Bailey, "Charged-spray deposition characteristics within cereal crops," *Industry Applications, IEEE Transactions on,* pp. 685-693, 1985.

[23] J. Marchant, A. Dix and J. Wilson, "The electrostatic charging of spray produced by hydraulic nozzles: Part II. Measurements," *J. Agric. Eng. Res.,* vol. 31, pp. 345-360, 1985.

[24] S. C. a. L. Cooper S.E., "Transient Characteristics of Charge Spray Deposition Occurring Under Action of Induction Taget Coronas: Space charge Polarity Effect," *The Institute of Physics ,Static Electrification Group,* Electrostatic'87,St Catherine's College,Oxford 8-12 April, 1987.

[25] J. R. Lake, "The deposition of electrostatically charged sprays on parts of targets shaded from the spray," *J. Agric. Eng. Res.,* vol. 39, pp. 9-18, 1988.

[26] A. Bologa and L. Makalsky, "Electrostatic pneumatic sprayer of water solutions," *J. Electrostatics,* vol. 23, pp. 227-233, 1989.

[27] I. Inculet and J. Fischer, "Electrostatic aerial spraying," *Industry Applications, IEEE Transactions on,* vol. 25, pp. 558-562, 1989.

[28] D. Giles, Y. Dai and S. Law, "Enhancement of spray electrodeposition by active precharging of a dielectric boundary," in *Institute of physics conference series,* 1991, pp. 33-38.

[29] S. E. Law, S. Cooper and R. Oetting, "Advances in air-assisted electrostatic crop spraying of conductive pesticides," in *American Society of Agricultural Engineers. Meeting,* 1992, .

[30] W. Machowski and W. Balachandran, "Design of electrostatic fog generator using a reverse field modelling technique," in *Industry Applications Conference, 1997. Thirty-Second IAS Annual Meeting, IAS'97., Conference Record of the 1997 IEEE,* 1997, pp. 1784-1789.

[31] S. Edward Law, J. Robert Cooke and S. C. Cooper, "Space charge suppression of electrostatic-induction spray charging," *J. Electrostatics,* vol. 40, pp. 603-608, 1997.

[32] M. Jahannama, A. Watkins and A. Yule, "Examination of electrostatically charged sprays for agricultural spraying applications," in *ILASS拟 Europe,* 1999, pp. 120-127.

[33] J. R. Cooke and S. E. Law, "Finite-element analysis of space-charge suppression of electrostatic-induction spray charging," *Industry Applications, IEEE Transactions on,* vol. 37, pp. 751-758, 2001.

[34] G. N. Laryea and S. No, "Development of electrostatic pressure-swirl nozzle for agricultural applications," *J. Electrostatics,* vol. 57, pp. 129-142, 2003.

[35] S. Zhao, G. Castle and K. Adamiak, "Comparison of conduction and induction charging in liquid spraying," *J. Electrostatics,* vol. 63, pp. 871-876, 2005.

[36] S. Zhao, G. Castle and K. Adamiak, "Factors affecting deposition in electrostatic pesticide spraying," *J. Electrostatics,* vol. 66, pp. 594-601, 2008.

[37] M. A. Latheef, J. B. Carlton, I. W. Kirk and W. C. Hoffmann, "Aerial electrostatic-charged sprays for deposition and efficacy against sweet potato whitefly (Bemisia tabaci) on cotton," *Pest Manag. Sci.,* vol. 65, pp. 744-752, 2009.

[38] Maynagh,B.M.,Ghobadian,M.J., andT.T. Hashjin, "Effect of Electrostatic Induction Parameters on Drroplets Charging for Agriculture Application," vol. J. Agric.Sci., pp. 249-257, 2009.

[39] B. F. Nader, G. P. Castle and K. Adamiak, "Effect of surface conduction on the dynamics of induction charging of particles," *J. Electrostatics,* vol. 67, pp. 394-399, 2009.

[40] D. Maski and D. Durairaj, "Effects of electrode voltage, liquid flow rate, and liquid properties on spray chargeability of an air-assisted electrostatic-induction spray-charging system," *J. Electrostatics,* vol. 68, pp. 152-158, 2010.

[41] D. Maski and D. Durairaj, "Effects of charging voltage, application speed, target height, and orientation upon charged spray deposition on leaf abaxial and adaxial surfaces," *Crop Protection,* vol. 29, pp. 134-141, 2010.

[42] N. Toljic, G. Castle and K. Adamiak, "Charge to radius dependency for conductive particles charged by induction," *J. Electrostatics,* vol. 68, pp. 57-63, 2010.

[43] A. Esehaghbeygi, A. Tadayyon and S. Besharati, "Comparison of Electrostatic and Spinning-discs Spray Nozzles on Wheat Weeds Control," *Journal of American Science,* vol. 12, pp. 6, 2010.

[44] A. Bayat, A. Bolat, A. Soysal, M. Güllü and H. Sarıhan, "Efficiency of different spray application methods in second crop maize," .

[45] R. Roten, A. Hewitt, M. Ledebuhr, H. Thistle, R. Connell, T. Wolf, S. Sankar, S. Woodward and S. Zydenbos, "Evaluation of spray deposition in potatoes using various spray delivery systems." *New Zealand Plant Protection,* vol. 66, pp. 317-323, 2013.

[46] R. S. Sasaki, M. M. Teixeira, H. C. Fernandes, Monteiro, Paulo Marcos de Barros, D. E. Rodrigues and C. B. d. Alvarenga, "Parameters of electrostatic spraying and its influence on the application efficiency," *Revista Ceres,* vol. 60, pp. 474-479, 2013.

[47] V. R. Mamidi, C. Ghanshyam, P. Manoj Kumar and P. Kapur, "Electrostatic hand pressure knapsack spray system with enhanced performance for small scale farms," *J. Electrostatics,* vol. 71, pp. 785-790, 2013.

[48] D. Martin and J. Carlton, "Airspeed and orifice size affect spray droplet spectrum from an aerial electrostatic nozzle for fixed-wing applications," *Appl. Eng. Agric.,* vol. 29, pp. 5-10, 2013.

[49] M. K. Patel, C. Ghanshyam and P. Kapur, "Characterization of electrode material for electrostatic spray charging: Theoretical and engineering practices," *J. Electrostatics,* 2012.

[50] G. Laryea, S. Kim and S. No, "Depositional studies of a charged spray application in an orchard," .

[51] M. Mokeba, D. Salt, B. Lee and M. Ford, "Simulating the dynamics of spray droplets in the atmosphere using ballistic and random-walk models combined," *J. Wind Eng. Ind. Aerodyn.,* vol. 67, pp. 923-933, 1997.

[52] P. Miller and B. Ellis, "Effects of formulation on spray nozzle performance for applications from ground-based boom sprayers," *Crop Protection,* vol. 19, pp. 609-615, 2000.

[53] D. Giles and E. Ben-Salem, "Spray droplet velocity and energy in intermittent flow from hydraulic nozzles," *J. Agric. Eng. Res.,* vol. 51, pp. 101-112, 1992.

[54] M. Ellis, C. Tuck and P. Miller, "The effect of some adjuvants on sprays produced by agricultural flat fan nozzles," *Crop Protection,* vol. 16, pp. 41-50, 1997.

[55] B. Ellis, C. Tuck and P. Miller, "How surface tension of surfactant solutions influences the characteristics of sprays produced by hydraulic nozzles used for pesticide application," *Colloids Surf. Physicochem. Eng. Aspects,* vol. 180, pp. 267-276, 2001.

[56] J. Marchant, A. Dix and J. Wilson, "The electrostatic charging of spray produced by hydraulic nozzles: Part I. Theoretical Analysis," *J. Agric. Eng. Res.,* vol. 31, pp. 329-344, 1985.

[57] N. Toljic, K. Adamiak, G. Castle, H. H. Kuo and H. C. Fan, "Three-dimensional numerical studies on the effect of the particle charge to mass ratio distribution in the electrostatic coating process," *J. Electrostatics,* vol. 69, pp. 189-194, 2011.

[58] N. Toljic, K. Adamiak and G. Castle, "Determination of particle charge to mass ratio distribution in electrostatic applications: A brief review," in *Proc. ESA Annual Meeting on Electrostatics,* 2008, .

[59] Y. Ru, H. Zhou and J. Zheng, "Design and Experiments on Droplet Charging Device for High-Range Electrostatic Sprayer," 2011.

[60] K. D. Kihm, B. Kim and A. McFarland, "Atomization, charge, and deposition characteristics of bipolarly charged aircraft sprays," *Atomization and Sprays,* vol. 2, 1992.

[61] J. Wilson, "A linear source of electrostatically charged spray," *J. Agric. Eng. Res.,* vol. 27, pp. 355-362, 1982.

[62] G. Laryea and S. No, "Spray characteristics of charge injected electrostatic pressure-swirl nozzle," *Zaragoza,* vol. 9, pp. 11, 2002.

[63] R. S. Sasaki[1], M. M. Teixeira[1], H. C. Fernandes[1], P. M. Monteiro[1], D. E. Rodrigues and C. B. Alvarenga[1], "Effect of space on droplets electrical charge during electrostatic spraying," 2012.

[64] D. Nuyttens, K. Baetens, M. De Schampheleire and B. Sonck, "Effect of nozzle type, size and pressure on spray droplet characteristics," *Biosystems Engineering,* vol. 97, pp. 333-345, 2007.

[65] K. Asano, "Electrostatic spraying of liquid pesticide," *J. Electrostatics,* vol. 18, pp. 63-81, 1986.

[66] S. C. Cooper and S. E. Law, "Bipolar spray charging for leaf-tip corona reduction by space-charge control," *Industry Applications, IEEE Transactions on,* pp. 217-223, 1987.

[67] S. E. Law and A. G. Bailey, "Perturbations of charged-droplet trajectories caused by induced target corona: LDA analysis," *Industry Applications, IEEE Transactions on,* pp. 1613-1622, 1984.

[68] S. E. Law, "Electrical interactions occurring at electrostatic spraying targets," *J. Electrostatics,* vol. 23, pp. 145-156, 1989.

[69] S. Carlsen, N. H. Spliid and B. Svensmark, "Drift of 10 herbicides after tractor spray application. 1. Secondary drift (evaporation)," *Chemosphere,* vol. 64, pp. 787-794, 2006.

[70] T. M. Wolf, R. Grover, K. Wallace, S. R. Shewchuk and J. Maybank, "Effect of protective shields on drift and deposition characteristics of field sprayers," *Canadian Journal of Plant Science,* vol. 73, pp. 1261-1273, 1993.

[71] N. Thompson and A. Ley, "Estimating spray drift using a random-walk model of evaporating drops," *J. Agric. Eng. Res.,* vol. 28, pp. 419-435, 1983.

[72] A. Hewitt, "Spray drift: impact of requirements to protect the environment," *Crop Protection,* vol. 19, pp. 623-627, 2000.

[73] K. Baetens, D. Nuyttens, P. Verboven, M. De Schampheleire, B. Nicolaï and H. Ramon, "Predicting drift from field spraying by means of a 3D computational fluid dynamics model," *Comput. Electron. Agric.,* vol. 56, pp. 161-173, 2007.

[74] K. Baetens, Q. Ho, D. Nuyttens, M. De Schampheleire, A. Melese Endalew, M. Hertog, B. Nicolaï, H. Ramon and P. Verboven, "A validated 2-D diffusion–advection model for prediction of drift from ground boom sprayers," *Atmos. Environ.,* vol. 43, pp. 1674-1682, 2009.

[75] R. Fox, M. Salyani, J. Cooper and R. Brazee, "Spot size comparisons on oil-and water-sensitive paper," *Appl. Eng. Agric.,* vol. 17, pp. 131-136, 2001.

[76] B. Sayıncı, S. Bastaban and J. Sánchez-Hermosilla, "Determination of Optimal Spot Roundness Variation Interval for Droplet Size Analysis on Water Sensitive Paper," 2011.

[77] R. D. Fox, R. Derksen, J. Cooper, C. Krause and H. Ozkan, "Visual and image system measurement of spray deposits using water-sensitive paper," *Appl. Eng. Agric.,* vol. 19, pp. 549-554, 2003.

[78] E. Cerruto, C. Aglieco, S. Failla and G. Manetto, "Parameters influencing deposit estimation when using water sensitive papers," *Journal of Agricultural Engineering,* vol. 44, pp. e9, 2013.

[79] F. Pezzi and V. Rondelli, "The performance of an air-assisted sprayer operating in vines," *J. Agric. Eng. Res.,* vol. 76, pp. 331-340, 2000.

[80] X. Martini, N. Kincy and C. Nansen, "Quantitative impact assessment of spray coverage and pest behavior on contact pesticide performance," *Pest Manag. Sci.,* vol. 68, pp. 1471-1477, 2012.

[81] Latheef,Kirk,Bouse,Carlton,Hoffmann, "Evalution of Aerial Delivery Systems for Spray Deposition and Efficiency Adainst Sweet Potato Whitefly on Cotton." vol. 24(4), pp. 415-422, 2008.

[82] M. Cunha, C. Carvalho and A. R. Marcal, "Assessing the ability of image processing software to analyse spray quality on water-sensitive papers used as artificial targets," *Biosystems Engineering,* vol. 111, pp. 11-23, 2012.

[83] J. Cunha, A. Farnese and J. Olivet, "Computer programs for analysis of droplets sprayed on water sensitive papers," *Planta Daninha,* vol. 31, pp. 715-720, 2013.

[84] C. Turner and K. Huntington, "The use of a water sensitive dye for the detection and assessment of small spray droplets," *J. Agric. Eng. Res.,* vol. 15, pp. 385-387, 1970.

[85] W. Hoffmann and A. Hewitt, "Comparison of three imaging systems for water-sensitive papers," *Appl. Eng. Agric.,* vol. 21, pp. 961-964, 2005.

[86] A. De Moor, J. Langenakens, E. Vereecke, P. Jaeken, P. Lootens and P. Vandecasteele, "Image analysis of water sensitive paper as a tool for the evaluation of spray distribution of orchard sprayers," *Aspects of Applied Biology,* vol. 57, pp. 329-342, 2000.

[87] A. Marçal and M. Cunha, "Image processing of artificial targets for automatic evaluation of spray quality," *Transactions of the ASAE (American Society of Agricultural Engineers),* vol. 51, pp. 811, 2008.

[88] Chaim, Pessoa, Neto and Hermes, "Comparison of microscopic method and computational program for pesticide deposition evalution of spraying," vol. 37(4), pp. 493-496, 2002.

[89] H. Zhu, M. Salyani and R. D. Fox, "A portable scanning system for evaluation of spray deposit distribution," *Comput. Electron. Agric.,* vol. 76, pp. 38-43, 2011.

[90] Salyani and Fox, "Performance of Image Analysis for Assessment of Simulation Spray Droplet Distribution," vol. 37(4), pp. 1083-1089, 1994.

[91] QUANTIFOL I nstrument Gmbh and Germany, "Water -sensitive paper for monitoring spray distribution," vol. http//www.QInstrument.com, pp. 1-14, .

[92] J. Wang, H. Mao and W. Hwang, "Experimental investigation of electrostatic spray of twin-fluid atomization," *Chem. Eng. Commun.,* vol. 197, pp. 213-222, 2009.

[93] Anonymous "http://www.exilim.eu/euro/exilimhighspeed/exfh25/specifications/," .

[94] Anonymous "http://www.solidsolutions.co.uk/solidworks/3D-CAD/Data-Sheets.aspx," .

[95] James H. Vincent, "**Aerosol Science for Industrial Hygienists**," vol. Pergamon Press, Elsevier Science, Inc., Tarrytown, NY, 1995.

[96] Anonymous "http://imagej.software.informer.com/1.4/," .

[97] Anonymous "http://www.watersensitivepaper.com/de/index.html," .

[98] Anonymous "http://www.teejet.com/english/home.aspx," .

[99] Anonymous "http://www.comsol.com/comsol-multiphysics," .

[100] Anonymous "http://3dprinting.com/what-is-3d-printing/," .

[101] D M Oosterhuis,F M Bourland, "**COTMAN crop management system** ," *Arkansas Agricultural Experiment Station. ; University of Arkansas (System). Division of Agriculture. ; Cotton Incorporated.,* vol. Chapter3, pp. pp 21-25, 2008.

[102] Anonymous "Contains the data on Lynxmotion AL05D robot manipulator can be found on website:" . http://www.lynxmotion.com/images/html/build143b.htm

[103] Anonymous "Instructions for assembling the robot manipulator AL05D from Lynxmotion wbsite http://www.lynxmotion.com/images/html/build103.htm ," accessed on 13 -4 -2014).

[104] Anonymous "Instructions for assembling the tracked vehicle TTRK-KT from Lynxmotion website," (accessed on 13 -4 -2014). http://www.arduino.cc/en/Main/ArduinoBoardMega2560

[105] Anonymous "Specifications of arduino mega obtained from Ardiona web site :" (accessed on 5-4-2014). http://www.cytron.com.my/p-shield-md10

[106] Anonymous "Specifications of the MD-10 dc motor drive shield for arduino obtained from citron website," (accessed on 7-4-2014). http://www.cytron.com.my/p-sn-hc-sr04

[107] Anonymous "Data sheets for HC-SR04 ultrasonic module obtained from citron website:" (accessed on 10-4-2014). http://www.cytron.com.my/p-sn-hc-sr04

[108] Anonymous "Inverse Kinematics of the AL05D manipulator obtained from Lynxmotion website," (accessed at 22-7-2014). http://www.lynxmotion.com/images/jpg/al5dbd.jpg

[109] F. Chao, Z. Chengsheng, K. Fanyu and W. Jing, "Effects of spray height and spray angle on spray deposition in tobacco plants," in *Industrial Electronics and Applications (ICIEA), 2011 6th IEEE Conference on,* 2011, pp. 2390-2393.

Appendix

Appendix : Information on Lynxmotion™ AL05d Robot Manipulator and TTRK-KT

Tracked Vehicle.

About the Robot Arm

The AL5D robotic arm delivers fast, accurate, and repeatable movement. The robot features: base rotation, single plane shoulder, elbow, wrist motion, a functional gripper, and optional wrist rotate. The AL5D robotic arm is an affordable system with a time tested rock solid design that will last and last. Everything needed to assemble and operate the robot is included in the kit, with several different software control options.

Note that we have tested the arm to hold at most <10oz at full reach without any additional products such as the wrist rotate upgrade installed on the arm (which decreases the payload). The lift capacity increases as the load is closer to the base, but depends on the configuration of the arm.

Image of AL5D Arm with optional wrist rotate.

The Mechanics

The aluminum robotic arm is made from our Servo Erector Set components for the ultimate in flexibility and expandability. The kit consists of black anodized aluminum brackets, Aluminum tubing and hubs, custom injection molded components, and precision laser-cut Lexan components. The arm uses 1 x HS-485HB in the base, 1 x HS-805BB in the shoulder, 1 x HS-755HB in the elbow, 1 x HS-645MG in the wrist, and 1 x HS-422 in the gripper.

Arm Control Options

We now have arm control options. They each have their own unique operating methodology and feature sets. They all incorporate advanced Inverse Kinematics to easily and accurately position the end effector in 3D space.

Gripper with Wrist Rotate.

- FlowBotics Studio is an easy to use graphical program which allows you to easily get your AL5 robot up and running without the need to create code. Use the software to manipulate the real arm using the virtual arm, and create, record and play back your own sequences. Software allows for wrist rotation and additional servos.

- The Dual Lynx Arm Controller program is a free download for a Windows PC. It allows up to two AL5 series arms to be controlled from a single SSC-32 servo controller. It allows the creation of sequences of motion and full editing of sequence steps. It uses a teach pendant style control panel to emulate an industrial arm control system. We also include the FlowStone source code so you can modify and customize the functionality to suit your purpose.

- RIOS is a Windows program for controlling the AL5 series of Robotic Arms with our SSC-32 servo controller. With RIOS, your robot can be taught sequences of motion via the mouse or joystick. The inverse kinematics engine makes positioning the arm effortless. This program uses external digital and analog inputs to affect the robot's motion for closed loop projects. If-then, for-next, and do-while, are supported for the inputs. External outputs can also be controlled.

- Alternately the servo motors can be controlled directly from a microcontroller. We sell the arm without electronics for this purpose.
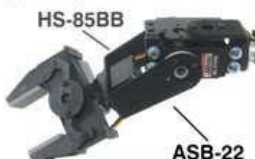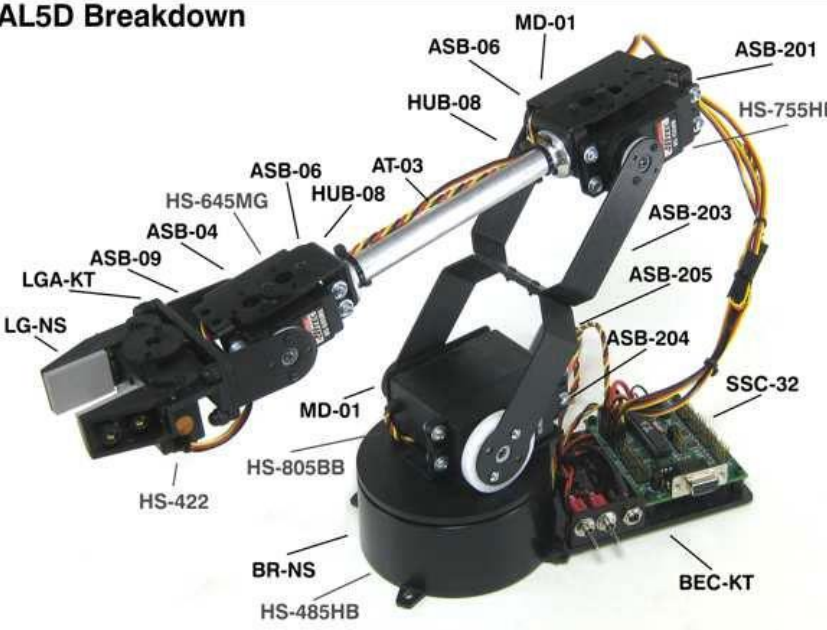

Injection Molded Base.

AL5D Breakdown

Light Weight Wrist Rotate — HS-85BB, ASB-22, Length: 4.50"

Medium Duty Wrist Rotate — HS-225MG, ASB-26, Length: 4.375"

Heavy Duty Wrist Rotate — HS-485HB, LPA-KT, Length: 3.875"

Labels: HS-85BB, ASB-22, HS-225MG, ASB-26, HS-485HB, LPA-KT, HS-645MG, ASB-04, ASB-09, LGA-KT, LG-NS, ASB-06, HUB-08, AT-03, MD-01, HS-805BB, HS-422, BR-NS, HS-485HB, MD-01, ASB-06, ASB-201, HUB-08, HS-755HB, ASB-203, ASB-205, ASB-204, SSC-32, BEC-KT

Alternate Gripper — HS-225MG, Adds (open): 0.75", Adds (closed): 1.25"

Vacuum Gripper (With Medium Duty Wrist Rotate) — Length: 3.875"

Dimensions and Specs
Shoulder to elbow: 5.75"
Elbow to wrist: 7.375"
Wrist to tip of gripper: 3.375"
Height (arm parked): approx. 7.25"
Height (reaching up): approx. 19.00"
Median forward reach: approx. 10.25"
Gripper opening: 1.25"
Alternate gripper opening: 1.875"
Weight: 31 oz
Range of motion per axis: 180°

SSC-32 Servo Connections
Channel 0: Base
Channel 1: Shoulder
Channel 2: Elbow
Channel 3: Wrist
Channel 4: Gripper open/close
Channel 5: Wrist rotate (optional)

Servo motion control: Local closed loop
Accuracy of motion per axis: Servo controller dependant (SSC-32=.09°)

About the Tri-Track Robot
The Lynxmotion Tri-Track Robot Kit is a robust chassis for your RC or autonomous robot experimentation. The robot is designed for indoor or outdoor use and performs well on many different surfaces. With the addition of the optional Base Rotate an arm or large sensor array can be added, or even a Johnny 5 style robot can be made! The chassis is designed to accept the Bot Board and/or the SSC-32. There's room for the Sabertooth 2 x 5 RC motor controller and an assortment of battery packs with room to spare. The robot is capable of carrying up to a 5lb payload.

The Mechanics
The robot chassis is made from ultra-tough laser-cut Lexan structural components, and custom aluminum brackets. By utilizing heavy duty polypropylene and rubber tracks with durable ABS molded sprockets the robot has excellent traction. It includes two 12vdc 50:1 gear head motors.

Controlling the Robot
The robot is currently available only as a basic rolling chassis kit. However, check out this page for a complete Johnny 5 Kit.

Powering Options
The robot is compatible with the following batteries and chargers.
  Chargers & Accessories
    > 7.2 - 12vdc Universal Smart Charger (USC-02)
    > NiMH Quick Connect (mates to battery) (BATC-01)
    > Battery Connector with Switch (WH-01)
  Batteries
    > 12 Volt Ni-MH 1600mAh Battery Pack (BAT-01)
    > 12 Volt Ni-MH 2800mAh Battery Pack (BAT-06)

Important!
To keep costs down we are not providing printed Assembly Guides. They are provided online, so you will need to print them when you order the kits. By providing the Assembly Guides online we can provide more detailed and up to date information than the old hardcopy method allowed.

Tri-Track isometric view.

Tri-Track with SES Arm.

Front view with base.

ations

Tracked Robot Specs

- Length = 10.00"
- Width = 11.00"
- Height = 5.00"
- Ground Clearance = 1.00"
- Deck Height = 3.00"
- Deck Dimensions = 7.25" W x 7.88" D
- Weight = 3.0 lbs (no batteries or electronics)
- Speed = 17.2 in/sec